AN ANALYTICAL MODEL OF IEEE 802.11 DCF FOR MULTI-HOP WIRELESS NETWORKS AND ITS APPLICATION TO GOODPUT AND ENERGY ANALYSIS

A THESIS

SUBMITTED TO THE DEPARTMENT OF ELECTRICAL AND

ELECTRONICS ENGINEERING

AND THE INSTITUTE OF ENGINEERING AND SCIENCES

OF BİLKENT UNIVERSITY

IN PARTIAL FULFILLMENT OF THE REQUIREMENTS

FOR THE DEGREE OF

DOCTOR OF PHILOSOPHY

By

Canan Aydoğdu

November 2010

I certify that I have read this thesis and that in my opinion it is fully adequate, in scope and in quality, as a thesis for the degree of Doctor of Philosophy.

Assoc. Prof. Dr. Ezhan Karaşan(Supervisor)

I certify that I have read this thesis and that in my opinion it is fully adequate, in scope and in quality, as a thesis for the degree of Doctor of Philosophy.

Prof. Dr. Hayrettin Köymen

I certify that I have read this thesis and that in my opinion it is fully adequate, in scope and in quality, as a thesis for the degree of Doctor of Philosophy.

Assist. Prof. Dr. İbrahim Körpeoğlu

I certify that I have read this thesis and that in my opinion it is fully adequate, in scope and in quality, as a thesis for the degree of Doctor of Philosophy.

Assoc. Prof. Dr. Nail Akar

I certify that I have read this thesis and that in my opinion it is fully adequate, in scope and in quality, as a thesis for the degree of Doctor of Philosophy.

Assoc. Prof. Dr. Elif Uysal Bıyıklıoğlu

Approved for the Institute of Engineering and Sciences:

Prof. Dr. Levent Onural
Director of Institute of Engineering and Sciences

ABSTRACT

AN ANALYTICAL MODEL OF IEEE 802.11 DCF FOR MULTI-HOP WIRELESS NETWORKS AND ITS APPLICATION TO GOODPUT AND ENERGY ANALYSIS

Canan Aydoğdu
Ph.D. in Electrical and Electronics Engineering
Supervisor: Assoc. Prof. Dr. Ezhan Karaşan
November 2010

In this thesis, we present an analytical model for the IEEE 802.11 DCF in multi-hop networks that considers hidden terminals and works for a large range of traffic loads. A goodput model which considers rate reduction due to collisions, retransmissions and hidden terminals, and an energy model, which considers energy consumption due to collisions, retransmissions, exponential backoff and freezing mechanisms, and overhearing of nodes, are proposed and used to analyze the goodput and energy performance of various routing strategies in IEEE 802.11 DCF based multi-hop wireless networks. Moreover, an adaptive routing algorithm which determines the optimum routing strategy adaptively according to the network and traffic conditions is suggested.

Viewed from goodput aspect the results are as follows: Under light traffic, arrival rate of packets is dominant, making any routing strategy equivalently optimum. Under moderate traffic, concurrent transmissions dominate and multi-hop transmissions become more advantageous. At heavy traffic, multi-hopping

becomes unstable due to increased packet collisions and excessive traffic congestion, and direct transmission increases goodput. From a throughput aspect, it is shown that throughput is topology dependent rather than traffic load dependent, and multi-hopping is optimum for large networks whereas direct transmissions may increase the throughput for small networks.

Viewed from energy aspect similar results are obtained: Under light traffic, energy spent during idle mode dominates in the energy model, making any routing strategy nearly optimum. Under moderate traffic, energy spent during idle and receive modes dominates and multi-hop transmissions become more advantageous as the optimum hop number varies with processing power consumed at intermediate nodes. At the very heavy traffic conditions, multi-hopping becomes unstable due to increased collisions and direct transmission becomes more energy-efficient.

The choice of hop-count in routing strategy is observed to affect energy-efficiency and goodput more for large and homogeneous networks where it is possible to use shorter hops each covering similar distances. The results indicate that a cross-layer routing approach, which takes energy expenditure due to MAC contentions into account and dynamically changes the routing strategy according to the network traffic load, can increase goodput by at least 18% and save energy by at least 21% in a realistic wireless network where the network traffic load changes in time. The goodput gain increases up to 222% and energy saving up to 68% for denser networks where multi-hopping with much shorter hops becomes possible.

Keywords: IEEE 802.11 DCF, distributed coordination function, analytical model, semi-Markov chain, multi-hop wireless networks, energy-efficiency, goodput, throughput, routing.

ÖZET

ÇOK-SEKMELİ TELSİZ AĞLAR İÇİN BİR ANALİTİK IEEE 802.11 DCF MODELİ VE MODELİN ULAŞTIRILAN İŞ İLE ENERJİ ANALİZİNE UYGULANMASI

Canan Aydoğdu
Elektrik ve Elektronik Mühendisliği Bölümü Doktora
Tez Yöneticisi: Doç. Dr. Ezhan Karaşan
Kasım 2010

Bu tezde, çok-sekmeli telsiz ağlarda saklı düğümleri göz önüne alan ve geniş bir trafik yük aralığında çalışan analitik bir IEEE 802.11 DCF modeli meydana koymaktayız. IEEE 802.11 DCF'e dayalı çok-sekmeli telsiz ağlarda, çarpışmaların ve yeniden iletimlerin sebep olduğu hız azalmasıyla saklı terminalleri göz önüne alan bir ulaştırılan iş (goodput) modeli; ve ek olarak, üstel geri çekilme, donma mekanizması ve düğümlerin kulak misafiri olmalarından kaynaklanan enerji harcamalarını içeren bir enerji modeli önerilmiş ve farklı sekme sayısının ulaştırılan iş ve enerji performansına etkisinin araştırılmasında kullanılmıştır. Dahası, ağ ve trafik durumuna göre en uygun yolatama yöntemini belirleyen bir uyarlanır yolatama algoritması ortaya atılmıştır.

Ulaştırılan iş açısından bakıldığında sonuçlar şöyledir: Hafif trafik altında paket üretim hızı baskındır ve herhangi bir sekme yöntemi eşdeğerde uygundur. Orta şiddette trafikte eşzamanlı gönderimler baskındır ve çok-sekmeli yolatama daha kârlıdır. Şiddetli trafik varlığında ise artan paket çarpışmaları ve trafik sıkışıklığı nedeniyle çok-sekmeli gönderim kararsız olmakta ve doğrudan gönderim ulaştırılan işi arttırmaktadır. Üretilen iş (throughput) açısından

bakıldığında, üretilen işin trafik yükünden çok ağ topolojisine bağımlı olduğu, çok-sekmeli iletimin büyük ağlar için en uygunken doğrudan iletimin küçük ağlar için üretilen işi arttırabildiği gösterilmiştir.

Enerji açısından bakıldığında benzer sonuçlar elde edilmektedir: Hafif trafikte, boş durumda tüketilen enerji baskın olup herhangi bir sekme yöntemini yaklaşık olarak en uygun yapmaktadır. Orta şiddette trafik altında, boş ve alış durumundaki enerji harcaması baskınlaşıp çok-sekmeli gönderim en uygun olmakta en uygun sekme sayısı ara düğümlerde harcanan işlem gücü ile değişmektedir. Çok ağır trafik yük durumunda, artan paket çarpışmaları nedeniyle çok-sekmeli iletim kararsız hale gelmekte ve doğrudan gönderim daha enerji-verimli olmaktadır.

Yolatama yönteminde kullanılan sekme sayısının ulaştırılan iş ve enerji verimliliğini, herbiri benzer mesafeleri kateden daha kısa sekmelerin kullanılmasının mümkün olduğu, büyük ve homojen ağlarda daha çok etkilediği gözlenmiştir. Sonuçlar, MAC seviyesinde kanal kapışmasını göz önüne alan ve sekme yöntemini dinamik olarak değiştiren çapraz-katmanlı bir yolatama yaklaşımının, gerçek bir telsiz ağda ağ trafik yükü zaman içinde değişirken ulaştırılan işi en az %18 arttırdığını ve en az %21 enerji tasarrufu sağladığını göstermiştir. Daha kısa sekmelerin mümkün olduğu yoğun ağlarda ulaştırılan iş %222 kadar artmış ve enerji tasarrufu %68'e çıkmıştır.

Anahtar Kelimeler: IEEE 802.11 DCF, dağıtık eşgüdüm fonksiyonu, analitik model, yarı-Markov zinciri, çok-sekmeli telsiz ağlar, enerji verimliliği, ulaştırılan iş, üretilen iş, yolatama.

ACKNOWLEDGMENTS

I would like to thank my thesis advisor, Assoc. Prof. Dr. Ezhan Karaşan, especially for his good intentions and understanding throughout my studies. I would like to thank him for letting me act free in choosing the topics of my researches-which motivated me to be passionately fond of my studies for years. And finally, I would like to thank him for the countless hours he spent with me discussing our research. His assistance during my time at Bilkent has been invaluable-my life has been enriched professionally and intellectually by working with him.

I would like to thank my daughters Damla and Duru for joining my life and delighting my studies. My Ph.D. studies would not have been so beautiful -and so organized- if I hadn't the hope of playing games with them when I returned home. It was just like finding two little rainbows at home... that sweep away all problems.

And finally, I would like to thank my husband Özgü for the past 16 years that are filled with his love and friendship.

Contents

List of Figures

List of Tables

List of Abbreviations and Notations

b	Backoff stage	34
B	Maximum counter value	42
BEB	Binary Exponential Backoff	4
CCW	Constant Contention Window	37
$EDCA$	Enhanced Distributed Channel Access	29
EPB	Energy Per Bit	19
E_{idle}	Idle energy per bit	130
$E_{overhear}$	Overhear energy per bit	128
E_{rx}	Receive energy per bit	128
E_{tx}	Transmit energy per bit	128
$\bar{G}$	Average node goodput	101
$G(i)$	Node goodput of node i	100
G_n	Network goodput	101
h	Number of hops of all paths in the network	41
IFQ	Interface queue between physical and MAC layers	41
k	Backoff counter value	42
$LACAR$	Load-Adaptive Contention-Aware Route selection algorithm	148
M	Maximum retry count	41
MAC	Medium Access Control	3

MCF	Mesh Coordination Function 29
n	Avg. # of nodes inside the carrier sensing range 57
$\bar{n}_M$	Avg. # retries 103
N	Total number of nodes in the wireless network 41
N_{drop}	Total number of unsuccessful transmissions per path per successful reception 128
N_{rxexc}	Avg. # of nodes inside S_{rxexc} 57
N_{rxint}	Avg. # of nodes inside S_{rxint}, including tx and rx 58
N_{succ}	Total number of successful transmissions per path per successful reception 128
NAV	Network Allocation Vector 33
p	Prob. of collision given transmission occurs 41
P_{coll}	Prob. that NAV is set for short duration given that carrier sensing is done with zero NAV 45
p_{cs}	Prob. that a node does carrier sensing with zero NAV 45
P_{idle}	Prob. that NAV is not set given that carrier sensing is done with zero NAV 45
$P_{ifq}(i)$	Prob. of packet drop at interface queue of node i 41
P_{succ}	Prob. that NAV is set for long duration given that carrier sensing is done with zero NAV 45
Pwr_{idle}	Idle power in Watts 127
Pwr_{rx}	Receive power in Watts 127

Dedicated to my daughters,
Damla and Duru...

Chapter 1

Introduction

Advances in wireless technology have led to various appealing networking applications for delivery of data, audio and video. A diverse range of these applications include real-time audio and streaming video delivery, remote monitoring through sensor networks, rapidly deployed and reconfigured emergency or military ad-hoc networking applications, under-water group communications, teleconferencing, home networking, etc. The wide span of these wireless networking applications is predicted to grow further and even replace wireline communications in the far future with the advances in technology as depicted by Edholm's law of bandwidth [1]. The logarithmic plot given in Fig. 1.1 taken from this study shows the data rates of wireless, wireline and nomadic[1] communications against time.

Applications that run on large wireless networks with limited range necessitate *multi-hopping* functionality, which is the act of transferring data through multiple hops via intermediate nodes. Multi-hopping is used in such wireless networks to extend the coverage when maximum transmit power of the source station is not enough to reach the destination. Multi-hopping becomes optional

[1]The author uses the term *nomadic* for communications that are connected to base stations with small ranges so that users are not fully mobile [1].

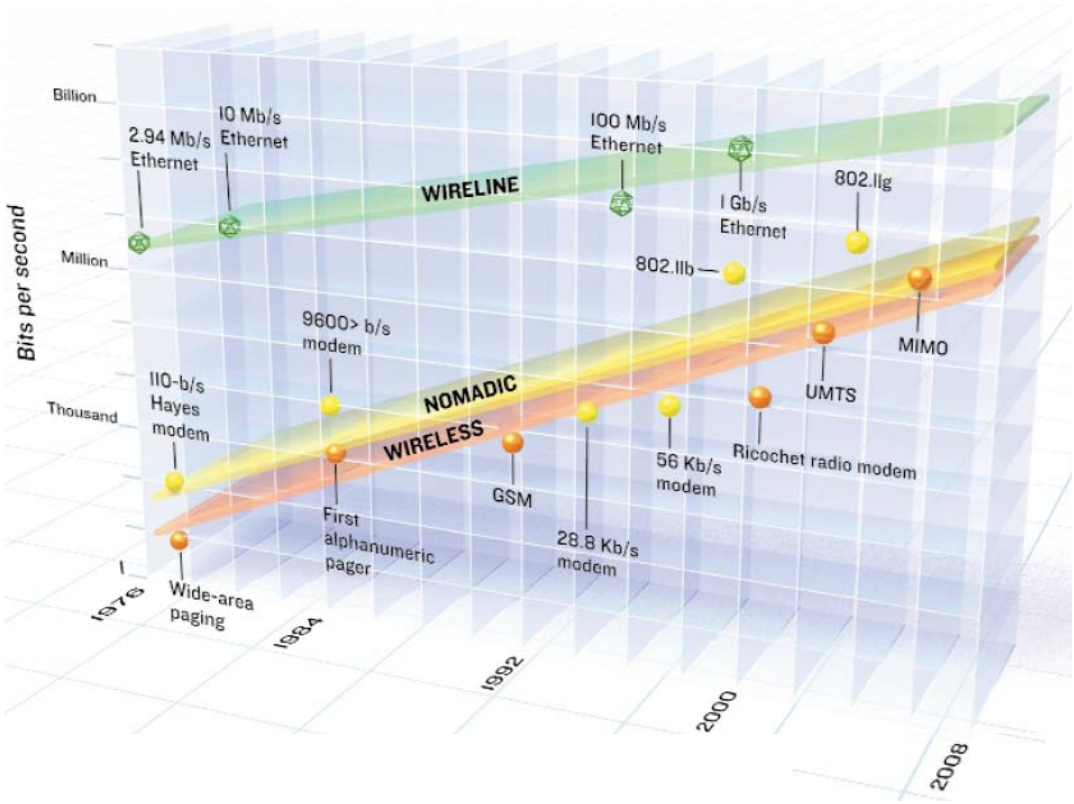

Figure 1.1: Advances in wireless technology fit the Edholm's law of bandwidth rule and predictions are that wireless data access will exceed wireline access in the far future [SOURCE: IEEE Spectrum [1]].

in denser wireless networks, or in denser parts of multi-hop networks, where possible intermediate nodes exist in between source and destination stations and the transmit power of the source station is enough to transmit directly to the destination.

The main technical challenge facing multi-hop wireless networks is that the two substantial resources, the energy and bandwidth, are limited. Energy is limited for mobile stations due to battery supplied appliances and bandwidth is limited due to the shared error-prone time-varying wireless nature of the communication channel. Overcoming these limitations requires innovative cross-layer designs for energy and bandwidth efficient protocols, which can be achieved through detailed analyzes of basic principles of multi-hop wireless networks with an extensive consideration of the layers of the protocol stack.

Figure 1.2: A multi-hop wireless ad-hoc sensor network, where each heat sensor is responsible of conveying information regarding an increase in the heat to the central office. An energy-efficient routing design in this network requires an answer to the basic question of "directly transmit or multi-hop?"

In this dissertation, we focus on routing in multi-hop wireless networks and find an answer to the following basic question: *"When should a routing algorithm use a single long hop or multiple short hops in wireless networks for enhancing a particular performance metric such as energy, goodput or throughput?"*. Fig. 1.2 illustrates an example of a wireless sensor network where the answer of the above question is important in designing an energy-efficient routing algorithm. Heat sensors are deployed in a forest devoted to signaling start of a fire to a central office so that fire is extinguished before it spreads. The main design challenge in this multi-hop wireless network is to design communication algorithms so as to minimize energy consumption, because the more the batteries of the sensors last the less the annual maintenance cost will be.

This dissertation extends the studies investigating the effect of routing on wireless network performance using a cross-layer approach, where the effects of medium access control (MAC) contention are incorporated. The goal of this

study is to reveal when multi-hopping becomes advantageous and to state guidelines for energy, goodput and throughput-efficient routing considering MAC contention.

In this dissertation we study the random medium access control protocol of the IEEE 802.11 standard [2], since most commercial wireless products are based on this standard. IEEE 802.11 is an open standard developed by the Institute of Electrical and Electronics Engineers (IEEE) and the primary MAC technique of 802.11 is the distributed coordination function (DCF), which is based on the carrier sense multiple access with collision avoidance (CSMA/CA) with binary slotted exponential backoff (BEB).

A more comprehensive statement of the problem studied in this dissertation may be given as follows: investigation of the basic question of whether to "directly transmit or multi-hop?" in order to increase the energy, goodput and/or throughput performance in IEEE 802.11 DCF based wireless networks using a cross-layer approach that considers

- MAC contention including BEB, freezing mechanisms, retransmissions, collisions, etc.,
- hidden terminal effect,

and works for

- a large range of traffic loads,
- any two-dimensional topology,
- any traffic patterns among nodes,
- networks where nodes may have any functionality: any combination of source, sink and relay.

This dissertation, initially inspired by the basic question of how to route in a multi-hop wireless network for enhanced energy/goodput/throughput performance, makes several contributions to the literature aside from providing an answer to the original starting problem. The main contributions of this dissertation are illustrated in Fig. 1.3.

Owing to the fact that existing models are inadequate for energy, goodput and throughput performance analysis for IEEE 802.11 DCF based multi-hop networks, an analytical model for IEEE 802.11 DCF is developed in this dissertation. Hence, the primary contribution of this study is the introduction of an analytical IEEE 802.11 DCF model for multi-hop networks which:

- considers hidden terminals,
- provides fairly accurate results for large range of traffic loads,

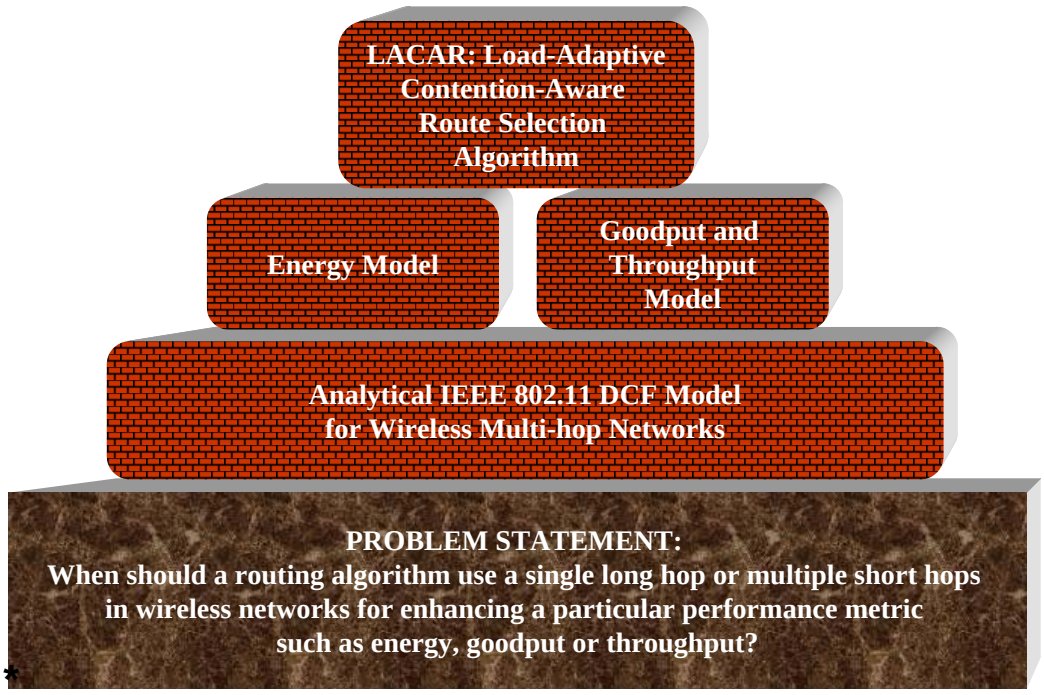

Figure 1.3: Main contributions of the dissertation: i) an analytical IEEE 802.11 DCF model, ii) goodput and throughput models, iii) an energy model and iv) a load-adaptive contention-aware route selection algorithm for IEEE 802.11 DCF based multi-hop networks.

- works for any given two-dimensional topology,
- increases the accuracy and scalability of the analytical model by joint use of fixed and variable slots
- allows each node to be both source and/or relay.

The second contribution is an analytical framework for calculation of the average node goodput and the average node throughput for the IEEE 802.11 DCF based multi-hop wireless networks, which considers carrier sensing, hidden terminal effect, non-optimum routing and analyzes the problem for a large range of traffic loads and for different network densities.

The third contribution is an analytical framework for the investigation of the energy-efficiency of routing strategies in IEEE 802.11 DCF based multi-hop wireless networks. To the best of our knowledge, this is the first study in multi-hop networks that includes the energy consumption due to MAC operations such as collisions, retransmissions, overhearing of nodes, BEB and freezing mechanisms.

Our final contribution is a load-adaptive contention-aware routing strategy for increasing the energy and goodput performance in IEEE 802.11 DCF based multi-hop networks. The results of our research show that traffic load adaptive cross-layer routing strategy significantly increases the energy and goodput performances of IEEE 802.11 DCF based multi-hop networks.

We demonstrate the effect of routing on the goodput, throughput and energy performance of multi-hop wireless networks. The analytic results obtained via the IEEE 802.11 DCF, the goodput/throughput and energy model, supported by simulations, demonstrate the following main results:

- Throughput is shown to increase for any routing strategy with increased traffic, whereas goodput exhibits a bell-shaped behavior for short hop routing as the traffic increases. The goodput results show that selection of routing strategy based on the traffic load increases goodput significantly. Under light traffic, arrival rate of packets is dominant, making any routing strategy equivalently optimum. Under moderate traffic, concurrent transmissions dominate and multi-hop transmissions become more advantageous. At heavy traffic, short hop routing becomes unstable due to increased packet collisions and excessive traffic congestion, and long hop routing becomes more stable and increases goodput. The choice of routing strategy is observed to affect goodput more for large and homogeneous networks where it is beneficial to use multiple short hops each covering similar distances.

- Energy-efficient routing strategy highly depends on the traffic load: Under light traffic, energy spent during idle mode is responsible for most of the energy consumed, making any routing strategy equally good. Under moderate traffic, energy spent during idle and receive modes dominates and multi-hop transmissions become more advantageous. At heavy traffic, short hop routing becomes unstable due to increased packet collisions and excessive traffic congestion, and long hop routing becomes more energy-efficient and stable. It is also shown that the processing power at intermediate nodes affects the optimum hop number, but only for a specific range of traffic loads.

- The proposed load-adaptive contention-aware routing algorithm (LACAR), which takes energy expenditure due to MAC contentions into account and dynamically changes the routing strategy according to the network traffic load, increases goodput by at least 18% and saves energy by at least 21% in a relatively less dense wireless network where the traffic load changes with time. The goodput gain increases up to 222% and energy savings

increase up to 68% for a denser network where short hop routing with higher number of hop-counts is possible.

The dissertation begins with a detailed explanation of technical background on multi-hop wireless networks, investigation of performance metrics in wireless networks with emphasis on goodput, throughput and energy, design challenges at layers of protocol stack and cross-layer design. Chapter 3 is devoted to the description of the analytical IEEE 802.11 DCF model for multi-hop wireless networks. The analytical IEEE 802.11 DCF model, as well as the analytical and simulation results for the model are presented here. Chapter 4 describes the goodput and throughput model for IEEE 802.11 DCF based multi-hop networks and presents corresponding results and conclusions. A theoretical framework to evaluate the energy consumption of IEEE 802.11 DCF based multi-hop networks is introduced in Chapter 5, where the results and conclusions regarding energy are presented. An adaptive routing approach for increasing the energy and goodput performance in IEEE 802.11 DCF based multi-hop networks is presented in Chapter 6, which contains the adaptive routing algorithm and its performance evaluation. This dissertation ends with conclusions and a discussion of future research directions in Chapter 7.

Chapter 2

Goodput, Throughput and Energy-Efficiency in Multi-Hop Wireless Networks

During the past decade, wireless services have evolved from basic voice communication to broadband multimedia services. However, users demand higher flexibility and higher mobility while requesting services with higher data-rate, lower latency, higher energy-efficiency. The wireless applications and services commercially available around the world today owe their existence to the evolution of the wireless technology advancements, and the technologies not achieved today need more advancements in the quality of service provided by wireless technologies.

Various wireless networking applications have emerged: personal area networks, distributed control systems and military applications, home networks, and a broad class of ad-hoc and sensor networking applications. The chief utilities of wireless networks such as easy deployment and reconfiguration, distributed nature and node redundancy are possible by means of battery powered mobile

devices, which bring together the problem of effective usage of energy resources. Although energy-constraints are not inherent to all wireless networks (for example, devices may be stationary and attached to a large energy source such as a vehicle), some of the most exciting applications lie in the category where energy-efficiency is an important design issue. Energy management is one of the most important problems in wireless communication and recent studies have addressed this topic [3].

In the next section, we introduce and define two major performance metrics in wireless networks: goodput/throughput and energy consumption. Goodput and throughput issues in multi-hop wireless networks and cross-layering techniques for enhancing goodput and throughput performance are examined in the next section. The energy-efficiency at layers of protocol stack is investigated in Sec. 2.2 with a discussion of various cross-layering techniques in increasing energy-efficiency.

2.1 Goodput and Throughput Performance in Multi-Hop Wireless Networks

Realization of many wireless services depends on delivering information with an acceptable data rate to the users. One factor that limits the data rate in wireless networks is the limited available bandwidth. Federal communications commissions in countries regulate which bandwidth particular networks can access with how much maximum power. This limits the amount of bandwidth that can be given to each user of the wireless network.

Providing goodput/throughput adequate for applications becomes complicated in wireless networks due to the lack of accurate knowledge of the state of the network, e.g., the quality of the radio links, availability of routers and their

resources [4]. The time varying conditions, error-prone wireless channel are also factors that decrease goodput/throughput in wireless networks. Furthermore, providing an adequate goodput/throughput for applications in a wireless network may become impossible when: 1) the size of the network grows beyond a certain level where network updates cannot be propagated within specific delay bounds, 2) the nodes are too mobile, and 3) when a node loses connectivity with the rest of the network. Thus, goodput/throughput in wireless networks is fundamentally different from traditional networks.

There are several definitions of goodput for different disciplines, that are listed as follows:

- In computer networks, goodput is defined to be the application level throughput, i.e. the number of useful bits per unit of time forwarded by the network from a certain source address to a certain destination, excluding protocol overhead, packet headers and retransmitted data packets.
- In communication systems theory, the typical measure of goodput equals the information transmission rate times the probability of success, assuming that the channel statistics remain unchanged. This calculation of goodput is not any more valid when scheduling decisions on rate and power change over time or when errors appear in an irregular fashion e.g. in bursts [5].
- Goodput may also be defined as the ratio of achieved user data rate over channel raw data rate [6].

The first definition is more general including the application layer mechanisms. In this dissertation we define goodput to be the network level throughput.

Throughput, on the other hand, is the link layer data rate of successful transmissions. Goodput is always lower than the throughput, which generally is lower than the channel capacity or bandwidth. The factors that cause lower goodput

than throughput are inclusion of the following items in calculation of throughput, which are excluded from goodput calculation:

- Transport layer, network layer and MAC layer protocol overhead due to management packets, control packets and packet headers.
- Retransmission of lost or corrupt packets due to transport layer automatic repeat request (ARQ), network or MAC layer retransmission mechanisms.

Goodput in multi-hop wireless networks is much lower than throughput, compared to single-hop networks or wireless local area networks (WLAN), because packets are also dropped at intermediate nodes. For a data packet dropped at some intermediate hop, the successful transmissions of this data packet at prior hops are counted in calculation of throughput, whereas these transmissions are excluded in goodput calculation. Hence, goodput is normally employed to give more accurate performance evaluation than throughput in multi-hop networks.

Both goodput and throughput are vulnerable to variations in channel quality, packet length, lower layer protocol efficiency, network load, inter-frame gaps between packets, packets-per-second ratings of devices that forward packets, hardware speeds, network design protocols, network topology, and so forth.

In this dissertation, we are specifically concerned with average node goodput and average node throughput, where average node goodput is defined as the *number of data bits per second received successfully by the destination, averaged over all nodes in the wireless network*. The average node throughput is defined as *the data rate of successful transmissions of a node, including retransmissions due to collisions* [7, 8].

2.1.1 Goodput and throughput issues at layers of the protocol stack

Multi-hop networks are expected to be an important part of future wireless network architectures due to their easy deployment, robustness and flexibility. The core idea of multi-hop wireless networks, forwarding of packets over multiple wireless hops, is a new quality in wireless communications and requires optimization of many research issues in order to meet the high goodput and throughput requirements in practical multi-hop wireless deployments. More powerful devices based on multiple radio interfaces that make use of channel diversity, optimized MAC protocols for accessing the multi-hop channel or scheduling links, new routing metrics are needed in order to support necessary improvements. Finally, the cross-layer design is important in order to get better access to the layers in order to enhance goodput and throughput performance. In this section, a review of some technology solutions at the physical, MAC and network layers, together with some cross-layer design examples to improve goodput and throughput performance in the literature are provided.

Physical layer

Physical layer has several properties affecting goodput and throughput. The antenna type, the modulation scheme, the rate and complexity of channel coding are physical layer features that impact goodput and throughput directly. Multi-Radio and Multi-Channel (MRMC) is also a means to improve throughput in multi-hop wireless networks. Multi-radio is attractive due to cheap and various hardware devices that can be simultaneously used due to the different sensing range, bandwidth and attenuation characteristics. Interference is reduced by multi-channel by which non-overlapping channels are used to transmit

or receive simultaneously. This way the use ratio of frequency spectrum is enhanced by improving the effective bandwidth of the whole network. A centralized static channel assignment in MRMC wireless mesh networks with the objective of maximizing overall end-to-end throughput, which we refer as goodput in this dissertation, is introduced in [9], which assigns the available channels to the bottleneck links of multi-hop flows iteratively. Simulation results conducted in ring and grid topologies show that the algorithm is effective in increasing the goodput.

The physical layer properties have also indirect effects on goodput and throughput performance by restraining multiple access and routing decisions through changing the error rate of the channel.

MAC layer

MAC layer is responsible for allocating wireless channels to contending users and scheduling the transmissions among them. It also realizes link error control, by which a destroyed frame on the link is retransmitted. The MAC layer affects goodput and throughput in various ways. The allocation of simultaneous transmissions affects interference, which in turn affects the error rate of packets, where increased error rate decreases goodput and throughput. Moreover, interference determines the signal to interference and noise ratio that affects the data rate. The link error control scheme at MAC affects the header size, the error rate, the collision probability, number of retransmissions, service time per packet metrics which have a direct effect on goodput and throughput.

Several MAC protocols for increasing goodput or throughput performance are proposed in the literature. A novel high-throughput MAC protocol, called Concurrent Transmission MAC (CTMAC) is presented in [10], which supports concurrent transmissions while allowing the network to have a simple design

with a single channel, single transceiver, and single transmission power architecture. CTMAC inserts additional control gap between the transmission of control packets (RTS/CTS) and data packets (DATA/ACK), which allows a series of RTS/CTS exchanges to take place between the nodes in the vicinity of the transmitting, or receiving node to schedule possible multiple, concurrent data transmissions. To safeguard the concurrent data transmission, collision avoidance information is included in the control packets and used by the neighboring nodes to determine to transmit or not. Simulation results show that a significant gain in throughput is obtained by the CTMAC protocol compared to the IEEE 802.11 DCF protocol.

Network layer

Network layer has two main functions: routing and mobility management. Regarding routing, the network layer determines the path from source to destination, and consequently selects a set of links. Routing protocols play the key role in multi-hop wireless networks since they control the formation, configuration and maintenance of the topology of the network. Routing protocols proposed for optimization of throughput have to consider other metrics depending on the application, mobility, energy, radio characteristics of nodes. For example a routing protocol proposed for optimization of goodput and throughput in an ad-hoc multi-hop wireless network has to consider energy-efficiency and mobility at the same time, whereas a routing protocol in a MRMC wireless mesh network should also select proper channel and radio, so that it can sufficiently make use of the advantage of MRMC.

Certain nodes that are located at critical positions in the multi-hop wireless network form network bottlenecks and are likely to get heavily loaded. Therefore, load balancing is an essential ingredient in improving the achievable throughput and goodput. Load balancing assumes to achieve the efficient traffic allocation,

efficient use of links, maximal use of network capacity, minimal resource consumption at the bottleneck nodes. In [11], it is shown that load balanced routing improves performance regardless of the nature of the underlying MAC protocol compared to conventional shortest widest path routing. And also, it is shown that an ideal load balanced routing protocol should take into account both the hop counts and the capacities when computing the optimal path.

2.1.2 Cross-layer design

The design of the OSI protocol stack where each layer operates independently results in poor performance for wireless networks, especially when energy is a constraint, leading to a necessity for a cross-layer design [12–42]. A cross-layer design requires the protocols of each layer to be developed within an integrated and hierarchical framework considering the interdependencies among them. On the other hand, a cross-layer design needs to be modified at all layers of the stack in case of an update and this might produce unintended interactions among layers, adaptation loops and performance degradation resulting in spaghetti-like codes if not maintained efficiently [18]. Furthermore, an efficient, flexible and comprehensive cross-layer signalling scheme is required [19]. The information that can be used in a cross-layer architecture and the layer to get it from are listed in Table 2.1. Some representative properties of each layer have the potential of affecting all the higher layers.

Different approaches for cross-layer design for optimization of throughput are reviewed in [43–45]. A technique to increase the throughput of wireless mesh networks, based on cooperative communications is introduced in [46], where two cooperative strategies, opportunistic relaying, and partial decoding, are proposed. Simulation results for Rayleigh and Rice fading show remarkable throughput gains of the cooperative strategies with respect to non-cooperative transmission.

Table 2.1: Some representative information that can be exchanged in a cross-layer architecture and where the information is available.

Layer	Information
Application	Topology control algorithms Traffic requirements Logical topology
Transport	Congestion window Timeout clock End-to-end packet loss rate End-to-end delay
Network	Network lifetime Physical topology Connectivity
Data Link/MAC	Link bandwidth Link quality Mac packet delay Data rate Power control Scheduling policy
Physical	Node location Movement pattern Transmit power (radio transmission range) Antenna type (multiple antennas etc.) (Residual) battery power SNR information

In [47], the authors have proposed a LEss remaining hop More Opportunity (LEMO) algorithm for multi-hop networks in order to achieve higher packet delivery ratio, which is a cross-layer MAC and routing algorithm. Through simulations, the performance of proposed LEMO algorithm is evaluated and compared with the legacy IEEE 802.11 DCF. Results show that the total packet delivery ratio is increased, which means that the throughput discrepancy among flows is reduced while the total flow throughput is enhanced.

IEEE802.11e is proposed and Additive Increase Multiplicative Decrease (AIMD) mechanism is combined to analyze the quality of service in cross layer in [48]. The combined technique enhanced the throughput by $30 - 40\%$. IEEE802.11e MAC employs a channel access function called hybrid coordination function. Their results showed that the interaction between transportation and MAC protocol has a significant impact on the achievable throughput in wireless networks.

2.2 Energy Performance in Multi-Hop Wireless Networks

Another performance goal in wireless networks, as important as providing goodput/thorughput, is energy-efficiency, because realization of many wireless services depends on battery powered devices. The relative importance of energy and goodput/throuput depends on the application. For example, the primitive design constraint for a wireless sensor network used for remote environment monitoring may be energy-efficiency, whereas it is goodput for a wireless mesh network set for a dublex video-conferencing application.

Wireless medium is accessed often by portable, lightweight devices that are supplied by a local battery. This limits the amount of energy available to each

user, requiring energy-efficient protocols in order to maximize node lifetime. It is foreseen that wireless interface will be the primary consumer of energy and energy-efficiency is expected to become the single most important figure of merit in 10 to 20 years time in ad-hoc networks [49].

Energy-efficiency in wireless networks can be defined as effective usage of power resources of nodes in the wireless network so that one of the following objective functions is satisfied:

1. Maximization of the network lifetime
2. Maximization of the lifetime of each individual node
3. Minimization of energy per bit delivered.

The first objective function aims prolonging the network lifetime. In [50], [51] network lifetime is defined as the time of the first node failure due to battery depletion since a single node failure can make the network become partitioned and further services be interrupted. The second objective function aims prolonging individual node lifetimes. This is achieved by various techniques in the literature: i) maximizing the fraction of surviving nodes in a network [52, 53], ii) maximizing the mean expiration time [54], and iii) maximizing the minimum residual battery energy among nodes [55].

The third objective function for achieving energy-efficiency is minimizing *energy per bit (EPB)* which is defined as the energy consumed for communicating one bit of information per flow. EPB includes the energy consumed at all layers of the protocol stack. The energy consumption is shaped by various modulation techniques, synchronization, header overhead, energy and time ratio of transmission-reception and standby modes, MAC techniques, retransmission strategies, routing, etc.

The first two objective functions regarding lifetime consider residual battery energies of nodes, whereas the last ignores it. The objective function that achieves the most energy-efficient operation is network and application dependent. For example, maximizing the lifetime of a wireless sensor network is generally a more crucial objective in terms of energy-efficiency compared to maximizing the lifetime of individual nodes, since connectivity of the network, compared to individual nodes, is more important for sustaining operability of the sensor network. On the other hand, in an office network, maximizing the lifetime of each individual node may gain importance since none of the clients may tolerate an unfair energy outage in the middle of a meeting. Furthermore, in an wireless network where throughput is of primary interest, such as data networks, EPB may become more important than the lifetimes of the network or nodes.

2.2.1 Energy-efficiency at layers of the protocol stack

Studies show that the significant consumers of power in typical laptop are the microprocessor (CPU), liquid crystal display (LCD), hard disk, system memory (DRAM), keyboard/mouse, CDROM drive, floppy drive, I/O subsystem, and the wireless network interface card [56, 57]. A typical example from a Toshiba 410 CDT mobile computer demonstrates that nearly 36% of power consumed is by the display, 21% by the CPU/memory, 18% by the wireless interface, and 18% by the hard drive. Consequently, energy conservation has been largely considered in the hardware design of the mobile terminal and in components such as CPU, disks, displays, etc. [58]. Significant additional power savings may result by incorporating low-power strategies into the design of network protocols used for data communication. Moreover, communication units of a large group of wireless networking applications are simple devices without a display and limited processing capabilities, where the power consumed by the wireless interface constitutes a larger fraction of the total power consumption than mentioned above.

Furthermore, authors in [59] showed that accessing local hard drives consumes significant power compared to reception of wireless data and thus, periodic broadcast of data over wireless communication channels can be considered as a supplement to a mobile user's secondary storage. Hence, considerable reduction in the wireless interface power consumption may provide a reduction in memory power consumption if such a method is used for storage.

Although a wireless interface is composed of the data link and the physical layers, energy saving at a wireless interface is not restricted by these layers. Any energy-efficient network or application layer operation reduce power consumption at the wireless interface.

Recent advances in wireless network protocols, the technical challenges to be considered within all layers of the protocol stack for energy-constrained wireless networks and possible approaches for solving them are investigated in [12], [13]. The areas of research for energy-efficient design and the corresponding protocol layers are summarized in Figure 2.1.

Physical layer

Physical layer has several properties affecting energy expenditure. The RF circuit features such as the power required to drive the RF modules, transmit power, transceiver complexity, antenna type and antenna beam coefficients accumulatively impact power consumption in transmit, receive and idle modes of operation. The modulation scheme, the rate and complexity of channel coding are additional physical layer features that impact energy consumption directly. These physical layer properties have also indirect effects on energy- efficiency, by restraining multiple access and routing decisions through changing the error rate of the channel.

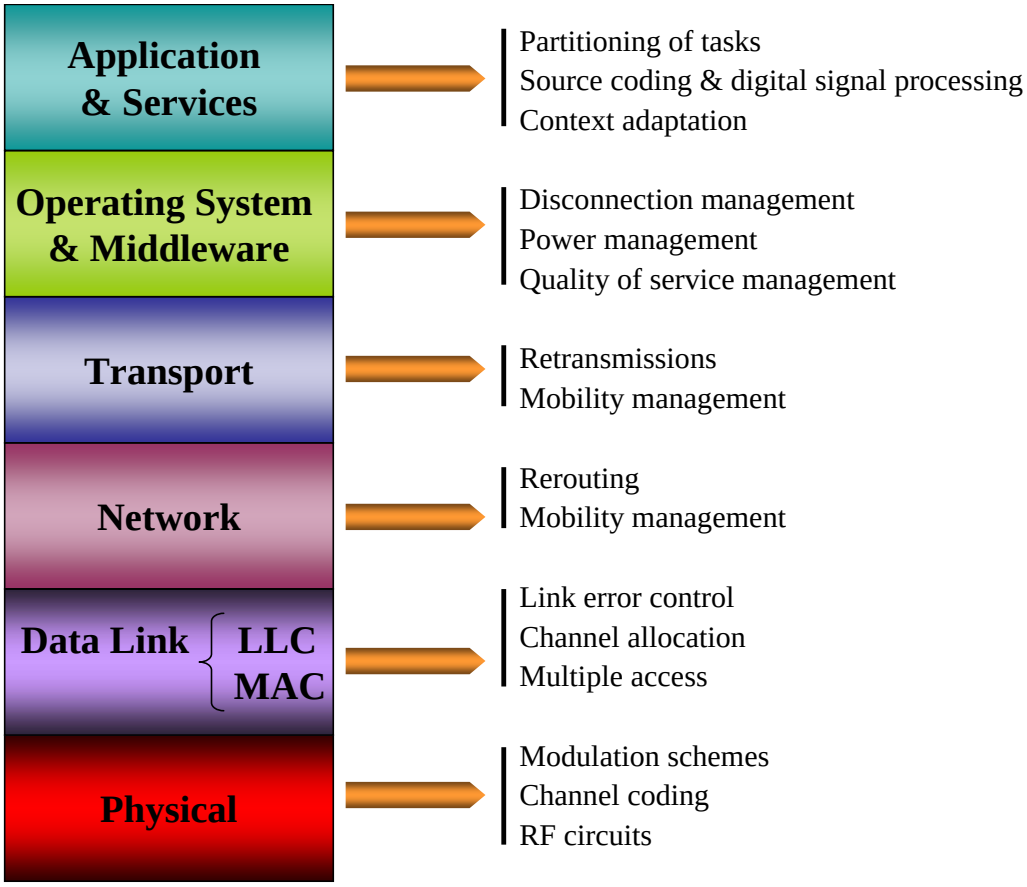

Figure 2.1: Protocol stack of a generic wireless network, and corresponding areas of energy efficient research.

MAC layer

The MAC layer affects energy expenditure in three ways: 1) The allocation of simultaneous transmissions imposes interference that impacts physical layer performance in terms of distinguishing the desired signal from the rest. Briefly, the MAC layer mainly controls interference that may lead to excessive energy consumption for transmit power adaptation at the transmitter or link retransmissions. 2) Depending on the scheduling scheme, nodes may switch to power-saving modes of operation. 3) The link error control scheme affects the energy consumption per packet. Ineffective maintenance of point-to-point retransmissions at the link layer may initiate end-to-end retransmissions at the transport layer, resulting in excessive energy consumption. Conversely, a strict link error control scheme

that results in frequent link layer retransmissions may also introduce additional power expenditure.

Network layer

Several power-aware routing protocols can be summarized as follows:

1. Minimum total transmission power routing (MTPR) selects the route with minimum sum of link transmission powers. Therefore, the route with more shorter hops and greater end-to-end delay is selected, where load balancing and fairness in energy-consumption are not supplied [14], [15].

2. Minimum battery cost routing (MBCR) selects the route with the maximum sum of residual battery powers. Hence, load balancing is considered and the lifetime of each node together with that of the network is extended. However, routes with nodes that have little energy may still be selected [15].

3. Min-max battery cost routing (MMBCR) selects the route with the maximum value of minimum residual battery energies of all possible routing paths. Each node's lifetime is maximized by this protocol and fairness in the way nodes are used is satisfied. But since, minimum transmission power paths are not necessarily chosen, the lifetime of all nodes may actually reduce [15].

4. Conditional max-min battery capacity routing (CMMBCR) uses the most energy-efficient routes while all modes have residual battery capacity above a threshold. Once nodes' energies fall below this threshold, routes with the lowest battery capacity are avoided. This routing protocol represents a compromise between MTPR and MMBCR [16].

5. Constrained shortest-path routing (CSPR), imposes a constraint on maximum transmission distance that controls the network topology. The longer

the maximum transmission distance, the more fully connected the network graph will be. For a given network topology, shortest path routing selects the minimum-energy path. The maximum distance constraint enables a trade-off between transmission energy and overall (source to destination) delay. Potential application of CSPR may be within clusters of target-tracking sensor networks [17].

Different routing strategies select different sets of links that result in different sets of concurrent transmitting links, influencing the MAC layer. For instance, spatially close routes increase interference and make it harder for MAC to resolve the transmission conflicts. However, none of the above mentioned routing algorithms consider increases in transmission power or degradation in link quality due to these concurrent transmissions, which can only be neglected when all simultaneous links use orthogonal channels without spatial reuse.

Mobility management is another responsibility of the network layer that affects energy-efficiency. The mobility pattern, the frequency of node additions/failures and link quality variations impact the amount of control traffic, which is another source of energy dissipation. Transport layer is responsible of end-to-end transmissions and becomes crucial for wireless networks due to error prone nature of the wireless channel. Congestion control mechanisms and retransmissions at this layer may result in energy waste.

2.2.2 Cross-layer design

Energy-efficiency is enhanced by cross-layer designs, some of which are summarized in this section with some examples.

Transmit power plays a key role in the development of energy-efficient cross-layer protocols. Wireless terminals capable of varying the transmit power acquire

different radio transmission ranges through power control. The level of transmit power affects all of the upper layer protocols, due to its effect on local neighborhood. Increasing radio transmission range may result in larger number of nodes in the neighborhood, affecting link quality, bandwidth, packet delay and scheduling [20–22] at the MAC layer; routing decisions at the network layer; retransmissions and congestion control mechanisms at the transport layer; logical topology (the users included in the network) and the type of applications at the application layer.

Signal to interference and noise ratio (SINR) determines the performance of the link. In case of a low SINR, power is consumed more either due to increased transmit power or increased number of retransmissions. Also a low SINR may require a reduction in data rate, affecting MAC layer properties such as packet delay and scheduling policies. An example for such cross-layering is given in [23], where SINR information is attached to RREQ packets and PREP packets propagate with rate adaptation at each hop providing the selection of the route with minimum MAC delay. A somewhat similar cross-layering is introduced in [24], where the network layer may discard packets in advance based on the channel conditions and link delay information passed from the MAC layer, together with traffic requirements information passed from the application layer. Another cross-layering method that passes the channel conditions and MAC delay information, but this time to the MAC layer scheduler, is proposed in [25]. The scheduler places the packet into the queue according to its estimated delay, where it may place a packet at the end of the queue if its corresponding channel is corrupted. Particular to CDMA channels, channel condition information can be used to change the spreading factor to adapt rate [26].

SINR information may also affect power control decisions at the MAC layer that constitutes the basics of the MAC protocol introduced in [27] where a frame format for slotted RTS/CTS structure for CSMA/CA is introduced. The SINR

of the slotted and successive RTS/CTS packets is measured and power control is done accordingly.

Monitoring the interference level and delaying packet transmissions [28], or marking packets indicating wireless channel related losses rather than congestion losses in order to reduce congestion window reductions [29], are methods for saving energy using SINR information.

Mobility pattern is another physical layer property of wireless networks that impacts all layers of the protocol stack. The frequency of link quality changes, node additions and failures depend on the movement pattern and affect power consumption due to additional amount of control packet flows that provide route updates, retransmissions and topology reconfigurations. Moreover, highly mobile systems impact connectivity of the network, requiring an increase in the transmit power [12], that increases power consumption.

Channel coding, multiple antenna techniques are shown to save transmission power. However, they are often highly complex and therefore require significant power for signal processing. This trade-off requires examination to determine if multiple antenna techniques and channel coding result in a net savings in energy [12].

Routing is shown to play a dominant role in reducing power consumption [21]. Cross-layer design of many energy-efficient routing protocols makes use of various physical layer information. A transmit power aware routing protocol that uses transmit power as a metric for shortest path routing to increase node and network lifetime is proposed in [30]. Since this cross-layer routing strategy leads to utilization of the same paths leading to battery depletions, battery power-aware strategy is introduced in conjunction with transmit power and lifetime is shown to increase by 45% in [31]. A cross-layer design for enhancing power-based routing protocols is proposed, where MAC layer information such as the number

of sucessfully received CTS and ACK messages are used in selecting paths with minimum probability of error [32]. A cross-layer design for routing when channel fading is present is proposed in [33], where the next hop is chosen to be the one that has the best channel condition to mitigate fading.

Goodput, throughput and energy-efficiency are enhanced by consideration of all protocol layers and exchange of relevant information among layers. However, an efficient cross-layering is possible by a correct and comprehensive knowledge of how network properties impact each layer's performance.

In the following chapters, the effect of long-hop and short-hop routing on goodput, throughput and energy performance in multi-hop wireless networks is investigated considering MAC contention. A cross-layer approach, which uses physical layer and MAC layer properties for the analysis of goodput, throughput and energy performance is developed. Since our concern is hop-count, an analytical model for MAC protocol for multi-hop networks is required in order to capture and understand the effect of MAC layer in this cross-layer architecture. In the next chapter, we propose an analytical model for the IEEE 802.11 DCF in multi-hop wireless networks, which is the MAC technique used in this dissertation for the cross-layer approach.

Chapter 3

An Analytical Model for IEEE 802.11 DCF

In order to investigate the effects of MAC layer on goodput, throughput and energy performance, the IEEE 802.11 technology, is chosen since most commercial wireless products are based on the IEEE 802.11 [2]. 802.11 is an open standard developed by the Institute of Electrical and Electronics Engineers (IEEE) in 1997. The original version specifies two raw data rates of 1 and 2 Mbps to be transmitted via infrared (IR) signals or by either frequency hopping or direct-sequence spread spectrum in the Industrial Scientific Medical (ISM) frequency band at 2.4 GHz. Widespread adoption of 802.11 networks occurred after ratification of the 802.11b and 802.11a in 1999.

The original IEEE 802.11 standard is supplemented by four different standards: 802.11a, 802.11b, 802.11g and 802.11n, where a summary of specifications is given in Table 3.1. 802.11b\g are currently the most widespread standards, since they operate in the free ISM band. 802.11a operates in 5 GHz band, and is not interoperable with 802.11b\g, except if using equipment that implements both standards. 802.11n builds upon previous 802.11 standards by adding

Table 3.1: Summary of the IEEE 802.11a\b\g\n protocols.

Protocol	Legacy	802.11a	802.11b	802.11g	802.11n	
Release date	1997	1999	1999	2001	2008	
Frequency (GHz)	2.4	5.0	2.4	2.4	2.4	or 5
Non-overlapping channels		12	3	3	3	12
Supported data rates (Mbps)	1,2	6,9,12,18, 24,36,48,54	1,2,5.5,11	1,2, 5.5,11, 6,9,12,18, 24,36,48,54	upto 130	upto 270
Max bandwidth per channel		54	11	54	130	270
Modulation technique	FHSS/ DSSS	OFDM	DSSS	OFDM	DSSS/OFDM/MIMO	
Range (meters)	20-100	35-120	38-140	38-140	70-250	70-250

MIMO (multiple-input multiple-output), where MIMO uses multiple transmitter and receiver antennas to allow for increased data throughput through spatial multiplexing and increased range by exploiting the spatial diversity.

802.11s is the IEEE 802.11 standard for Mesh Networking, the draft of which is approved in 2009. It specifies an extension to the IEEE 802.11 MAC to solve the inter-operability problem by defining an architecture and protocol that support both broadcast/multicast and unicast delivery using radio-aware metrics over self-configuring multi-hop topologies.

The primary MAC technique of 802.11 is the distributed coordination function (DCF), which is CSMA/CA technique with binary slotted exponential backoff. Stations in a IEEE 802.11s based network implement the mesh coordination function (MCF). The mandatory part of MCF relies on the contention based protocol known as Enhanced Distributed Channel Access (EDCA), which itself is an improved variant of the basic 802.11 DCF. Using DCF, a station transmits a single frame of arbitrary length. With EDCA, a station may transmit multiple frames whose total transmission duration may not exceed a limit [60]. EDCA mechanism allows service differentiation in IEEE 802.11 networks by using up to four different channel access functions that each execute independent

backoff counters. The difference in absolute values of timers and the maximum contention window allows the differentiation of traffic types [61]. The mesh deterministic access (MDA) mechanism is introduced in IEEE 802.11s that allows access for a certain period with lower contention than other periods without using MDA. IEEE 802.11s is based on an exchange of congestion information of nodes in the neighborhood in order to resolve congestion in the network [62]. Unfortunately, the IEEE 802.11s standard has not been finalized yet and experiments with real 802.11s deployments show that multi-hop networks carry the aggregation of locally generated and forwarded traffic and are threatened with saturation, which is a problem to be solved on the medium access side [60].

In this dissertation, we have chosen DCF as the MAC protocol in multi-hop wireless networks for the investigation of the effects of MAC layer on energy and goodput performance. Although MCF is the medium access control protocol for the mesh networking standard IEEE 802.11s, the immaturity of the standard and the unavailability of technical documents during the period that this study has been conducted prohibited an analysis based on MCF. Moreover, DCF is the basic medium access control protocol used by the widespread IEEE 802.11 legacy and IEEE 802.11a\b\g\n technologies, and is also the basis of EDCA and MCF.

Recently, there has been great interest on evaluating the performance of IEEE 802.11 DCF in multi-hop wireless networks. IEEE 802.11 DCF defines a MAC protocol for wireless local area networks that solves the hidden terminal problem in wireless local area networks where single-hop communications take place. By the incorporation of ad-hoc systems in future forth generation wireless systems, the IEEE 802.11 standard is adopted as the de-facto MAC standard in multi-hop wireless networks and understanding the performance of the standard in multi-hop wireless networks has gained importance [63]. The IEEE 802.11 DCF

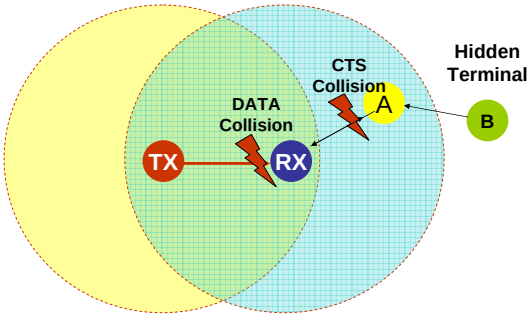

Figure 3.1: DATA packet collision due to hidden terminal problem in a multi-hop wireless network.

performance changes when switching from local area network to multi-hop wireless network environment in three major aspects: i) paths in multi-hop networks are multi-hop whereas they are single-hop in local area networks, ii) traffic handled by each node is the node's own traffic and the relay traffic, iii) the behavior of each node depends not only on the nodes in the carrier sensing range but also on hidden nodes that are placed outside the carrier sensing range (so that collisions occur also due to hidden terminals).

In multi-hop wireless networks RTS/CTS handshake mechanism is not enough to solve the hidden terminal problem. As illustrated in Fig. 3.1, the DATA frame of a transmission from the transmitter tx to the receiver rx collides, if there exists a hidden terminal B, which is hidden from node rx and sends to node A during the transmission of CTS frame sent by rx. In this hidden terminal topology, node A doe not receive the CTS frame successfully and may transmit something during the DATA frame of the $tx \rightarrow rx$ transmission. If there were no hidden terminals, then RTS/CTS mechanism would avoid DATA collisions completely, but with hidden terminals the colliding RTS and CTS frames at nodes can not avoid DATA collisions.

There are several simulation based studies in the literature investigating the performance of IEEE 802.11 DCF multi-hop wireless networks [63, 64]. Simulation based studies are useful in obtaining some knowledge of the complicated

behavior of IEEE 802.11 DCF in multi-hop wireless networks, however analytical models are more effective in providing an insight on the functionality of the protocol. As the network scenarios, traffic patterns and physical layer techniques change, simulations alone become inefficient to get insights into the impacts of MAC protocols on system performance. An analytical model of IEEE 802.11 DCF gives the opportunity to examine the impact of various physical layer parameters (such as data rate, contention window size, packet size, etc.), network layer parameters (routing strategy, connectivity, etc.), transport layer parameters (traffic pattern, congestion window, etc.) on the IEEE 802.11 DCF layer and on the performance metrics such as the throughput and energy-efficiency.

In order to achieve an energy consumption or goodput analysis in multi-hop networks with IEEE 802.11 DCF, an analytical model describing the performance of IEEE 802.11 DCF in multi-hop networks is required. Existing models are limited to either unsaturated or saturated traffic conditions, omit important aspects of multi-hop networks and work for small topologies. Hence, an analytical model for IEEE 802.11 DCF in multi-hop networks is developed in this chapter, which is the primary contribution of this dissertation. The analytical model for IEEE 802.11 DCF based multi-hop wireless networks:

- considers hidden terminals,
- provides fairly accurate results for large range of traffic loads,
- works for any given two-dimensional topology,
- increases the accuracy and scalability of the analytical model by joint use of fixed and variable slots
- allows each node to be both source and/or relay.

A semi-Markov chain (SMC) based model for the behavior of a IEEE 802.11 DCF node in a multi-hop wireless network is proposed, since SMC models are shown

to predict the DCF behavior better than discrete-time Markov chain (DTMC) models [7,65]. In the analysis of IEEE 802.11 DCF, the collision probability and network allocation vector (NAV) setting probabilities together with the probabilities governing the SMC are obtained first. Several MAC layer parameters (instead of fitting a probability distribution to them) are calculated, some of which can be counted as follows: i) the first and second moments of the service time, ii) the probability of packet drops due to retry count, iii) the probability of packet drops due to exceeding the buffers at the interface queues, iv) relay traffic at each node, v) the expected NAV durations.

Several approaches that differ our solution methodology from that of the literature are: i) joint usage of variable and fixed length slots for discretizing time, ii) redefinition of channel state probabilities as NAV setting probabilities. The major approaches of the proposed analytical model and how it improves the assumptions and limitations of previous models are discussed in detail in Sec. 3.3.

After an introduction to IEEE 802.11 DCF function, a literature review of existing analytical models for IEEE 802.11 DCF are given in the next two sections. The major attributes of the proposed DCF model are given in Sec. 3.3. In Sec. 3.4, we present the analytical model for the IEEE 802.11 DCF in multi-hop wireless networks, which is used by the following two chapters for analyzing the energy consumption and goodput of various routing strategies. The underlying assumptions of the analytical IEEE 802.11 DCF model, the basics of the model, information regarding states and state transitions of the SMC, state residence times, geometry related notations, calculation of NAV setting probabilities and the probability of collision are given in this section. Finally, analytical model results are compared with simulation results in Sec. 3.5 under various PHY and MAC parameters.

3.1 Distributed Coordination Function

In this section, the basic features of DCF are presented and for a more thorough description the reader is refered to [2]. DCF is the fundamental MAC technique of the IEEE 802.11 wireless LAN standard. DCF employs a distributed CSMA/CA algorithm with either basic access or with an optional RTS/CTS control mechanism. In DCF, before attempting a transmission the station ensures that the channel is idle by listening the channel and initiating backoff procedures accordingly. Exponential backoff procedure adopted by DCF includes uniform random selection of counter value in the interval $(0, 2^b W_0 - 1)$, where b is the backoff stage and W_0 is the minimum contention window. The backoff stage is doubled after every failed transmission and reset to 0 after a successful transmission. The backoff counter is decremented as long as the channel is idle and frozen if it is busy, and reactivated if it is idle again. Each decrement of backoff counter lasts for σ duration which is the SlotTime defined in [2].

RTS/CTS exchange mechanism involves exchange of Request-to-Send (RTS) and Clear-to-Send (CTS) frames prior to sending the DATA packet. An RTS frame and a corresponding CTS reply, that are frames shorter than the DATA packet, inform neighbors of the DATA packet length. Thus, stations overhearing RTS/CTS transmissions defer their transmission for the duration of the data packet by setting their network allocation vector (NAV).

In single-hop networks, RTS/CTS exchange diminishes the hidden terminal problem and collisions occur only if two RTS frames collide, so that collision of DATA packets in basic access is replaced by the shorter RTS frame collisions. In a multi-hop network, RTS/CTS exchange does not eliminate the hidden terminal problem totally but is still more effective in terms of system performance compared to basic access owing to shorter collision durations.

3.2 IEEE 802.11 DCF Models

There are various studies conducted for modelling IEEE 802.11 DCF in single-hop networks [7,66–71]. Bianchi proposed a two-dimensional Markov chain (MC) to analyze the performance of the DCF function of the IEEE 802.11 protocol in single-hop saturated networks [7]. This model is extended in [66] to incorporate the unsaturated traffic conditions by the addition of W_0 extra backoff states [8, 66, 72]. Unsaturated networks, are considered in [67] by adding a single state instead of W_0 states, corresponding to the case that the node has no packets to send. The MC in this work becomes 3-dimensional by the addition of the queue size. Although this study is claimed to include multi-hop networks, the analysis is validated through simulation for single-hop networks. In this study, each node is allowed to be either relay or source.

Despite various studies conducted for modelling IEEE 802.11 DCF in single-hop networks [7, 66–71], there are few analytical modelling efforts for multi-hop networks [8, 72–74]. Owing to the comparable complexity increase when switching from single-hop to multi-hop network architecture, the existing analytical models are based on simplified assumptions that do not reflect the realistic dynamics of the IEEE 802.11 DCF system. Authors in [72] give an analytical model for multi-hop wireless networks for unsaturated traffic loads ignoring the hidden terminals and assuming that each node is either relay or source. The hidden terminal problem is eliminated in the analysis in [8] by the assumption of RTS/CTS mode with busy-tone, where unsaturated traffic load is assumed. The analysis in [67] also ignores the existence of hidden terminals and moreover assumes that each node is either relay or source. The hidden terminal problem is included in the analysis of IEEE 802.11 DCF for a 3-node network in [73] and for string topologies of variable sizes in [74]. These two articles point out important aspects of modelling in multi-hop networks. [73] points out that prior modelling of IEEE 802.11 DCF, based on variable length slot notion, may be misleading and

fixed length slots should be used instead. Also the channel state probabilities used by modelling single-hop networks is replaced by probabilities of freezing the backoff counter. The analysis in [73] is made by assuming a constant contention window size as opposed to the binary exponential backoff where the window size is doubled by each failure. The authors in [74] pointed out the existence of an optimum offered load for maximizing the throughput. The analytical model in [73] works for only a 3-node topology and the analytical model in [74] works for string topologies. An analytical model of the IEEE 802.11 DCF that considers hidden terminals, gives each node the joint functionality of being a source and relay, works for various traffic loads in various multi-hop topologies does not exist in the literature to the best of our knowledge.

3.3 Major Attributes of the Proposed IEEE 802.11 DCF Model

Owing to the fact that the existing analytical models of IEEE 802.11 DCF systems are inadequate for an energy-efficiency analysis in multi-hop wireless networks, an analytical model for IEEE 802.11 DCF for multi-hop wireless networks is developed in this dissertation. The major attributes of the proposed DCF model together with the limitations and assumptions of the previous DCF models are described in this section.

3.3.1 Semi-Markov chain

Analytical models in [7, 8, 66–73] are based on a Markov chain that is used for the calculation of probability of transmission. We want to emphasize that the chain is not Markov as stated in these studies, instead it is semi-Markov due to the state dependent residence times and the steady state solution of a SMC is

obtained by weighting the discrete time MC with average residence times [75]. The probability of transmission in these studies is calculated by the solution of the relevant discrete time Markov chain, because there exists a probability of transmission at the beginning of each variable length slot and diminishes to zero for the rest of the slot. The analytical IEEE 802.11 DCF model proposed in this dissertation is built on top of a SMC that models the behavior of a single IEEE 802.11 based node in a multi-hop network.

3.3.2 Joint use of fixed and variable slots

Most of the IEEE 802.11 DCF models are based on discretizing time into variable length slots, where a slot is either the constant $SlotTime$, or the variable time interval between two consecutive backoff counter decrements [2]. A limitation stemming from variable slot length is mentioned in [73] and it is pointed out that there might not be as many backoff slots as are implied by equations set for the channel states, and it is shown that the error in finding throughput for various physical layer parameters grows for smaller contention window size, larger packet sizes and lower data rates. Thus, a model that views the channel time as a succession of fixed length slots of $SlotTime$ proposed in [73]. In this work, the duration of time where NAV is set is discretized into fixed length slots only, whereas the duration of sending a successful transmission or a collision is not divided into fixed slots of length $SlotTime$.

The major drawback of using fixed length slots in the analysis is the increase in number of states in the Markov chain used to model the behavior of IEEE 802.11 DCF node, so that the analysis becomes not tractable. The analysis in [73] is based on the assumption of constant contention window (CCW) instead of binary exponential backoff, in order to limit the number of states in the Markov chain. But the CCW assumption hinders the dynamics of the IEEE 802.11 DCF and the results obtained do not reflect the exact operation of DCF.

In this dissertation, a solution methodology different from the literature is developed where a joint usage of fixed and variable length slots is adopted. The SMC is developed and solved based on variable slot notion, whereas MAC parameters such as collision probability and NAV setting probabilities are developed based on fixed length slot notion. Variable length slot notion ensures that the number of states of the SMC is kept relatively small, so that BEB is included in the analysis, reflecting the real dynamics of the IEEE 802.11 DCF. On the other hand, the fixed slot notion used in developing MAC parameters ensures that our analysis is not prone to the errors pointed out by [73]. This way, the weaknesses of variable slot length analysis are eliminated, while keeping the SMC state size small enough to be computationally efficient even with BEB.

3.3.3 From channel state probability towards NAV setting probability

In studies modelling IEEE 802.11 DCF in single-hop and multi-hop networks [7,8,66–72], the successful, collision and idle channel is denoted by channel state probabilities. However this representation is not appropriate for multi-hop networks, because the channel state perceived by a node may not be the actual state of the channel when hidden nodes exist. For example, two concurrent successful transmissions in the channel of a node are perceived as a collision. Also, a node perceives a successful channel if it successfully receives an RTS or CTS frame that collides at the relevant receivers. In [73], instead of distinguishing among channel states the probability of freezing/not freezing the backoff counter is used. But NAV duration takes only one value and leads to insufficient accuracy in large multi-hop networks. We observed that a discrimination among NAV durations is necessary and the duration of NAV varies if it contains at least one DATA transmission. We switch from channel state probability notion to NAV

setting probability notion and discriminate between events that set the NAV for long and short durations.

3.3.4 Large range of traffic loads

The existing analytical models for IEEE 802.11 DCF for both single-hop and multi-hop networks work under either unsaturated [8, 72, 76] or saturated [7, 65, 67, 73, 74] traffic loads. By saturated traffic load we mean the condition where there is always one packet waiting in the queue upon finishing processing of the last packet. Among the studies for multi-hop networks, the analytical models in [8, 72] are limited to unsaturated traffic loads whereas the analytical models in [73,74] are limited to saturated traffic loads. In this dissertation, we develop an analytical model for multi-hop networks that operates in any traffic load ranging from light to heavy traffic conditions.

3.3.5 Any given topology and traffic pattern

Unlike previous studies that have focused on analyzing IEEE 802.11 behavior by considering hidden terminals in multi-hop networks under assumptions of specific network (e.g., [73, 74]), the proposed model accurately works for various network topologies and traffic patterns considered in this study.

3.3.6 Not only RTS collisions

Existence of hidden terminals in multi-hop networks results in collisions other than collision of RTS frames. An RTS or CTS frame that is not received correctly by neighbors inside the carrier sensing range may cause collision of other types of frames. In the analysis carried out in this dissertation, collisions of RTS, CTS,

DATA or ACK frames with each other are also considered in the calculation of the probability of collision.

3.4 IEEE 802.11 DCF Model for Multi-Hop Wireless Networks

Basics of the proposed IEEE 802.11 DCF model is introduced in this section after an overview of assumptions. The states of the SMC and calculation of the state residence times are explained next. Geometry related notations, NAV setting probabilities and collision probability are described next.

3.4.1 Assumptions

Several simplifying assumptions also made by several previous studies [7, 8, 65, 67, 73, 74, 76] are adapted in order to provide an analytically tractable solution to the problem: 1) unified disk radio model, 2) Poisson offered traffic, 3) bit error-free channel, 4) stationary nodes. The unified disk graph model states that a communication is successful if and only if no simultaneous transmissions exist within a certain interference range from the receiver. This channel model is used since it is simple and generally used to model the behavior of CSMA/CA networks such as IEEE 802.11.

No assumption is imposed neither on the topology nor on the traffic pattern. But, we assume that the topology information regarding the placement of nodes and the traffic pattern, i.e. the source destination pairs and the average traffic on each route, are available. In order to be able to compare the energy-efficiency of routing strategies, a comparison is conducted using the same topology and traffic pattern where all nodes in the network are assumed to adapt the same

routing strategy: each generated packet traverses a path of h hops. Thus, source destination pairs are selected so that a reasonable h-hop path exists. Nodes are assumed to conduct power control with infinitely variable levels and transmit with the minimum required power to reach the next hop. The receiving range is assumed to be equal to the carrier sensing range and the interference range. The receiving range is the maximum distance from the source at which a packet can be successfully received, whereas the carrier sensing range is the maximum distance from the emitter at which a transmission is detected and the interference range is the maximum distance from a receiver where nodes cause interference. The capture effect is neglected in this study, where we assume that two packets received at the same time always collide.

Each node is assumed to use the IEEE 802.11 DCF in conjunction with the RTS/CTS exchange as the MAC protocol. Although the RTS/CTS handshake mechanism introduces an overhead, it is shown to improve IEEE 802.11 performance in multi-hop wireless networks when hidden nodes are present [77]. In case of a collision, packets are retransmitted according to BEB until the maximum retry count (M) is reached. At each transmission attempt of a node, regardless of the number of retransmissions, each packet collides with a conditional probability p, conditioned on the fact that the particular node is attempting a transmission. Packets are dropped after M unsuccessful retries with probability p^M or due to overflow of the finite sized interface queue (IFQ), that reside between MAC and physical layers, with probability $P_{ifq}(i)$ at each node i for $1 \leq i \leq N$, where N is the total number of nodes in the wireless network. $P_{ifq}(i)$ is calculated in Sec. A assuming an $M/G/1/K$ interface queue with buffer size of K, including the packet in service. In our model, a single value is used for p which corresponds to the average conditional collision probability taken over all links, whereas $P_{ifq}(i)$ is different for each node.

3.4.2 Basics of IEEE 802.11 DCF model

The IEEE 802.11 DCF behavior of a node is modelled by the SMC given in Fig. 3.2, which captures both the transmit and the receive states of the node. The state diagram is Markov since the future state of the node given the present state is independent of the past state; and it is semi-Markov due to state dependent residence times [75]. The SMC is two-dimensional, where the first dimension is the backoff stage and the second is the backoff counter value. Backoff states of the SMC are represented by the notation (b, k), where b is the backoff stage and k is the backoff counter value. The maximum backoff stage is limited by M and the maximum counter value is limited by B.

The maximum backoff counter value at stage b is W_b where,

$$W_b = \begin{cases} W_0, & b = 0' \\ 2^b W_0, & 0 \leq b < B \\ 2^B W_0, & B \leq b < M. \end{cases} \tag{3.1}$$

$b = 0'$ corresponds to the backoff stage when the IFQ is empty. The backoff states at which the backoff counter is frozen are represented by $(b, k)^S$ and $(b, k)^C$, for $k \neq 0$, where NAV is set for a long and short duration, respectively.

The backoff states at which backoff counter is frozen is represented by the notation $(b, k)^S$ and $(b, k)^C$, for $k \neq 0$, in case of perception of a successful channel or collision channel respectively. The successful transmitting states are the $(b, 0)^S$ states, and the transmit collision states are the $(b, 0)^C$ states.

The SMC models not only saturated but also unsaturated traffic conditions. The unsaturated traffic conditions are incorporated by the $IDLE$, $IDLE^S$ and $IDLE^C$ states and the backoff states $(0', k)$, for $1 \leq k < W_0$, which correspond to states entered just after a successful transmission or after a packet is dropped due to M, in case there is no packet in the queue. The $IDLE$ state represents the state in which the node has no packet to transmit and the backoff counter

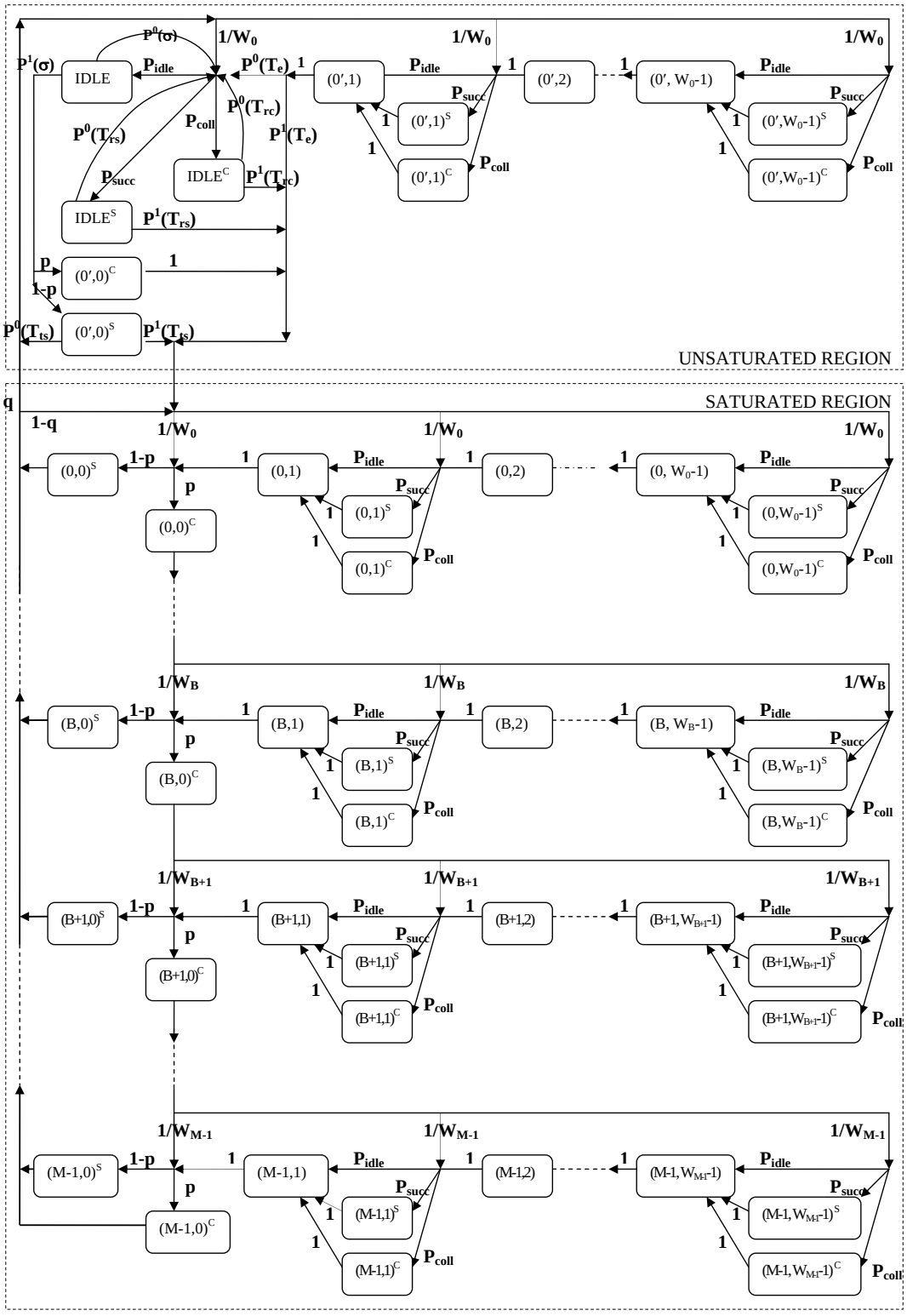

Figure 3.2: SMC model for a IEEE 802.11 DCF based node

value is zero. The node has three options in such condition: it perceives the

channel as idle ($IDLE$), or it sets its NAV due to perception of a successful channel ($IDLE^S$), or sets its NAV due to a collision channel ($IDLE^C$).

$(0', 0)^S$ represents the first successful transmission and $(0', 0)^C$ represents the first collision of a packet after $IDLE$ state. $(b, 0)^S$ and $(b, 0)^C$, for $0 \leq b < M$ represent the states where a successful transmission and collision occurs respectively.

The states of the SMC are grouped in five categories according to state residence times as follows:

1. Idle States: The $IDLE$ state where the node is idle waiting in unsaturated region and the backoff states (b, k), for $b \in \{0', [0, M)\}$ and $k \in [1, W_b)$, are called as *idle states*. The state residence time of idle states is denoted by σ, which is also equal to a $SlotTime$.

2. Transmit Success States: These are the states $(b, 0)^S$ for $b \in \{0', [0, M)\}$ with state residence time T_{ts}, where a successful transmission occurs.

3. Transmit Collision States: These are the states $(b, 0)^C$ for $b \in \{0', [0, M)\}$ with state residence time T_{tc}, where a collision occurs.

4. Receive Success States: These are the states $IDLE^S$ and $(b, k)^S$ for $b \in \{0', [0, M)\}$ and $k \in [1, W_b)$ with state residence time T_{rs}, where the NAV is set and the backoff counter is frozen for at least one DATA reception duration.

5. Receive Collision States: These are the states $IDLE^C$ and $(b, k)^C$ for $b \in \{0', [0, M)\}$ and $k \in [1, W_b)$ with residence time T_{rc}, where NAV is set and contains no DATA reception.

The steady state probabilities of being in idle, transmit success, transmit collision, receive success and receive collision state categories are represented by π_{idle},

π_{ts}, π_{tc}, π_{rs} and π_{rc}, respectively, and are calculated by summing up the steady state probabilities of all the states in the corresponding category. A detailed description of states and state transition probabilities of the SMC given in Fig. 3.2 are presented in the next section.

T_e is the average time spent during the backoff stages $(0', k)$ for $k \in [1, W_0)$ and is calculated by $T_e = \frac{W_0\bar{\sigma}}{2}$, where $\bar{\sigma}$ is the average NAV duration given by

$$\bar{\sigma} = P_{succ}(T_{rs} + \sigma) + P_{coll}(T_{rc} + \sigma) + P_{idle}\sigma. \tag{3.2}$$

The average slot duration is denoted by $\bar{\sigma_n}$ and is given by

$$\bar{\sigma_n} = \tau p T_{tc} + \tau(1-p)T_{ts} + p_{cs}\bar{\sigma}, \tag{3.3}$$

where p_{cs} is the probability that a node does carrier sensing with zero NAV and is calculated by summing up the idle states of the discrete time Markov Chain.

The channel state probability notion introduced in analytical modelling of DCF for single-hop networks is transformed here into NAV setting probability notion for multi-hop networks due to existence of hidden terminals. The decision on setting NAV is given at certain instants of time as shown in Fig. 3.3, corresponding to time instants when the node does carrier sensing and the NAV is zero. Thus NAV setting probabilities are conditioned on the fact that the node does carrier sensing with zero NAV. Three NAV setting probabilities are defined: i) P_{idle} is the probability that NAV is not set, ii) P_{succ} is the probability that NAV is set for a long duration that contains at least one DATA reception and iii) P_{coll} is the probability that NAV is set for a short duration that does not contain any DATA reception.

The probability of transmission, τ, introduced by [7] and adopted by further studies, is calculated by summation of steady state probabilities of the transmit success and the transmit collision states of the discrete time Markov chain (DTMC) describing the behavior of a IEEE 802.11 node. τ is found by assuming equal residence time for the MC given in Fig. 3.2, which corresponds to the

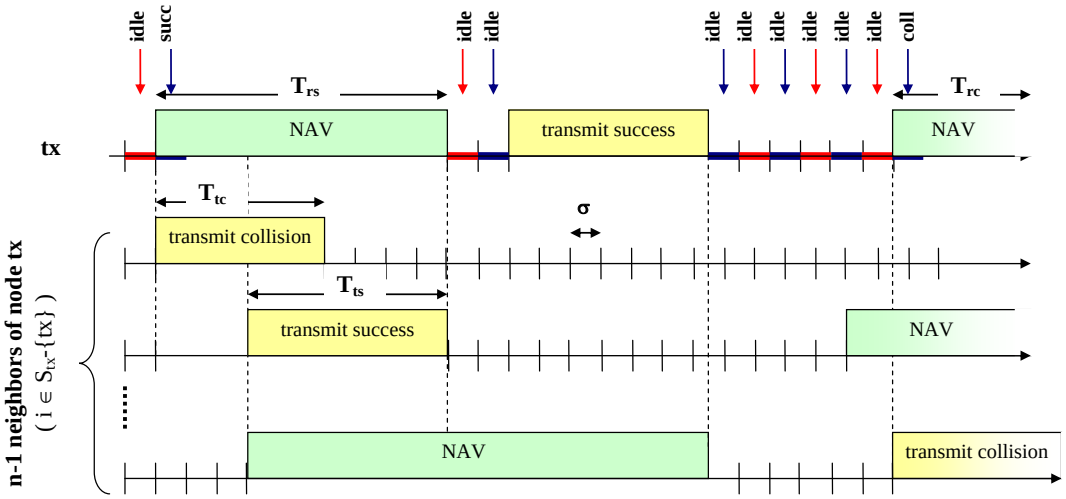

Figure 3.3: Time instants at which NAV setting probabilities P_{idle}, P_{succ} and P_{coll} are calculated

solution of the DTMC, because transmission probability is nonzero for the first σ duration of a transmission state and is zero for the rest of the residence time. Denoting the steady state probabilities of the DTMC by π^{DTMC}, τ becomes

$$\tau = \sum_{b \in \{0', [0,M)\}} (\pi^{DTMC}_{(b,0)^S} + \pi^{DTMC}_{(b,0)^C}). \tag{3.4}$$

In fact, the MC given in Fig. 3.2 is semi-Markov but τ is obtained by the solution of the DTMC since the probability of transmission is nonzero for only the first σ portion of state residence times. Note that, the summation of the steady state probabilities of the transmit states of the DTMC gives the *probability of transmission* whereas the same summation for the SMC gives the *probability that a node is transmitting*.

The conditional collision probability p is different for each link, since the links in the network are not homogeneous. This leads to a computationally untractable analytical model, where each link should be modelled by a separate SMC and SMC's as many as links is to be solved in parallel at each round of fixed point iterations. In order to simplify the analysis, an average p is found which is averaged over all links weighted by the traffic carried over each link. Extensive simulations conducted with various topologies and traffic patterns demonstrate that finding an average p in the analysis results with reasonable errors while maintaining

tractable computations for regular topologies, whereas the error increases with the irregularity of the topology and traffic pattern.

The packet arrivals to IFQ at a node follow the Poisson process with average rate λ_t. Packets are served using the first in first out discipline by a single server. The service time is a non-negative random variable denoted by random variable T_S, which has a discrete probability of $Pr(T_S = t_s(i))$ for T_S being $t_s(i)$, expressed as:

$$\begin{aligned} \Pr\{T_S = t_s(i)\} &= \begin{cases} (1-p)p^i & \text{if } 0 \le i < M \\ p^M & \text{if } i = M \end{cases} \\ t_s(i) &= \begin{cases} T_{ts} + iT_{tc} + \sum_j^{i+1} W_j \frac{\bar{\sigma}}{2} & \text{if } 0 \le i < M \\ MT_{tc} + \sum_j^{M} W_j \frac{\bar{\sigma}}{2} & \text{if } i = M. \end{cases} \end{aligned} \tag{3.5}$$

Thus, IFQ can be modelled as an M/G/1/K queue where K represents the maximum number of packets in the queue, and can be solved by the techniques in [78]. P_{ifq} corresponds to the steady-state probability of K packets in the queueing system, whereas q corresponds to the probability that the node's buffer is empty after the node finishes processing a packet in backoff. The calculation of P_{ifq} and q is given in Appendix A.

Between each node pair (i, j) in the network there is a generated Poisson traffic with rate $\lambda_o(i, j)$. The total traffic at node i is $\lambda_t(i)$ given by

$$\lambda_t(i) = \lambda_o(i) + \lambda_r(i), \tag{3.6}$$

where $\lambda_o(i)$ is the average traffic generated by node i given by

$$\lambda_o(i) = \sum_j \lambda_o(i, j),$$

and $\lambda_r(i)$ is the total relay traffic. Let P_{kl} be the sequence of nodes traversed by the path between nodes k and l. For $i \in P_{kl}$, define the set Q_{kli} as the set of nodes on path P_{kl} that precede node i. $\lambda_r(i)$ is calculated by summing up all the relay traffic crossing node i:

$$\lambda_r(i) = \sum_{k,l \neq i : i \in P_{kl}} \lambda_o(k, l)(1 - p^M)^{|Q_{kli}|} \prod_{j \in Q_{kli}} (1 - P_{ifq}(j)). \tag{3.7}$$

The relay traffic is not Poisson because of packet drops at the IFQ and at the intermediate nodes due to the retry limit. In order to simplify the analysis, we assume that the relay traffic is Poisson and hence the overall traffic arriving at a node is Poisson with rate $\lambda_t(i)$. Hence, the probability of receiving no packets in a duration of t, denoted by $P^0(t)$, and the probability of receiving one or more packets during t, denoted by $P^1(t)$, become as follows:

$$P^0(t) = e^{-\lambda t}, \tag{3.8}$$

$$P^1(t) = 1 - e^{-\lambda t}. \tag{3.9}$$

The analytic model is solved through fixed point iterations, since no closed form solution exists. The convergence of the fixed point iterations is not investigated and left as a future work, but for all the scenarios that we studied, the fixed point iterations always converged.

3.4.3 State categories and state transitions

The states of the SMC are grouped in five categories according to state residence times. For ease of understanding each of the above categories are described separately together with the state transition probabilities from each, where the transition probability from state a to state b is denoted by $P_{a \to b}$:

Idle states:

The $IDLE$ state where the node is idle waiting in unsaturated region and the backoff states (b, k) and $(0', k)$, for $1 \leq k < W_0$ and $0 \leq b < M$, are called as *idle states*. The state residence time of idle states is denoted by σ, which is also equal to a *SlotTime* defined in [2].

The backoff counter is decremented if the channel is idle or frozen with probability P_{succ} or P_{coll} corresponding to the following state transitions for $2 \leq k < W_0$:

$$\begin{aligned}
P_{(b,k)\rightarrow(b,k-1)} &= P_{idle}, \\
P_{(b,k)\rightarrow(b,k-1)^S} &= P_{succ}, \\
P_{(b,k)\rightarrow(b,k-1)^C} &= P_{coll}, \\
P_{(0',k)\rightarrow(0',k-1)} &= P_{idle}, \\
P_{(0',k)\rightarrow(0',k-1)^S} &= P_{succ}, \\
P_{(0',k)\rightarrow(0',k-1)^C} &= P_{coll}.
\end{aligned} \tag{3.10}$$

Upon expiration of the backoff counter in unsaturated region, a node with empty queue enters the $IDLE$, $IDLE^S$ and $IDLE^C$ states. If a new packet arrives during time spent in the backoff procedure, the node enters the $(0, k)$ backoff states in order to transmit the newly arrived packet. The average time spent during the unsaturated backoff stages $(0', k)$ is denoted by T_e and the probabilities of receiving no packets ($P^0(T_e)$) or more than one packets ($P^1(T_e)$) during T_e determine the state transitions. The transitions from the $(0', 1)$ are as follows for $0 \leq k < W_0$:

$$\begin{aligned}
P_{(0',1)\rightarrow IDLE} &= P^0(T_e)P_{idle}, \\
P_{(0',1)\rightarrow IDLE^S} &= P^0(T_e)P_{succ}, \\
P_{(0',1)\rightarrow IDLE^C} &= P^0(T_e)P_{coll}, \\
P_{(0',1)\rightarrow(0,k)} &= P^1(T_e)P_{idle}/W_0, \\
P_{(0',1)\rightarrow(0,k)^S} &= P^1(T_e)P_{succ}/W_0, \\
P_{(0',1)\rightarrow(0,k)^C} &= P^1(T_e)P_{coll}/W_0, \\
P_{(0',1)\rightarrow(0,0)^S} &= P^1(T_e)(1-p)/W_0, \\
P_{(0',1)\rightarrow(0,0)^C} &= P^1(T_e)p/W_0.
\end{aligned} \tag{3.11}$$

T_e is calculated by multiplying the average NAV duration, $\bar{\sigma}$, with the average number of stages $\frac{W_0}{2}$:

$$\begin{aligned} &P^0(T_e) = e^{-\lambda T_e}, \\ &P^1(T_e) = 1 - e^{-\lambda T_e}, \\ &T_e = \tfrac{W_0 \bar{\sigma}}{2}, \\ &\bar{\sigma} = P_{succ}(T_{rs} + \sigma) + P_{coll}(T_{rc} + \sigma) + P_{idle}\sigma. \end{aligned} \tag{3.12}$$

A node with no packet in the queue resides in the $IDLE$ state as long as the channel is idle, visits $IDLE^S$ or $IDLE^C$ states upon setting of NAV due to a successful or collision channel. If a packet is received then the transmit states $(0', 0)^S$ or $(0', 0)^C$ are visited. Hence, the transitions form the $IDLE$ state are as follows:

$$\begin{aligned} &P_{IDLE \to IDLE} = P^0(\sigma) P_{idle}, \\ &P_{IDLE \to IDLE^S} = P^0(\sigma) P_{succ}, \\ &P_{IDLE \to IDLE^C} = P^0(\sigma) P_{coll}, \\ &P_{IDLE \to (0',0)^S} = P^1(\sigma)(1-p), \\ &P_{IDLE \to (0',0)^C} = P^1(\sigma) p. \end{aligned} \tag{3.13}$$

Transmit success states:

These are the states $(0', 0)^S$ and $(b, 0)^S$ for $0 \leq b < M$ with state residence time is T_{ts}, where a successful transmission occurs. After each successful transmission, the backoff contention window is reset to W_0 and backoff is initiated [2]. If the queue is empty upon the successful transmit, then the unsaturated backoff states, $(0', k)$, or $IDLE, IDLE^S, IDLE^C$ states are visited. If there is a waiting packet in IFQ, then the saturated region backoff states, $(0, 0)^S$ or $(0, 0)^C$ are visited. The transitions from the transmit success states $(0', 0)^S$ for $1 \leq k < W_0$ are

given by:

$$
\begin{aligned}
P_{(0',0)^S \to (0,k)} &= P^1(T_{ts}) P_{idle}/W_0, \\
P_{(0',0)^S \to (0,k)^S} &= P^1(T_{ts}) P_{succ}/W_0, \\
P_{(0',0)^S \to (0,k)^C} &= P^1(T_{ts}) P_{coll}/W_0, \\
P_{(0',0)^S \to (0',k)} &= P^0(T_{ts}) P_{idle}/W_0, \\
P_{(0',0)^S \to (0',k)^S} &= P^0(T_{ts}) P_{succ}/W_0, \\
P_{(0',0)^S \to (0',k)^C} &= P^0(T_{ts}) P_{coll}/W_0, \\
P_{(0',0)^S \to IDLE} &= P^0(T_{ts}) P_{idle}/W_0, \\
P_{(0',0)^S \to IDLE^S} &= P^0(T_{ts}) P_{succ}/W_0, \\
P_{(0',0)^S \to IDLE^C} &= P^0(T_{ts}) P_{coll}/W_0.
\end{aligned}
\tag{3.14}
$$

The transitions from the transmit success states $(b,0)^S$, for $0 \leq b < M$ and $1 \leq k < W_0$, are as follows:

$$
\begin{aligned}
P_{(b,0)^S \to (0,k)} &= (1-q) P_{idle}/W_0, \\
P_{(b,0)^S \to (0,k)^S} &= (1-q) P_{succ}/W_0, \\
P_{(b,0)^S \to (0,k)^C} &= (1-q) P_{coll}/W_0, \\
P_{(b,0)^S \to (0',k)} &= q P_{idle}/W_0, \\
P_{(b,0)^S \to (0',k)^S} &= q P_{succ}/W_0, \\
P_{(b,0)^S \to (0',k)^C} &= q P_{coll}/W_0, \\
P_{(b,0)^S \to IDLE} &= q P_{idle}/W_0, \\
P_{(b,0)^S \to IDLE^S} &= q P_{succ}/W_0, \\
P_{(b,0)^S \to IDLE^C} &= q P_{coll}/W_0, \qquad .
\end{aligned}
\tag{3.15}
$$

Transmit collision states:

These are the states $(b,0)^C$ and $(0',0)^C$ for $0 \leq b < M$ with state residence time is T_{tc}, where a failed transmission occurs. After each collision, the back-off contention window is doubled if maximum retry count is not exceeded, else contention window is reset to W_0 and the packet dropped. Thus, the transitions

from the transmit collision states $(0',0)^C$ for $1 \leq k < W_0$ are as follows:

$$\begin{aligned}
P_{(0',0)^C \to (0,k)} &= P_{idle}/W_0, \\
P_{(0',0)^C \to (0,k)^S} &= P_{succ}/W_0, \\
P_{(0',0)^C \to (0,k)^C} &= P_{coll}/W_0, \\
P_{(0',0)^C \to (0,0)^S} &= (1-p)/W_0, \\
P_{(0',0)^C \to (0,0)^C} &= p/W_0.
\end{aligned} \tag{3.16}$$

The transitions from the transmit collision states $(b,0)^C$, for $0 \leq b < M-1$ and $1 \leq k < W_0$, are given by:

$$\begin{aligned}
P_{(b,0)^C \to (b+1,k)} &= P_{idle}/W_0, \\
P_{(b,0)^C \to (b+1,k)^S} &= P_{succ}/W_0, \\
P_{(b,0)^C \to (b+1,k)^C} &= P_{coll}/W_0, \\
P_{(b,0)^C \to (b+1,0)^S} &= (1-p)/W_0, \\
P_{(b,0)^C \to (b+1,0)^C} &= p/W_0.
\end{aligned} \tag{3.17}$$

The transitions from the transmit collision state $(M-1,0)^C$, where the maximum retry count is reached, for $1 \leq k < W_0$ are expressed as:

$$\begin{aligned}
P_{(M-1,0)^C \to (0,k)} &= (1-q)P_{idle}/W_0, \\
P_{(M-1,0)^C \to (0,k)^S} &= (1-q)P_{succ}/W_0, \\
P_{(M-1,0)^C \to (0,k)^C} &= (1-q)P_{coll}/W_0, \\
P_{(M-1,0)^C \to (0,0)^S} &= (1-q)(1-p)/W_0, \\
P_{(M-1,0)^C \to (0,0)^C} &= (1-q)p/W_0, \\
P_{(M-1,0)^C \to (0',k)} &= qP_{idle}/W_0, \\
P_{(M-1,0)^C \to (0',k)^S} &= qP_{succ}/W_0, \\
P_{(M-1,0)^C \to (0',k)^C} &= qP_{coll}/W_0, \\
P_{(M-1,0)^C \to IDLE} &= qP_{idle}/W_0, \\
P_{(M-1,0)^C \to IDLE^S} &= qP_{succ}/W_0, \\
P_{(M-1,0)^C \to IDLE^C} &= qP_{coll}/W_0.
\end{aligned} \tag{3.18}$$

Receive success states:

These are the states $IDLE^S$, $(b,k)^S$ and $(0',k)^S$ for $1 \leq k < W_0$ and $0 \leq b < M$, where the NAV is set for at least one DATA transmission duration. The state residence time is T_{rs}. Transitions from the receive success states are as follows for $0 \leq b < M$ and $1 \leq k < W_0$:

$$\begin{aligned}
&P_{(0',k)^S \to (0',k)} = 1, \\
&P_{(b,k)^S \to (b,k)} = 1, \\
&P_{IDLE^S \to (0,k)} = P^1(T_{rs}) P_{idle}/W_0, \\
&P_{IDLE^S \to (0,k)^S} = P^1(T_{rs}) P_{succ}/W_0, \\
&P_{IDLE^S \to (0,k)^C} = P^1(T_{rs}) P_{coll}/W_0, \\
&P_{IDLE^S \to (0,0)^S} = P^1(T_{rs})(1-p)/W_0, \\
&P_{IDLE^S \to (0,0)^C} = P^1(T_{rs}) p/W_0, \\
&P_{IDLE^S \to IDLE} = P^0(T_{rs}) P_{idle}, \\
&P_{IDLE^S \to IDLE^S} = P^0(T_{rs}) P_{succ}, \\
&P_{IDLE^S \to IDLE^C} = P^0(T_{rs}) P_{coll}.
\end{aligned} \tag{3.19}$$

Receive collision states:

These are the states $IDLE^C$, $(b,k)^C$ and $(0',k)^C$ for $1 \leq k < W_0$ and $0 \leq b < M$, where the NAV is set and contains no DATA transmission. In case the node is the receiver or the listener of an unsuccessful RTS/CTS exchange, the receive collision states are visited with residence time of T_{rc}. Transitions from receive

collision states are as follows for $0 \leq b < M$ and $1 \leq k < W_0$:

$$
\begin{aligned}
&P_{(0',k)^C \rightarrow (0',k)} = 1, \\
&P_{(b,k)^C \rightarrow (b,k)} = 1, \\
&P_{IDLE^C \rightarrow (0,k)} = P^1(T_{rc}) P_{idle} / W_0, \\
&P_{IDLE^C \rightarrow (0,k)^S} = P^1(T_{rc}) P_{succ} / W_0, \\
&P_{IDLE^C \rightarrow (0,k)^C} = P^1(T_{rc}) P_{coll} / W_0, \\
&P_{IDLE^C \rightarrow (0,0)^S} = P^1(T_{rc})(1-p) / W_0, \\
&P_{IDLE^C \rightarrow (0,0)^C} = P^1(T_{rc}) p / W_0, \\
&P_{IDLE^C \rightarrow IDLE} = P^0(T_{rc}) P_{idle}, \\
&P_{IDLE^C \rightarrow IDLE^S} = P^0(T_{rc}) P_{succ}, \\
&P_{IDLE^C \rightarrow IDLE^C} = P^0(T_{rc}) P_{coll}.
\end{aligned}
\tag{3.20}
$$

3.4.4 State residence times

The residence time of a node in transmit success state includes the duration required for transmission of a single successful DATA packet together with the control frames. This duration can not be extended with neighboring nodes in the transmit range of the successfully transmitting node, since these nodes are not allowed to send anything until the end of the reception of ACK plus a carrier sensing duration of DIFS. Thus, the residence time of transmit success state is as follows:

$$T_{ts} = T_{RTS} + T_{CTS} + T_{DATA} + T_{ACK} + 3SIFS + DIFS, \tag{3.21}$$

where $T_{RTS}, T_{CTS}, T_{DATA}$ and T_{ACK} correspond to transmission times of RTS, CTS, DATA and ACK frames respectively. Transmission time of control frames is calculated by dividing the number of bits of control frame by the basic rate of the communication and transmission time of DATA packet is calculated by dividing the number of bits of the PLCP header by the basic rate and the rest of the packet by data rate [2].

The residence time in transmit collision state can not be extended by neighboring transmissions, since the source node of the collision is not allowed to receive anything during the CTSTimeout so that it is not allowed to set its NAV. The additional DIFS duration is added since the backoff procedure starts after carrier sensing. The transmit collision state residence time, T_{tc}, is calculated as follows (assuming that DATA collisions are neglected):

$$T_{tc} = T_{RTS} + T_{CTSTimeout} + DIFS. \tag{3.22}$$

The NAV duration is assumed to take two possible values: T_{rs} and T_{rc}. Such a division of NAV duration, different from [73] where only one NAV duration is assumed, is required for a more precise modelling of the IEEE 802.11 MAC. In case the node receives successful or collided DATA destined for itself or the NAV is set for at least the duration of one DATA frame, the state residence time T_{rs} is equal to T_{ts}, neglecting the time difference of $T_{RTS} + SIFS$ in case the NAV is set by a CTS frame. In a multi-hop network, the NAV may be extended by two or more DATA receptions or collisions. But to simplify the analysis, we assume that overlap of two DATA receptions occur at most when the traffic gets saturated, so that T_{rs} is calculated as:

$$T_{rs} = T_{ts} + (1 - q)\frac{T_{ts}}{2}. \tag{3.23}$$

A receive success residence time, is expanded by a second receive success event by the average amount given by the second term with probability $1 - q$ in saturated traffic conditions.

When the node itself is the receiver of a successful transmission, then the NAV is set for a duration equal to $T_{ts} - T_{RTS} - SIFS$ and cannot be extended by neighboring transmissions. In the calculation of T_{rs}, we ignore the difference of reception time in order to simplify the model.

In case the node is the receiver or the listener of an unsuccessful RTS/CTS exchange, the NAV is set by T_{rc}. In a multi-hop network, two or more RTS/CTS

collisions may overlap. Neglecting more than two RTS/CTS collision overlaps, and assuming that an expansion occurs under saturated traffic conditions, T_{rc} is calculated as:

$$T_{rc} = 1.5RTS + EIFS + (1-q)\frac{EIFS}{2}. \tag{3.24}$$

There may be a collision of RTS with RTS, an RTS with CTS, or a CTS with CTS (the collisions with the DATA packet are neglected). We assume that the duration of RTS and CTS frames are equal in order to simplify the analysis. Depending on the assumption a collision is extended by half RTS duration on the average. After each perceived collision, the station waits for EIFS idle time before taking an action. NAV is extended by an average amount of $\frac{EIFS}{2}$ with probability $(1-q)$.

3.4.5 Steady state probabilities

The steady state probabilities of the SMC in Fig. 3.2 are solved by techniques in [75], due to state dependent state residence times. The steady state probability of a state (b,k) is denoted by the notation $\pi_{(b,k)}$. The steady state probability of being in idle state is represented by π_{idle} and is calculated by summing up the steady state probabilities of idle states. Likewise the steady state probability of being in the transmit success, transmit collision, receive success and receive collision states are represented by $\pi_{ts}, \pi_{tc}, \pi_{rs}$ and π_{rc} respectively and are calculated by summing up the steady state probabilities of the corresponding states

explained in Section 3.4.3:

$$\begin{aligned}
\pi_{idle} &= \sum_{b\in\{0',[0,M)\},k\neq 0} \pi_{(b,k)} + \pi_{IDLE}, \\
\pi_{ts} &= \sum_{b\in\{0',[0,M)\}} \pi_{(b,0)^S}, \\
\pi_{tc} &= \sum_{b\in\{0',[0,M)\}} \pi_{(b,0)^C}, \\
\pi_{rs} &= \sum_{b\in\{0',[0,M)\},k\neq 0} \pi_{(b,k)^S} + \pi_{IDLE^S}, \\
\pi_{rc} &= \sum_{b\in\{0',[0,M)\},k\neq 0} \pi_{(b,k)^C} + \pi_{IDLE^C}.
\end{aligned} \tag{3.25}$$

3.4.6 Geometry related notations

The analysis is based on a transmission from node tx to a receiver node rx. The probability of collision of this transmission from $tx \rightarrow rx$ and the NAV setting probabilities of node tx are calculated in the analysis. Definitions regarding the geometry of the nodes that are required in the analysis for the calculation of NAV setting probabilities and probability of collision are explained in next two sections.

S_{tx}: The carrier sensing region of a transmitter tx is denoted by S_{tx}. A fixed number of n nodes are assumed to be within this carrier sensing region of each node.

S_{rxexc}: The part of a receiver carrier sensing region which is not exposed to the transmitter carrier is called as the *receiver exclusive region* [8], and is denoted by S_{rxexc} for the transmission from tx to rx (Fig. 3.4(a)).

N_{rxexc}: The average value of number of nodes in receiver exclusive areas of nodes inside the carrier sensing range of the node tx is denoted by N_{rxexc}, and is found by averaging over all possible receivers inside the carrier sensing region of the transmitter. Let us assume that the network is homogeneous and the

distortion resulting at the edges of the network is negligible, so that N_{rxexc} is equal for any transmitter tx. Since all possible receivers are located at the same distance apart from the tx and the network is homogeneous, N_{rxexc} calculated for any receiver rx becomes equal.

S_{rxint}: The intersection area of carrier sensing regions of the transmitter and receiver is denoted by S_{rxint}.

N_{rxint}: The average number of nodes inside S_{rxint}, including the transmitter and receiver, is denoted by N_{rxint}.

$S_{exc}^{tx\rightarrow i}$: Let us denote the part of the carrier sensing region of any node $i \in S_{tx}$, which is not exposed to the transmitter carrier by $S_{exc}^{tx\rightarrow i}$.

$S_{int}^{tx\rightarrow i}$: The intersection area of carrier sensing regions of the transmitter and receiver is denoted by $S_{int}^{tx\rightarrow i}$.

$ntx_{exc}^{i\rightarrow j}$: The number of possible intended receivers of a node i that are inside the region $S_{exc}^{i\rightarrow j}$. Each node has six possible intended receivers inside its carrier sensing range, and the number of transmitters in a specific portion of the carrier sensing range is required for the analysis, which is obtained by this value.

The part of the carrier sensing region of any node $i \in S_{tx}$, which is not exposed to the transmitter carrier is denoted by $S_{exc}^{tx\rightarrow i}$ (Fig. 3.4(a)), whereas the intersection area of carrier sensing regions of tx and node $i \in S_{tx}$ is denoted by $S_{int}^{tx\rightarrow i}$. The number of possible intended receivers of a node j that are inside the region $S_{exc}^{i\rightarrow j}$ is denoted by $ntx_{exc}^{i\rightarrow j}$. $S_{txSrxint}$ and $S_{intSrxint}$ are the regions formed by borders of carrier sensing regions of nodes tx, rx and $i \in S_{rxint} - \{tx\}$ (Fig. 3.4(c)), whereas $S_{txSrxexc}$, $S_{rxSrxexc}$, $S_{intSrxexc}$ and $S_{excSrxexc}$ are the regions determined by the borders of carrier sensing regions of nodes tx, rx and $j \in S_{rxexc}$ (Fig. 3.4(d)). The ratio of number of nodes inside regions $S_{exc}^{tx\rightarrow i}$,

$S_{txSrxint}$, $S_{intSrxint}$, $S_{txSrxexc}$, $S_{rxSrxexc}$, $S_{intSrxexc}$ and $S_{excSrxexc}$ to n are represented by R_{exc}, $R_{txSrxint}$, $R_{intSrxint}$, $R_{txSrxexc}$, $R_{rxSrxexc}$, $R_{intSrxexc}$ and $R_{excSrxexc}$, respectively.

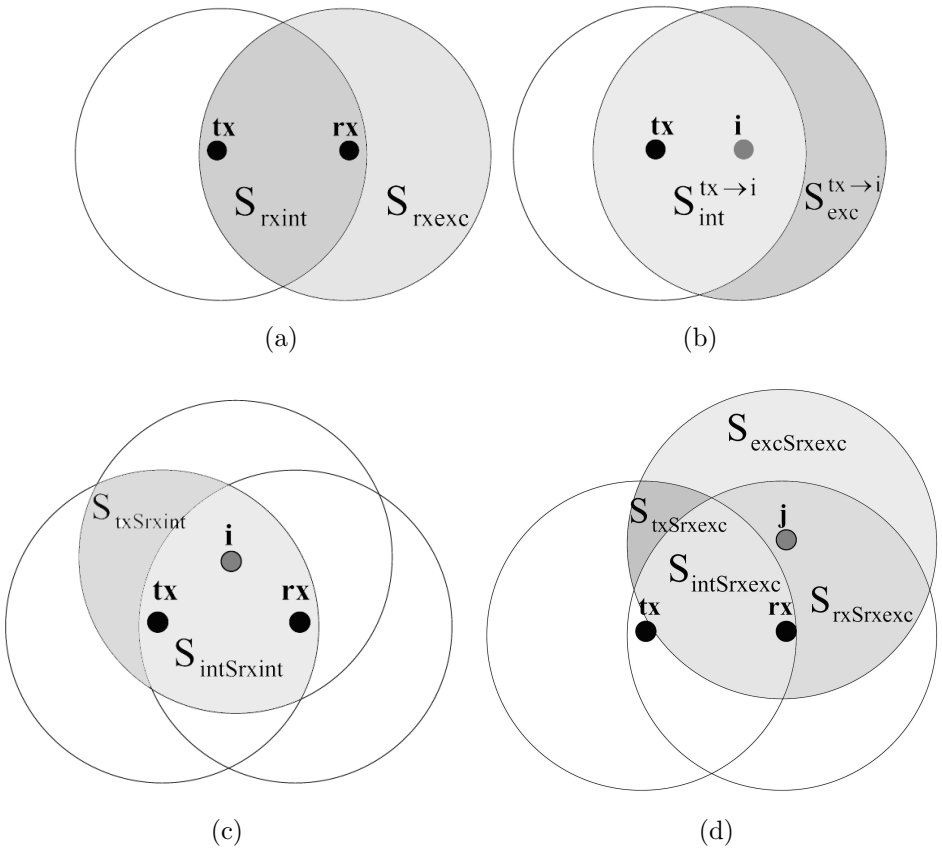

Figure 3.4: Illustration of carrier sensing regions a) S_{rxexc} and S_{rxint}, b) $S_{exc}^{tx \to i}$ and $S_{int}^{tx \to i}$, c) $S_{txSrxint}$ and $S_{intSrxint}$ formed by nodes tx, rx and $i \in S_{rxint} - \{tx\}$, d) $S_{txSrxexc}$, $S_{rxSrxexc}$, $S_{intSrxexc}$ and $S_{excSrxexc}$ formed by nodes tx, rx and $j \in S_{rxexc}$

Although the variables n, N_{rxexc}, N_{rxint}, $R_{txSrxint}$, $R_{intSrxint}$, $R_{txSrxexc}$, $R_{rxSrxexc}$, $R_{intSrxexc}$ and $R_{excSrxexc}$ are different for each $tx - rx$ pair for an arbitrary topology, average values obtained via a traffic weighted averaging operation over all links in the network are used. For a regular topology, calculation of these variables for a single node is enough since each node has the same value.

3.4.7 NAV setting probabilities

The channel state probability notion mentioned in analytical modelling of DCF in single-hop networks is transformed into NAV setting probability notion in multi-hop networks due to existence of hidden terminals. The decision on setting the NAV is given at certain instants of time shown in Fig. 3.3, corresponding to time instants when the node does carrier sensing and the NAV is zero. Thus NAV setting probabilities are conditional probabilities conditioned on the fact that the node does carrier sensing with zero NAV. Three NAV setting probabilities are defined:

1. P_{idle}: the probability that the NAV is not set,
2. P_{succ}: the probability that the NAV is set for a long duration that contains at least one DATA transmission,
3. P_{coll}: the probability that the NAV is set for a short duration that does not contain any DATA transmission,

given that the node does carrier sensing with zero NAV.

Node tx does not set its NAV during a fixed time slot of length σ, if the $n-1$ nodes inside S_{tx} do not start a transmission. Since the analysis is transmission based rather than packet based, by *start of a transmission*, we allude the first σ portion of an RTS frame of a successful transmission or collision, and the first σ portion of a CTS response of a successful reception. Denoting the probability of starting a successful transmission (collision), i.e., start sending the RTS of a successful transmission or CTS response to a node $i \in S_{exc}^{tx \to i}$ (i.e., start sending RTS of a collision), as τ_s (τ_c), and assuming that the probability of not starting a transmission, $1-\tau_s-\tau_c$, is same and independent for each of the $n-1$ nodes, P_{idle}, is in the product form and it is expressed as follows:

$$P_{idle} = (1-\tau_s-\tau_c)^{n-1}. \tag{3.26}$$

τ_s and τ_c are obtained by dividing the steady state probabilities of the states at which a successful transmission and a collision is started, respectively, by $\pi^{NAV}_{allowed}$, which is the sum of the steady state probabilities of allowed states at the instants of time where node tx is carrier sensing with zero NAV. The derivation is based on the fixed length slot notion, so that the states of the SMC are divided into states of residence times of σ. Hence τ_s and τ_c are given by:

$$\begin{aligned}
\tau_s &= \frac{1}{\pi^{NAV}_{allowed}}(\pi_{ts}\frac{\sigma}{T_{ts}} + K_1\pi_{rs}\frac{\sigma}{T_{ts}}),\\
\tau_c &= \frac{1}{\pi^{NAV}_{allowed}}\pi_{tc}\frac{\sigma}{T_{tc}},\\
\pi^{NAV}_{allowed} &= 1 - \pi_{ts}\frac{T_{ts}-\sigma}{T_{ts}} - \pi_{tc}\frac{T_{tc}-\sigma}{T_{tc}}\\
&\quad - K_1\pi_{rs}\frac{T_{ts}-T_{RTS}-SIFS-\sigma}{T_{ts}}\\
&\quad - (1-R_{exc})(\pi_{rs}\frac{T_{rs}-\sigma}{T_{rs}} + \pi_{rc}\frac{T_{rc}-\sigma}{T_{rc}}),
\end{aligned} \tag{3.27}$$

where K_1, averaged over each node $i \in S_{tx} - \{tx\}$, is the ratio of successful receptions from any node $j \in S^{tx\to i}_{exc}$ to the total receptions.

K_1 is the fraction of successful receptions that are destined to the node $i \in S_{tx} - \{tx\}$ from a node $j \in S^{tx\to i}_{exc}$. There are $ntx^{tx\to i}_{exc}$ possible transmitters of node i inside $S^{tx\to i}_{exc}$ and $1/{k_1}^{th}$ of their transmission is destined to node i. So the fraction of receptions that are destined to node i to the number of receptions around node i equals $\frac{ntx^{tx\to i}_{exc}}{k_1(n-1)}$ and K_1 is calculated by averaging over all $i \in S_{tx} - \{tx\}$:

$$K_1 = \frac{\sum_{i\in S_{tx}-\{tx\}} \frac{ntx^{tx\to i}_{exc}}{k_1(n-1)}}{n-1}. \tag{3.28}$$

P_{succ} is the probability that the node sets its NAV for a duration that contains at least one DATA transmission given that the node is carrier sensing with zero NAV. Node tx sets its NAV for a duration that contains at least one DATA reception in case, one node is transmitting -either successful or failure- and rest of the $n-1$ nodes are not, or at least two successful transmissions occur, corresponding

to probability

$$P_{succ} = (n-1)(\tau_s + \tau_c)(1-\tau_s-\tau_c)^{n-2} + 1 - (1-\tau_s)^{n-1} - (n-1)\tau_s(1-\tau_s)^{n-2}. \tag{3.29}$$

The first term in (3.29) represents the probability that one node is transmitting -either successful or failure- and rest of the $n-1$ nodes are not transmitting. Note that if there is only one failure among $n-1$ nodes, then node tx receives a successful RTS setting the NAV for as long as at least one DATA transmission. The rest of the terms in (3.29) correspond to the probability of at least two successful transmissions. Note that if there is only one failure among $n-1$ nodes, then node tx receives a successful RTS setting the NAV for as long as at least one DATA transmission.

P_{coll}, the probability that the node sets its NAV for a short duration that contains no DATA reception, given that the node is carrier sensing with zero NAV, is given by

$$P_{coll} = 1 - P_{idle} - P_{succ}. \tag{3.30}$$

The NAV setting probabilities are functions of the variables τ_s, τ_c and $\pi_{allowed}^{NAV}$, that are given in (3.27) and that are derived based on the fixed length slot notion, so that the states of the SMC are divided into states of residence times of σ transforming to a DTMC. A portion of the obtained DTMC that is used in calculation of NAV setting probabilities is shown in Fig. 3.5.

The states at which a successful transmission is started are indicated by T_S-labelled states in Fig. 3.5. A successful transmission is started by a node $i \in S_{tx} - \{tx\}$ during the first σ duration of transmit success states, corresponding to the steady state probability $\pi_{ts}\frac{\sigma}{T_{ts}}$, and during the first σ duration of a specific portion of receive success states, where a CTS reply to a node $j \in S_{exc}^{tx\rightarrow i}$ is started, corresponding to $K_1\pi_{rs}\frac{\sigma}{T_{ts}}$. The multiplicand K_1 gives the fraction of successful receptions from nodes inside $S_{exc}^{tx\rightarrow i}$ that are destined to node i only. Hence, the

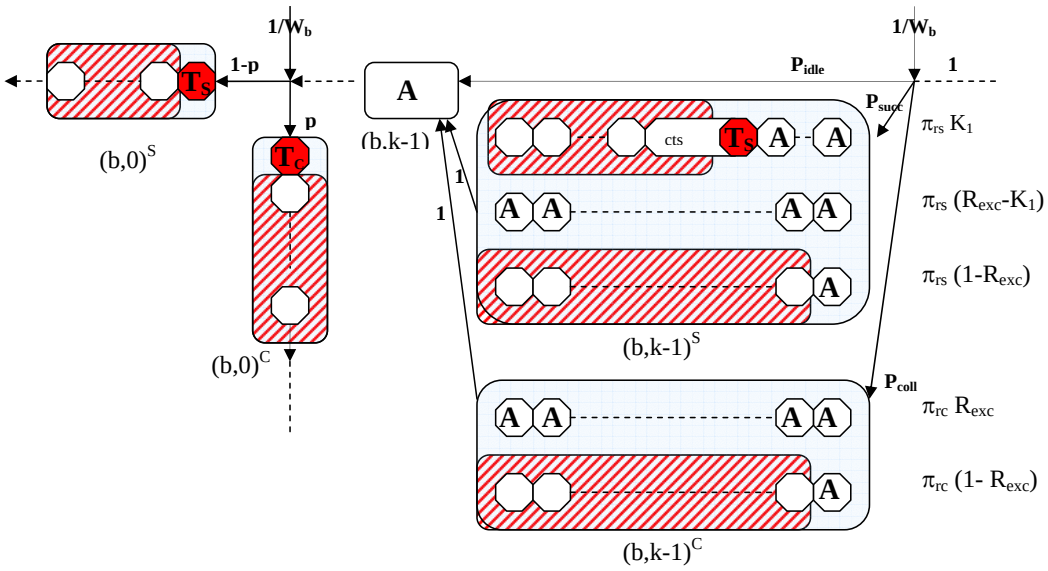

Figure 3.5: Calculation of NAV setting probabilities based on fixed-slot notion

steady state probability of the T_S-labelled states constitutes the numerator of τ_s given in (3.27). The state at which a collision is started is indicated by the T_C-labelled state in Fig. 3.5, corresponding to the first σ duration of transmit collision states. The steady state probability of the T_C-labelled state, $\pi_{tc}\frac{\sigma}{T_{tc}}$, gives the numerator of τ_c.

The A-labelled states shown in Fig. 3.5 together with the T_S-labelled and T_C-labelled states are the states that node $i \in S_{tx} - \{tx\}$ is allowed to be at while carrier sensing with zero NAV. The sum of the steady state probabilities of these states corresponds to $\pi^{NAV}_{allowed}$. Note that nodes are not allowed to transmit anything, and receive a successful transmission or a collision from any node $j \in S_{tx} - \{tx\}$, excluding the first σ duration of receive success and receive collision states.

3.4.8 Probability of collision

An RTS or CTS frame that is not received correctly by neighbors inside the carrier sensing range may cause collision of frames other than RTS frames due

to hidden terminals in multi-hop networks. In this dissertation, collisions among RTS, CTS, DATA or ACK frames with each other are also considered in the calculation of probability of collision. Let us denote the σ duration prior to RTS transmission from $tx \rightarrow rx$ with Δ_0, the first σ portion of RTS transmission with Δ_1 and the time duration afterwards up to the first σ portion of the CTS frame with Δ_2 as illustrated in Fig. 3.6. An RTS/CTS transmission from $tx \rightarrow rx$ is successful if and only if all the Events A, B and C take place, given that a transmission occurs:

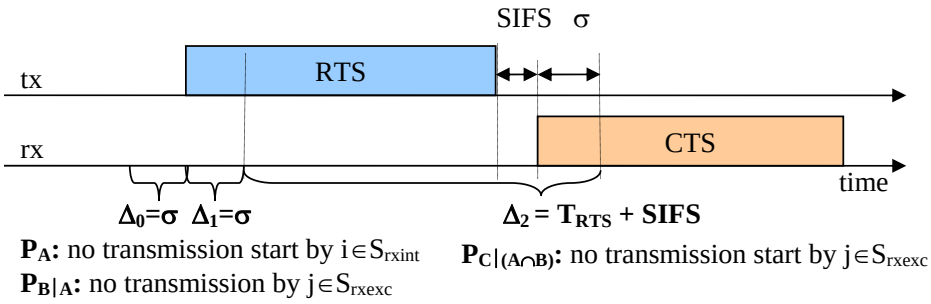

Figure 3.6: Illustration of events for calculation of probability of collision

1. Event A: No node $i \in S_{rxint} - \{tx\}$ *starts a transmission* during Δ_0 and Δ_1. The probability of Event A corresponds to $P_A = \prod_{k=0}^{1}(1-\tau_{A_k})^{Nrxint-1}$, where τ_{A_0} is the probability that node $i \in S_{rxint} - \{tx\}$ starts a transmission during Δ_0 and τ_{A_1} is the probability that node $i \in S_{rxint} - \{tx\}$ starts a transmission during Δ_1.

2. Event B: No node $j \in S_{rxexc}$ *is transmitting* during Δ_1. The probability of Event B given that Event A occurs is denoted by $P_{B|A}$ and is calculated by $P_{B|A} = (1 - \tau_B)^{N_{rxexc}}$, where τ_B is the probability that node $j \in S_{rxexc}$ is transmitting during Δ_1, given that Event A occurs.

3. Event C: No node $j \in S_{rxexc}$ *starts a transmission* during Δ_2. The probability of Event C given that Events A and B occur is denoted by $P_{C|(A\cap B)}$ and corresponds to the probability $P_{C|(A\cap B)} = (1-\tau_C)^{Nrxexc\frac{\Delta_2}{\sigma}}$, where τ_C is

the probability that node $j \in S_{rxexc}$ starts a transmission during Δ_2, given that Events A and B occur.

Since the analysis is transmission based rather than packet based, by *start of a transmission*, we allude the first σ portion of an RTS frame of a successful transmission or collision, and the first σ portion of a CTS response of a successful reception.

The events A, B and C are dependent on each other and an RTS/CTS exchange scheme is successful if all of the three events occur. Thus, the probability of collision is given by:

$$\begin{aligned} p &= 1 - P_{(A \cap B \cap C)} \\ &= 1 - P_A P_{B|A} P_{C|(A \cap B)} \\ &= 1 - \{(1-\tau_{A_0})(1-\tau_{A_1})\}^{N_{rxint}-1} \{(1-\tau_B)(1-\tau_C)^{\frac{\Delta_2}{\sigma}}\}^{N_{rxexc}}. \end{aligned} \tag{3.31}$$

The calculation of τ_{A_0}, τ_{A_1}, τ_B and τ_C is based on the fixed length time slot notion and is given by

$$\tau_i = \frac{\pi^i_{transmit}}{\pi^i_{allowed}}, \text{ for } i = \{A_0, A_1, B, C\}, \tag{3.32}$$

where $\pi^i_{transmit}$ corresponds to the sum of steady state probabilities of states where nodes have the opportunity to transmit and $\pi^i_{allowed}$ corresponds to the sum of steady state probabilities of allowed states for $i = \{A_0, A_1, B, C\}$. The calculation of P_A, $P_{B|A}$ and $P_{C|(A \cap B)}$ is based on the fixed length time slot notion and is given in detail next.

Calculation of P_A:

Recall that, this is the probability that no nodes in the S_{rxint} region (excluding the tx) start a transmission during Δ_0 and Δ_1. In fact, the probability that a node $i \in S_{rxint} - \{tx\}$ starts a transmission is dependent on the behavior of the

rest of the nodes inside S_{rxint}. But independence is assumed in order to simplify the analysis. Thus P_A corresponds to the probability

$$P_A = \{(1 - \tau_{A_0})(1 - \tau_{A_1})\}^{Nrxint-1}. \tag{3.33}$$

τ_{A_0} is the probability that node $i \in S_{rxint} - \{tx\}$ starts a transmission during Δ_0. The numerator of τ_{A_0}, $\pi^{A_0}_{transmit}$ corresponds to the sum of steady state probabilities of states where node $i \in S_{rxint}$ during Δ_0 has the opportunity to transmit. These are the states where the first σ portion of a collided RTS is sent and the first σ portion of a CTS response to a transmitter $k \in S^{tx \to i}_{exc}$ is sent. $\pi^{A_0}_{transmit}$ is calculated by summing up the steady state probabilities of the T-labelled states shown in Fig. 3.7. The A-labelled states plus the T-labelled states give us the allowed states, the sum of steady state probabilities of which corresponds to $\pi^{A_0}_{allowed}$. There are certain states that node i cannot be in during Δ_0 since p is conditioned on occurrence of a transmission from $tx \to rx$. For example, node i cannot be in transmit success states, since any transmission of node i during Δ_0, given that a transmission from $tx \to rx$ starts during Δ_1, would be a collision. Also, node i cannot be in transmit collision state, excluding the first and last σ duration of a collision, since node i being in these states would suppress the $tx \to rx$ transmission. Likewise, node i cannot receive from nodes inside $S_{txSrxint}$ and $S_{intSrxint}$, excluding the first and last σ duration of receive success and receive collision states, for the same reasoning.

$$\tau_{A_0} = \frac{\pi^{A_0}_{transmit}}{\pi^{A_0}_{allowed}}, \tag{3.34}$$

where

$$\begin{aligned}
\pi^{A_0}_{transmit} &= \pi_{tc}\frac{\sigma}{T_{tc}} + K_A\pi_{rs}\frac{\sigma}{T_{ts}}, \\
\pi^{A_0}_{allowed} &= 1 - \pi_{ts} - \pi_{tc}\frac{T_{tc} - 2\sigma}{T_{tc}} - K_A\pi_{rs}\frac{T_{ts} - 2\sigma}{T_{ts}} \\
&\quad - R_{txSrxint}(\pi_{rs}\frac{T_{rs} - 2\sigma}{T_{rs}} + \pi_{rc}\frac{T_{rc} - 2\sigma}{T_{rc}}) \\
&\quad - R_{intSrxint}(\pi_{rs}\frac{T_{rs} - 2\sigma}{T_{rs}} + \pi_{rc}\frac{T_{rc} - 2\sigma}{T_{rc}}).
\end{aligned} \tag{3.35}$$

K_A represents the fraction of successful receptions that are destined to node $i \in S_{rxint} - \{tx\}$ from a transmitter $\in S_{exc}^{tx \to i}$ and is calculated by averaging over all $i \in S_{rxint} - \{tx\}$, given by

$$K_A = \frac{\sum_{i \in S_{rxint} - \{tx\}} \frac{ntx_{exc}^{tx \to i}}{k_A(n-1)}}{N_{rxint} - 1}. \tag{3.36}$$

Not all of the transmissions of a transmitter $\in S_{exc}^{tx \to i}$ is destined to node $i \in S_{rxint} - \{tx\}$, but only $1/{k_A}^{th}$ of transmissions. $R_{txSrxint}$ and $R_{intSrxint}$ denote average of the fraction of receptions from regions $S_{txSrxint}$ and $S_{intSrxint}$ respectively averaged over all $i \in S_{rxint} - \{tx\}$ (Fig. 3.4(c)). Node i can be in the first σ portion of receive success or receive collision states from nodes inside $S_{txSrxint}$ and $S_{intSrxint}$.

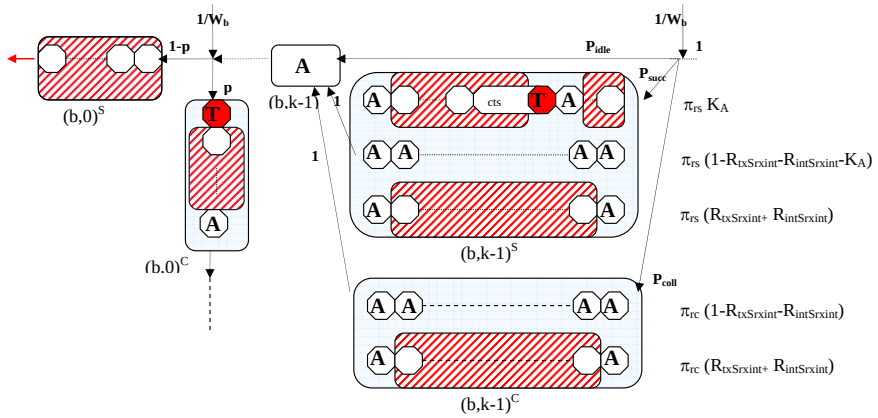

Figure 3.7: Illustration of states for calculation of τ_{A_0} of P_A.

τ_{A_1} is the probability that node $i \in S_{rxint} - \{tx\}$ starts a transmission during Δ_1. The A-labelled and T-labelled states used in calculation of $\pi_{transmit}^{A_1}$ and $\pi_{allowed}^{A_1}$ are shown in Fig. 3.8. Some allowed states during Δ_0 shown in Fig. 3.8 are not allowed during Δ_1. For example, node $i \in S_{rxint}$ is not allowed to be in idle states, since it receives the transmission from $tx \to rx$ during Δ_1. Also, node i cannot be in the last σ duration of transmit collision or receive states since node i being in these states would suppress the $tx \to rx$ transmission.

$$\tau_{A_1} = \frac{\pi_{transmit}^{A_1}}{\pi_{allowed}^{A_1}}, \tag{3.37}$$

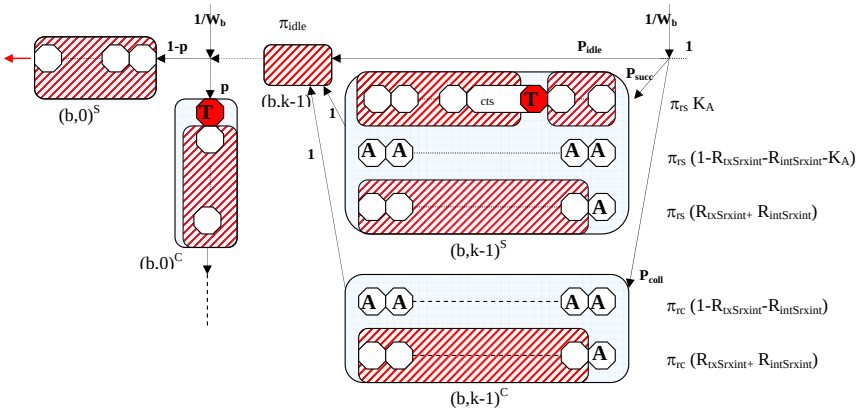

Figure 3.8: Illustration of states for calculation of τ_{A_1} of P_A.

where

$$\begin{aligned}
\pi^{A_1}_{transmit} &= \pi_{tc}\frac{\sigma}{T_{tc}} + K_A\pi_{rs}\frac{\sigma}{T_{ts}}, \\
\pi^{A_1}_{allowed} &= 1 - \pi_{idle} - \pi_{ts} - \pi_{tc}\frac{T_{tc}-\sigma}{T_{tc}} - K_A\pi_{rs}\frac{T_{ts}-\sigma}{T_{ts}} \\
&\quad - R_{txSrxint}(\pi_{rs}\frac{T_{rs}-\sigma}{T_{rs}} + \pi_{rc}\frac{T_{rc}-\sigma}{T_{rc}}) \\
&\quad - R_{intSrxint}(\pi_{rs}\frac{T_{rs}-\sigma}{T_{rs}} + \pi_{rc}\frac{T_{rc}-\sigma}{T_{rc}}).
\end{aligned} \tag{3.38}$$

Calculation of $P_{B|A}$:

Recall that this is the probability that no node $j \in S_{rxexc}$ is transmitting during Δ_1, given that none of the nodes $\in S_{rxint} - \{tx\}$ starts a transmission during Δ_1. Independence of behavior of a node $j \in S_{rxexc}$ on behavior of the rest of the nodes $\in S_{rxexc}$ is assumed. Then $P_{B|A}$, corresponds to the probability

$$P_{B|A} = (1 - \tau_B)^{N_{rxexc}}. \tag{3.39}$$

τ_B is the probability that node $j \in S_{rxexc}$ is transmitting (i.e. making a successful transmission or collision, or making a successful reception destined to itself) during Δ_1, given that nodes $\in S_{rxint} - \{tx\}$ do not start a transmission. The numerator of τ_B, $\pi^B_{transmit}$ corresponds to the sum of steady state probabilities of states where nodes in S_{rxexc} during Δ_1 have the opportunity to transmit. These

are the T-labelled states shown in Fig. 3.9. The denominator of τ_B, $\pi^B_{allowed}$ corresponds to the sum of steady state probabilities of allowed states for nodes in S_{rxexc} during Δ_1, corresponding to A-labelled plus T-labelled states. Hence τ_B becomes as follows:

$$\tau_B = \frac{\pi^B_{transmit}}{\pi^B_{allowed}}, \tag{3.40}$$

where

$$\begin{aligned}
\pi^B_{transmit} &= \pi_{ts}\frac{T_{ts} - DIFS}{T_{ts}} + \pi_{tc}\frac{T_{RTS}}{T_{tc}} \\
&\quad + K_B\pi_{rs}\frac{T_{CTS} + T_{DATA} + T_{ACK} + 2SIFS}{T_{ts}}, \\
\pi^B_{allowed} &= 1 - R_{intSrxexc}(\pi_{rs} + \pi_{rc}) \\
&\quad - R_{txSrxexc}(\pi_{rs}\frac{T_{rs} - \sigma}{T_{rs}} + \pi_{rc}\frac{T_{rs} - \sigma}{T_{rs}}) \\
&\quad - R_{rxSrxexc}(\pi_{rs}\frac{T_{rs} - DIFS}{T_{rs}} - \pi_{rc}\frac{T_{rc} - EIFS}{T_{rc}}).
\end{aligned} \tag{3.41}$$

K_B represents the fraction of successful receptions that are destined to node $j \in S_{rxexc}$ from a transmitter $\in S^{rx\to j}_{exc}$ and is calculated by averaging over all $j \in S_{rxexc}$, given by

$$K_B = \frac{\sum_{j\in S_{rxexc}} \frac{ntx^{rx\to j}_{exc}}{k_B(n-1)}}{N_{rxexc}}. \tag{3.42}$$

$R_{txSrxexc}$, $R_{rxSrxexc}$ and $R_{intSrxint}$ are the fraction of receptions from the regions $S_{txSrxexc}$, $S_{rxSrxexc}$ and $S_{intSrxint}$ respectively averaged over all $j \in S_{rxexc}$ (Fig. 3.4(d)). Node j is not allowed to be in receive states from nodes inside $S_{txSrxexc}$, except the first σ portion, since a transmission is perceived after σ duration by the PHY layer. Node j is not allowed to receive from $S_{intSrxexc}$ due to conditioning of occurrence of Event A. Node j can not receive from nodes inside $S_{rxSrxexc}$ during the busy periods of received transmissions, i.e., $T_{rs} - DIFS$ and $T_{rc} - EIFS$, since this implies that some node inside S_{rxexc} is transmitting where this probability is already captured by taking the power N_{rxexc} of $1 - \tau_B$.

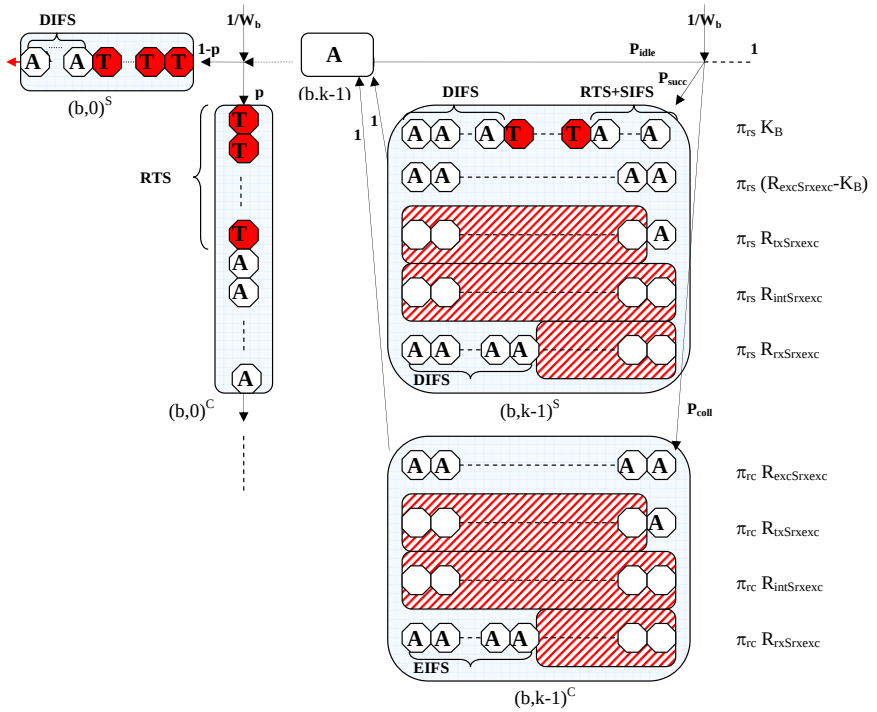

Figure 3.9: Illustration of states for calculation of $P_{B|A}$.

Calculation of $P_{C|(A\cap B)}$:

This is the probability that no nodes inside S_{rxexc} region starts a transmission during Δ_2, which is shown in Fig. 3.6, given that events A and B occur and is expressed as

$$P_{C|(A\cap B)} = (1-\tau_C)^{Nrxexc}. \tag{3.43}$$

τ_C is the probability that node $j \in S_{rxexc}$ starts a transmission, given that events A and B occur. The numerator of τ_C, $\pi^C_{transmit}$ corresponds to the sum of steady state probabilities of states where nodes in S_{rxexc} during Δ_2 have the opportunity to start transmission. The denominator of τ_C, $\pi^C_{allowed}$, corresponds to the sum of steady state probabilities of allowed states for nodes in S_{rxexc} during Δ_2. The T-labelled states where a transmission can be started and the A-labelled states which constitute the allowed states together with the T-labelled states are shown in Fig. 3.10. Hence τ_C becomes as follows:

$$\tau_C = \frac{\pi^C_{transmit}}{\pi^C_{allowed}}, \tag{3.44}$$

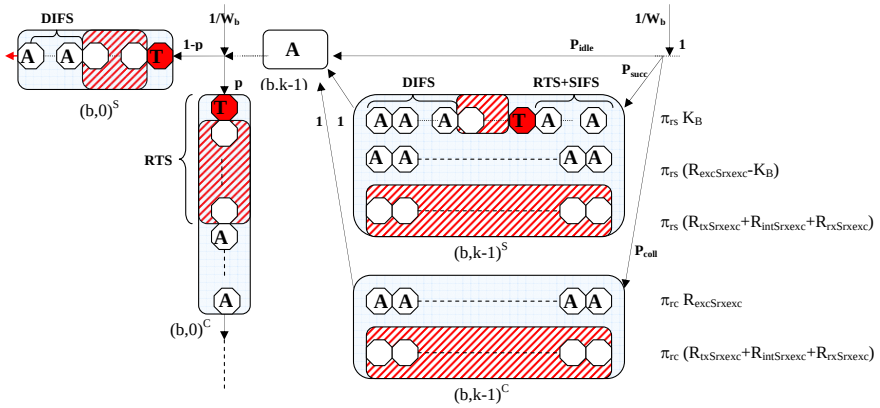

Figure 3.10: Illustration of states for calculation of $P_{C|(A\cap B)}$.

where

$$\begin{aligned}
\pi^C_{transmit} &= \pi_{ts}\frac{\sigma}{T_{ts}} + \pi_{tc}\frac{\sigma}{T_{tc}} + K_B\pi_{rs}\frac{\sigma}{T_{ts}}, \\
\pi^C_{allowed} &= 1 - \pi_{ts}\frac{T_{ts}-\sigma-DIFS}{T_{ts}} - \pi_{tc}\frac{T_{RTS}-\sigma}{T_{tc}} \\
&\quad - K_B\pi_{rs}\frac{T_{ts}-T_{RTS}-SIFS-\sigma-DIFS}{T_{ts}} \\
&\quad - (1-R_{excSrxexc})(\pi_{rs}+\pi_{rc}).
\end{aligned} \tag{3.45}$$

Node $j \in S_{rxexc}$ cannot be transmitting a successful transmission, a collision or a CTS response to some node $k \in S_{excSrxexc}$, except the first σ portion, due to condition on occurrence of Event B. Node j cannot receive from nodes inside $S_{txSrxexc}$ during Δ_2 since these nodes are silenced already by the transmission from $tx \rightarrow rx$. Node j cannot receive from nodes inside $S_{intSrxexc}$ due to condition on the Event A. Node j cannot receive from nodes inside $S_{rxSrxexc}$ due to condition on the Event B.

As a result, combining (3.33), (3.39) and (3.43), p is calculated as:

$$p = 1 - \{(1-\tau_{A_0})(1-\tau_{A_1})\}^{N_{rxint}-1}((1-\tau_B)(1-\tau_C)^{\frac{\Delta_2}{\sigma}})^{N_{rxexc}}. \tag{3.46}$$

Table 3.2: Parameters used for both the analytical model and simulation runs.

Data rate	11 Mbps
Basic rate	1 Mbps
PLCP rate	1 Mbps
W_0	32
B	3
Short retry count (SRC)	7
Long retry count (LRC)	3
SlotTime	20μs
DATA	1072 bytes
RTS	44 bytes
CTS	44 bytes
ACK	44 bytes
SIFS	10μs
DIFS	50μs
EIFS	412μs
IFQ buffer size	5
RxSensitivity	-70 dBm
path loss exponent (η)	3

3.5 Numerical Results

In this section, computed analytical results for probability of transmission (τ), probability of collision (p), NAV setting probabilities ($P_{idle}, P_{succ}, P_{coll}$) and average NAV duration ($\bar{\sigma_n}$) are compared with simulation data for varying traffic loads and various topologies. The effects of contention window size, DATA packet size and maximum retry count on probability of transmission and collision are investigated.

There exists no closed form solution for calculation of the probability of transmission, probability of collision and NAV setting probabilities in the proposed analytical IEEE 802.11 DCF model. The DCF model is solved through fixed point iterations. A flowchart is given in Fig. 3.11 that illustrates the solution

methodology of the analytical DCF model in order to be helpful for implementation.

The accuracy of the proposed analytical IEEE 802.11 DCF model is studied for different topologies deployed in a fixed area: two hexagonally placed regular topologies, one 127-node topology with $h = \{1, 3\}$ and one 469-node regular topology with $h = \{1, 2, 3, 6\}$; and 32 randomly generated topologies (10 with 10, 10 with 20, 5 with 50, 4 with 100 and 3 with 200 nodes) with $h = \{1, 3\}$ are compared through analysis and simulations. The effects of contention window size, DATA packet size and maximum retry count on probability of transmission and collision are investigated for the 469-node hexagonal topology. For the hexagonal topologies, source-destination pairs are chosen so that all possible linear paths carry traffic, while for the random topologies all source destination pairs that have a three-hop path in between are chosen. Fixed routing is used as the routing algorithm for both the analysis and simulations. Each path is traversed either by direct transmission or by multi-hopping. In case of multi-hopping, transmission power is reduced so as to reach the next hop. The hexagonal topologies are homogeneous in topology and traffic distribution, whereas the random topologies have no homogeneity.

The simulations are conducted using Network Simulator 2, version ns-allinone-2.34 [79]. The parameters used for both the analytical model and the simulations are listed in Table 3.2. Fixed point iterations are carried with a precision of 10^{-10}.

The run time of the analytical calculations and simulations are compared in Table 3.3 for the hexagonal topologies and one instance of the random topologies for $\lambda_o = 1$ packets/sec. The simulation duration is taken to be equal to a duration required to generate an average of 6000 packets per node. The results are obtained on an Intel Xeon CPU X5355 at 2.66 GHz with a physical cache of 4096 KB, and a RAM of size 16GB with 8GB swap. The simulation run times

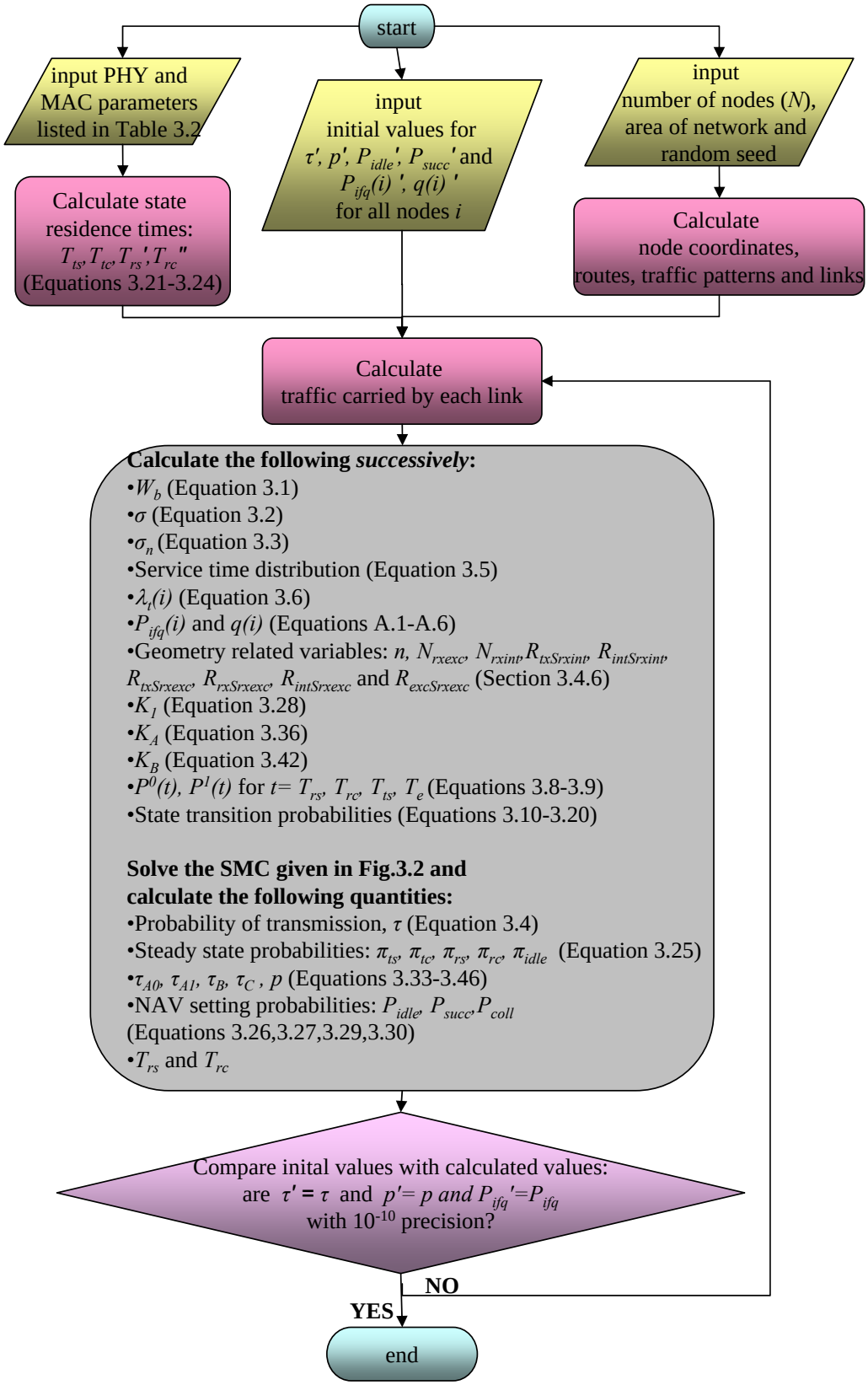

Figure 3.11: Flowchart of the solution of the analytical IEEE 802.11 DCF model.

Table 3.3: Comparison of run time of calculations of analytical IEEE 802.11 DCF model with simulations.

		Run time (sec)						
		Random topologies					Hexagonal topologies	
		N=10	N=20	N=50	N=100	N=200	N=127	N=469
Simulation	h=1	67.034	345.701	748.258	2464.891	23415.655	544.080	10786.374
	h=3	119.725	461.579	897.116	2999.148	5227.212	648.768	5670.547
Model	h=1	103.931	138.482	149.423	394.972	23658.753	160.946	199.536
	h=3	115.823	141.771	159.157	220.927	2361.916	167.370	147.961

are generally higher than the run time of DCF model calculations with a few exceptions. The run time of the simulations and analytical DCF model increases in parallel with increasing size and irregularity of topologies. In terms of run time, the DCF model provides shorter run times compared with simulations, except the 200-node random topology. Run time is longer for the 100-node random topology compared with the hexagonal 127-node topology and longer for the 200-node random topology compared with the hexagonal 469-node topology. This stems from the fact that each link in a random topology has a different transmit power and different number of contending nodes, where the number of links is at most for the 200-node random topology. Furthermore, extensive simulations carried with different physical layer parameters and under higher number of nodes have shown that, simulations obtained via Network Simulator 2 have memory problems, which limits the simulation duration, the number of nodes, the interface queue buffer size, etc. Trial of different simulation durations have shown that limiting the simulation duration to smaller values results in incorrect results, due to the transient behavior of the network. Thus, all of the simulation results are obtained by removing the transient behavior of the network, which is done by removing the first half of the simulation duration and by taking the simulation duration equal to the duration required to generate an average of 6000 packets per node. The analytical DCF model proposed in this dissertation provides better run time and memory requirements, together with a flexibility in solving larger networks with no limitation on interface queue buffer size.

3.5.1 Probability of transmission

The probability of transmission, τ, for random topologies and random traffic patterns is given in Fig. 3.12, whereas the probability of transmission for regular hexagonal topologies and regular traffic patterns is plotted in Fig. 3.13. The probability of transmission is almost zero for light traffic loads, where one station generates less than 1 packet per second on the average. τ tends to increase for moderate loads and becomes constant after a certain breakpoint for all topologies and routing strategies considered. Under heavy traffic loads, τ is more for multi-hopping for large networks and τ is more for direct transmission for 10-node and 20-node random networks. Also note that τ decreases with the increasing size of the network for all routing strategies.

Let us call the average traffic load per node after which the curves become constant as saturation load, and denote it as λ_{sat}. The value of λ_{sat} for τ is observed to depend on the network size and routing strategy. λ_{sat} decreases with the increase in network density and direct transmissions, i.e. with the increase in number of contenting stations. As a result, the saturation load for τ decreases with increasing number of contending stations.

The analytical model is fairly well in calculating τ for the light traffic loads. For moderate traffic loads, the error in analytical model increases, but the general behavior of curves obtained by simulations and analytic calculations is similar. For the heavy traffic loads, the analytical model obtains τ for the hexagonal topologies with an error of at most 42% for multi-hopping and at most 10% for direct transmissions. The error is more for random topologies, where τ is calculated with an error of about 66% for multi-hopping and 20% for direct transmissions for the 200-node random topology. The error increases for the smaller random topologies, where the irregularity of the topology and traffic increase. The general characteristic of the τ curves calculated with the analytical model fit the simulation results for most of the topologies considered, except

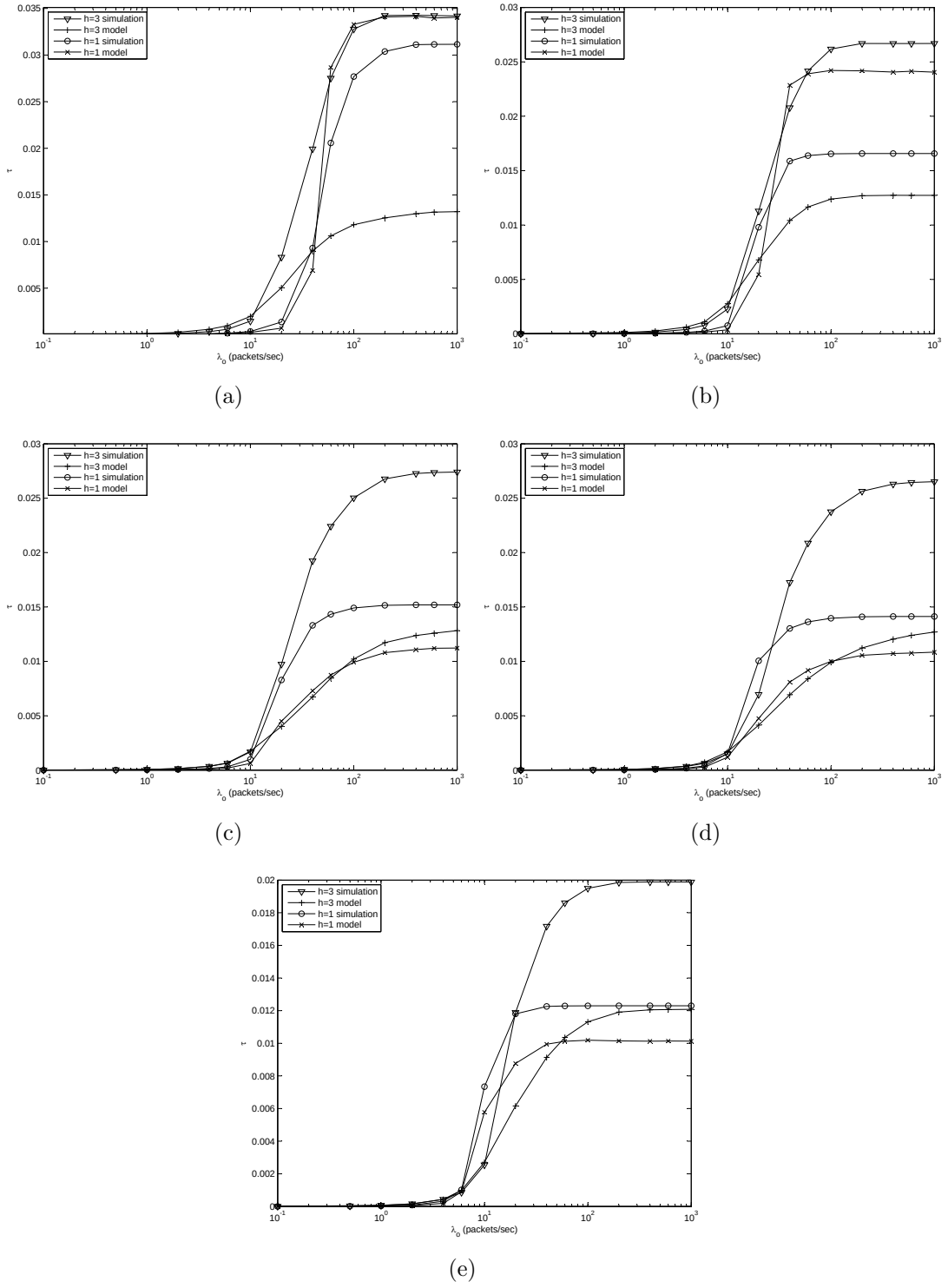

Figure 3.12: Probability of transmission obtained from analytical model and simulations for: a) 10-node, b) 20-node, c) 50-node, d) 100-node, e) 200-node random topologies and random traffic patterns

the 10-node and 20-node random topologies for heavy traffic loads, where τ is increased by direct transmissions. This result shows that the analytical model

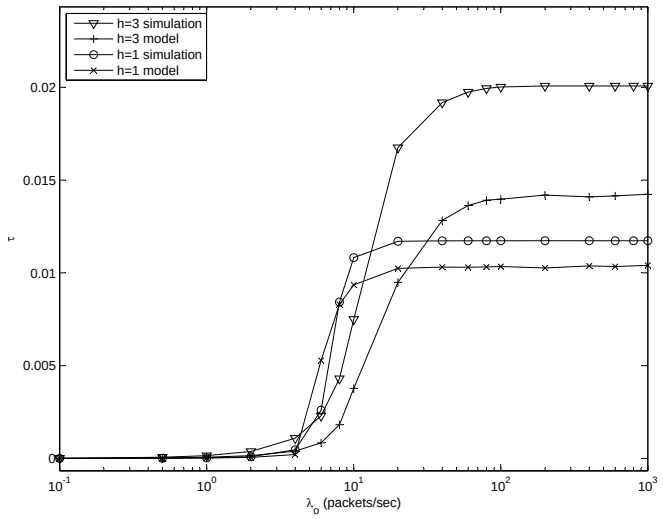

(a)

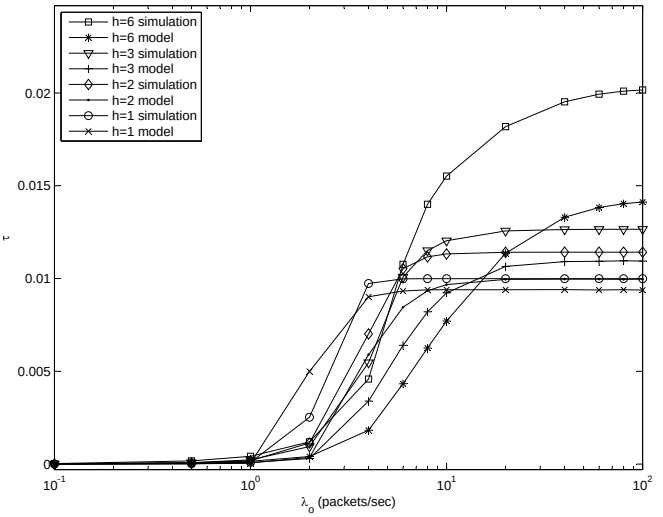

(b)

Figure 3.13: Probability of transmission obtained from analytical model and simulations for: a) 127-node and g) 469-node hexagonal topologies and regular traffic patterns

is insufficient for determining τ for small topologies due to the average analysis conducted where p of all links is averaged.

3.5.2 Probability of collision

The probability of collision, p, for random topologies and random traffic patterns is plotted in Fig. 3.14, whereas the probability of transmission for regular

hexagonal topologies and regular traffic patterns is given in Fig. 3.15. The

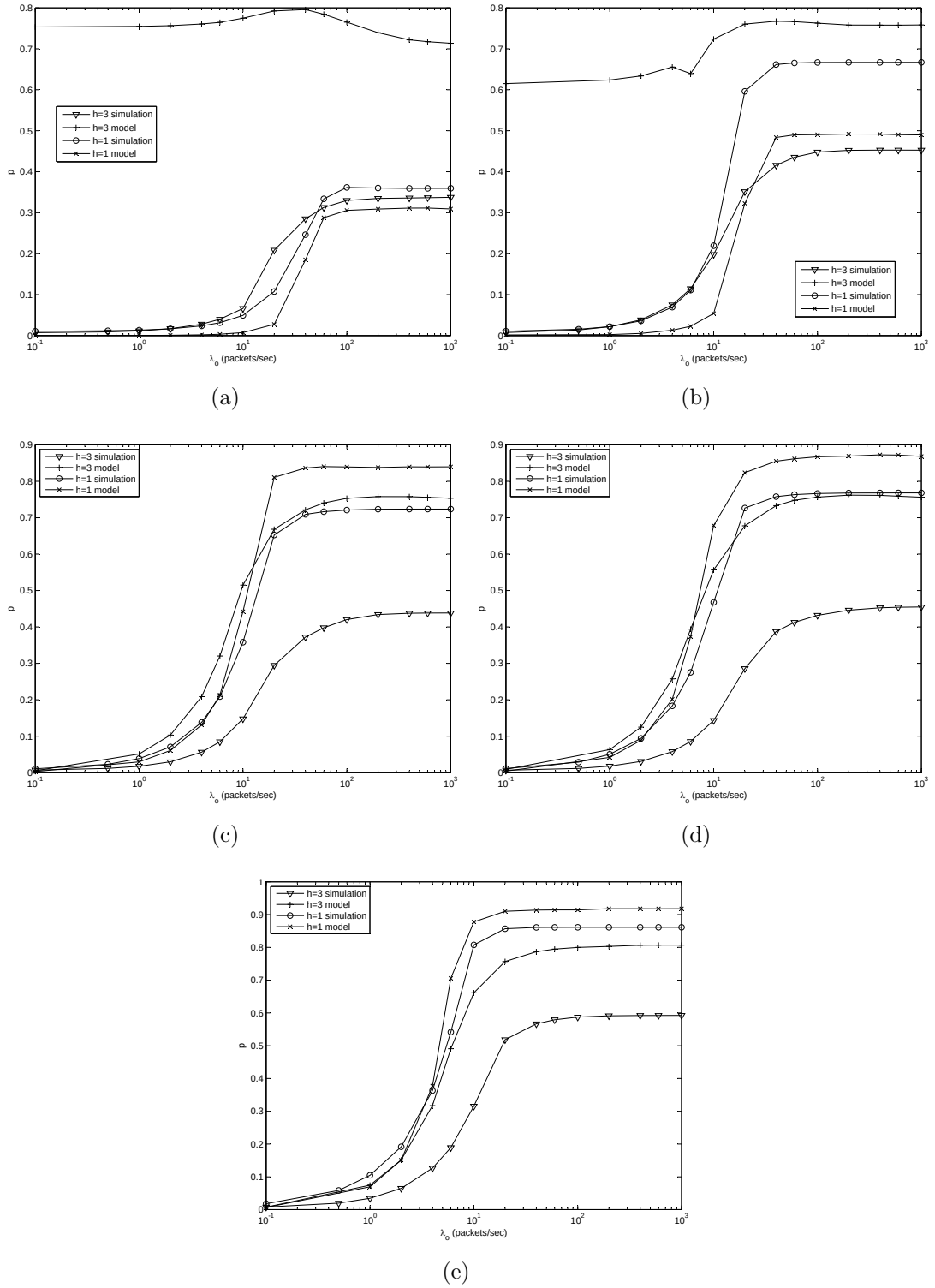

Figure 3.14: Probability of collision obtained from analytical model and simulations for: a) 10-node, b) 20-node, c) 50-node, d) 100-node, e) 200-node random topologies and random traffic patterns

probability of collision is small but nonzero for light traffic loads, and increases

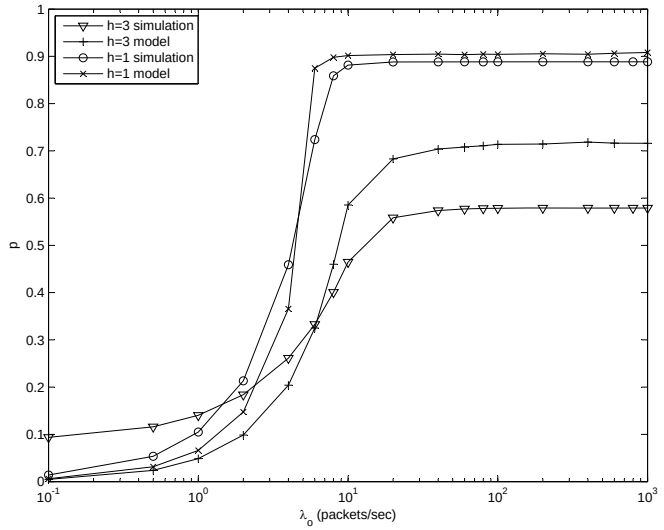

(a)

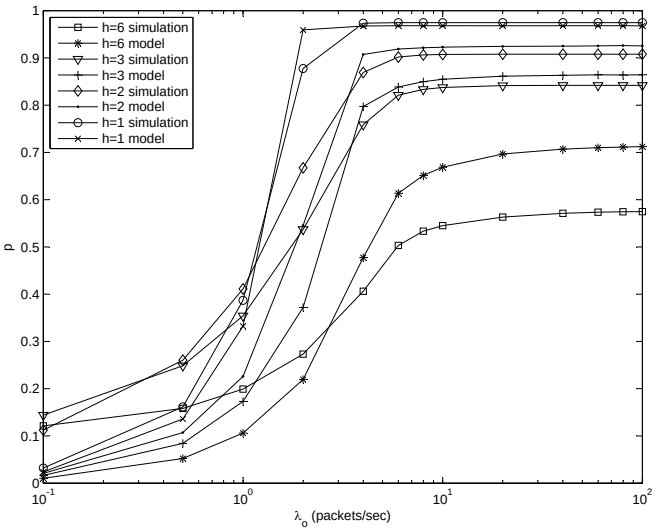

(b)

Figure 3.15: Probability of collision obtained from analytical model and simulations for: a) 127-node and g) 469-node hexagonal topologies and regular traffic patterns

sharply for moderate traffic loads becoming constant after saturation load for all topologies and routing strategies considered. Under heavy traffic loads, p is more for direct transmissions, where the number of contending stations is more than that of multi-hop transmissions. Also note that p increases with the increasing size of the network for all routing strategies.

The value of λ_{sat} for p is observed to depend on the network size and routing strategy, where λ_{sat} decreases with the increase in network density and direct transmissions, i.e. with the increase in number of contenting stations.

The analytical model is fairly well in calculating p for the hexagonal topologies with an error of about 0.6% for multi-hopping and 18% for direct transmissions for the 469-node hexagonal topology under heavy traffic loads. The error is more for random topologies, where p is calculated with an error of about 5% for multi-hopping and 25% for direct transmissions for the 200-node random topology. The error increases for the smaller random topologies, where the irregularity of the topology and traffic increase. The general characteristic of the p curves calculated with the analytical model fit the simulation results for most of the topologies considered, except the multi-hopping case of 10-node and 20-node random topologies, where irregularity of small topologies result in larger errors for an averaged p. This result shows that the analytical model is insufficient for determination of p in the context of routing strategy.

3.5.3 NAV setting probabilities

Probability of setting the NAV for a long duration, P_{succ}, for random topologies and random traffic patterns is depicted in Fig. 3.16, whereas the probability of transmission for regular hexagonal topologies and regular traffic patterns is given in Fig. 3.17. Probability of setting the NAV for a short duration, P_{coll}, for random topologies and random traffic patterns is plotted in Fig. 3.18, whereas the probability of transmission for regular hexagonal topologies and regular traffic patterns is given in Fig. 3.19. Probability of not setting the NAV, P_{idle}, for random topologies and random traffic patterns is depicted in Fig. 3.20, whereas the probability of transmission for regular hexagonal topologies and regular traffic patterns is shown in Fig. 3.21. P_{succ} and P_{coll} are close to zero for light traffic loads, whereas they increases sharply under moderate traffic loads and become

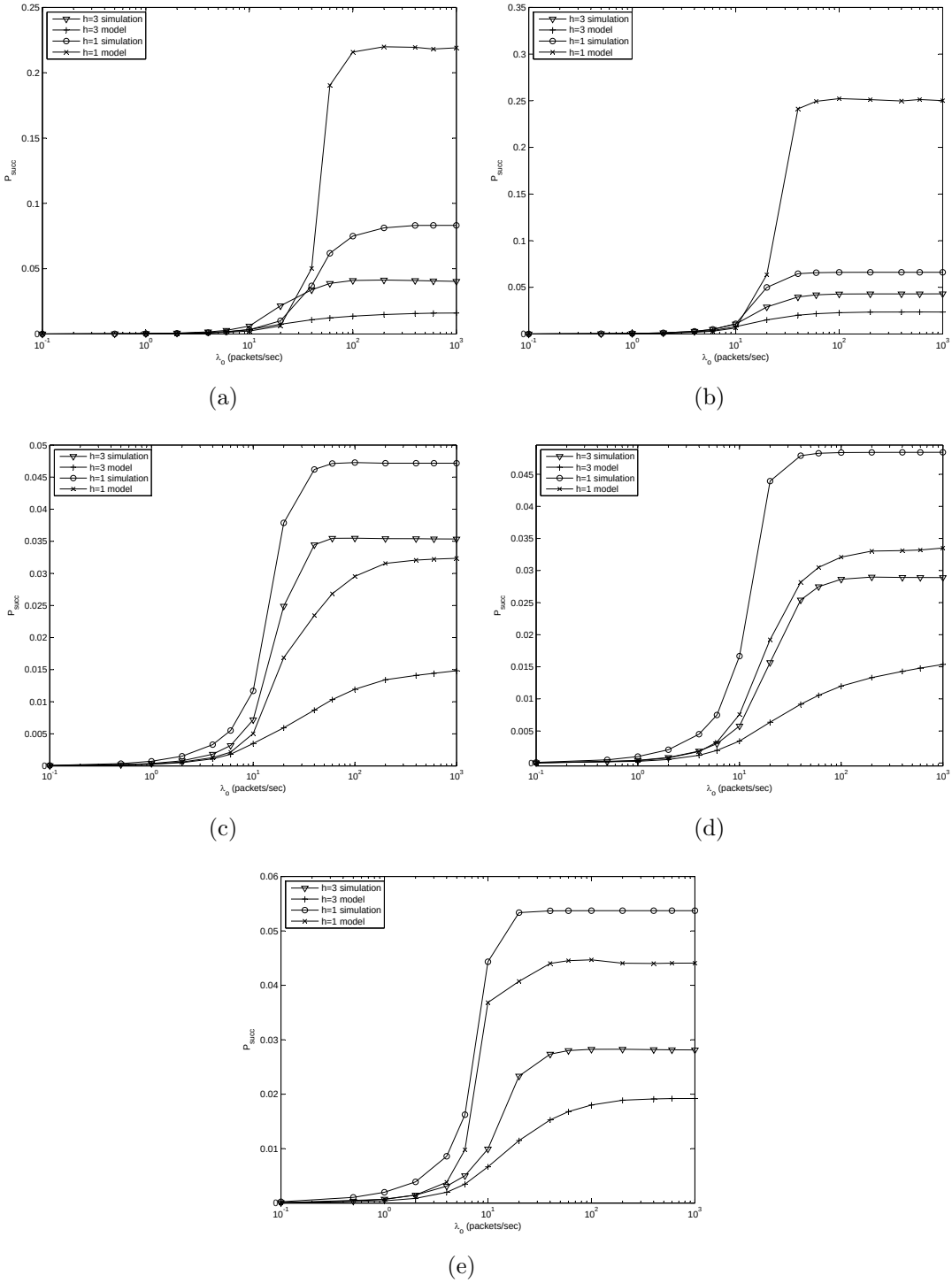

Figure 3.16: Probability of setting the NAV for a long duration, P_{succ}, obtained from analytical model and simulations for: a) 10-node, b) 20-node, c) 50-node, d) 100-node, e) 200-node random topologies and random traffic patterns

constant for heavy traffic loads, whereas P_{idle} exhibits a complementary behavior. Under light traffic, nodes are mostly idle, but start to set their NAV for long or

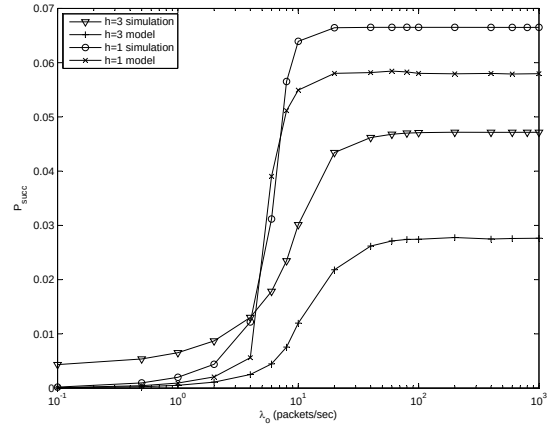

(a)

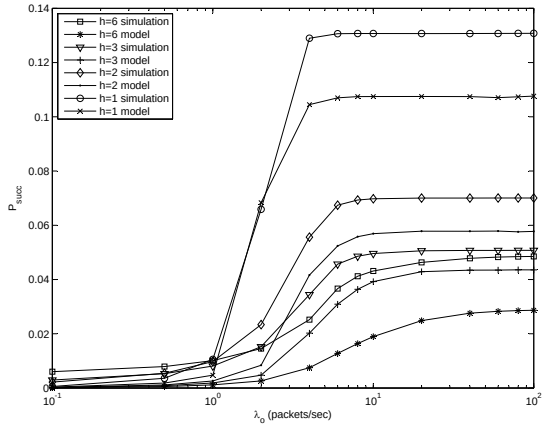

(b)

Figure 3.17: Probability of setting the NAV for a long duration, P_{succ}, obtained from analytical model and simulations for: a) 127-node and g) 469-node hexagonal topologies and regular traffic patterns

short durations as the traffic load gets heavier. For the topologies considered, P_{succ} is always higher than P_{coll}, where the difference among them gets smaller as the network size grows. For example, P_{succ} is almost five times of P_{coll} for the 50-node random topology, whereas it is only twice as much for the 200-node random topology.

Under heavy traffic, P_{succ} and P_{coll} is more for direct transmissions compared to multi-hop transmissions, whereas P_{idle} is less. By direct transmission, the number of contending stations is more, which results with overhearing of more transmissions -either successful or failure- and less idle waiting.

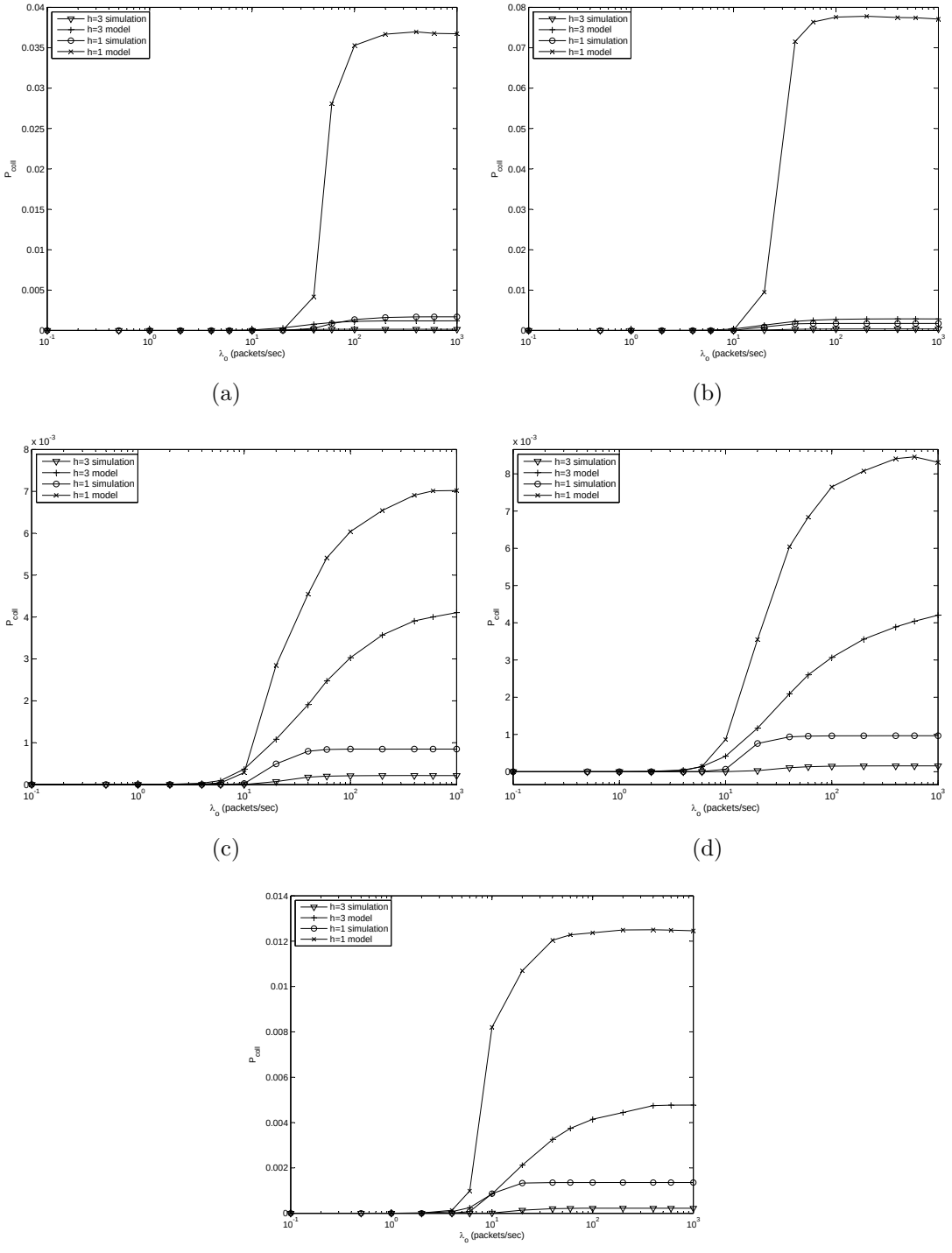

Figure 3.18: Probability of setting the NAV for a short duration, P_{coll}, obtained from analytical model and simulations for: a) 10-node, b) 20-node, c) 50-node, d) 100-node, e) 200-node random topologies and random traffic patterns

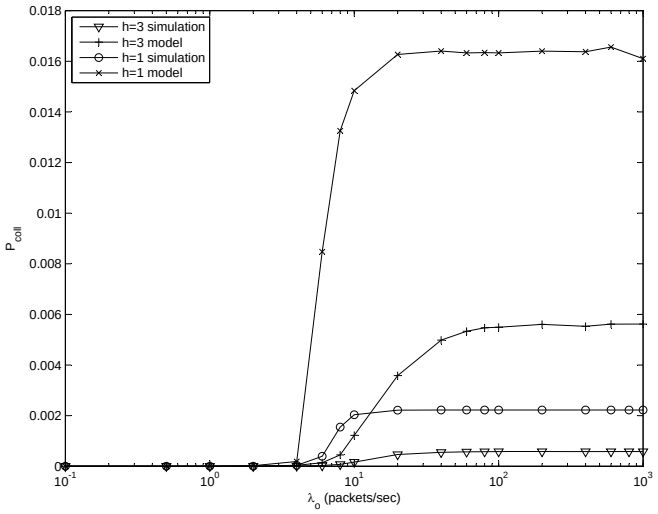

(a)

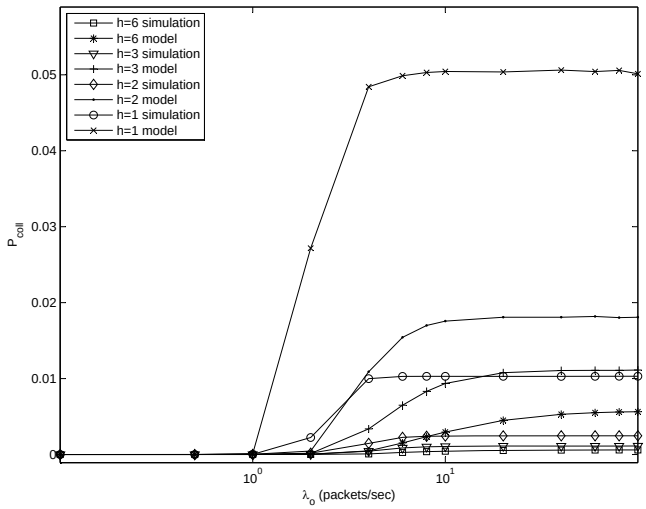

(b)

Figure 3.19: Probability of setting the NAV for a short duration, P_{coll}, obtained from analytical model and simulations for: a) 127-node and g) 469-node hexagonal topologies and regular traffic patterns

3.5.4 Average slot duration

Instead of giving the state residence times separately, the average slot duration, $\bar{\sigma_n}$, for random topologies and random traffic patterns is plotted in Fig. 3.22, whereas the probability of transmission for regular hexagonal topologies and regular traffic patterns is depicted in Fig. 3.23. The analytical model is fairly well in calculation of $\bar{\sigma_n}$ for all topologies and traffic loads considered. Although some errors exist, simulation and analytical curves exhibit a parallel behavior.

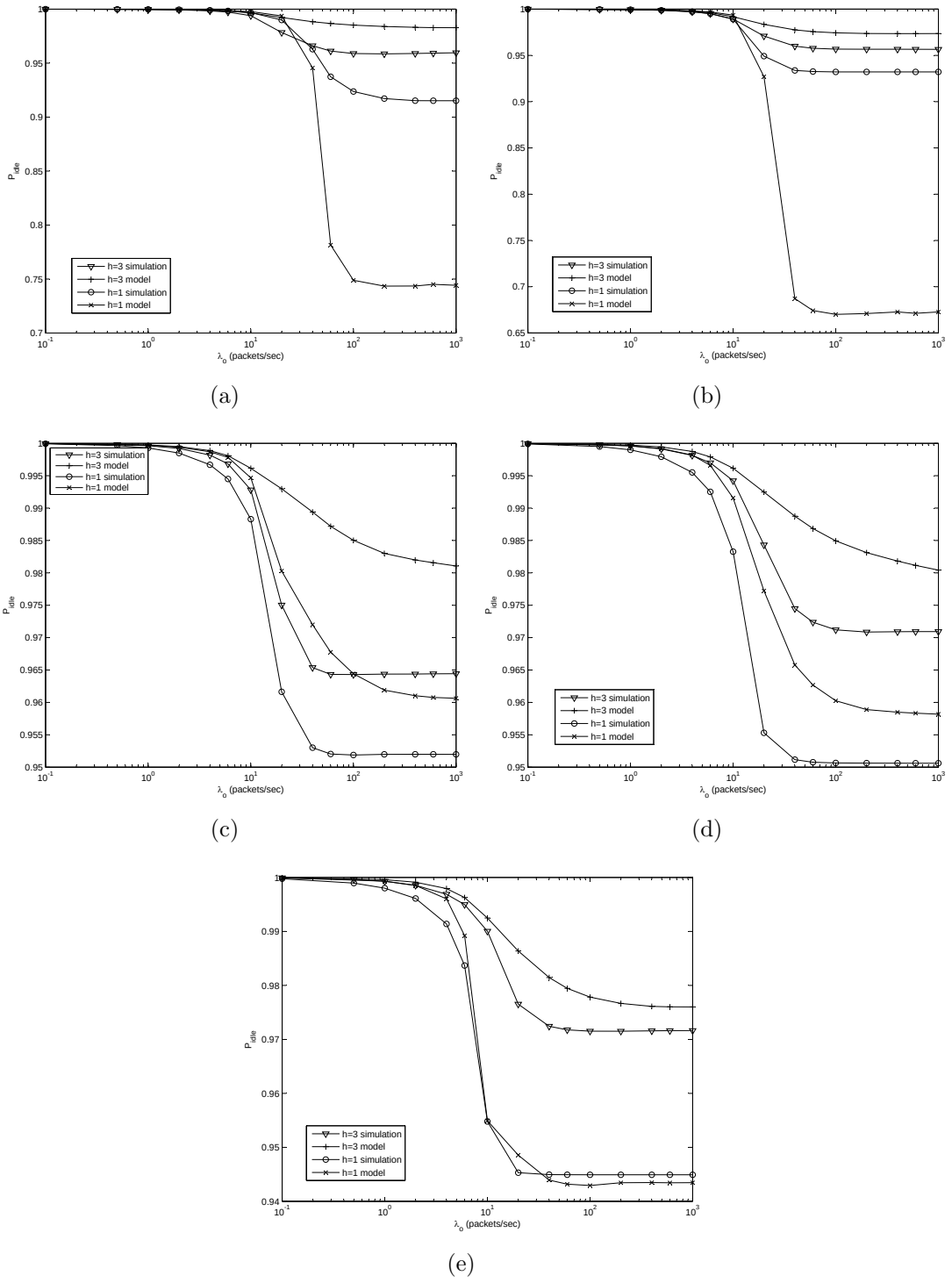

Figure 3.20: Probability of not setting the NAV, P_{idle}, obtained from analytical model and simulations for: a) 10-node, b) 20-node, c) 50-node, d) 100-node, e) 200-node random topologies and random traffic patterns

$\bar{\sigma_n}$ is large for direct transmissions. The reason for this is observed to be the increased T_{rs} that results due to overlapping of more than two overhearing of

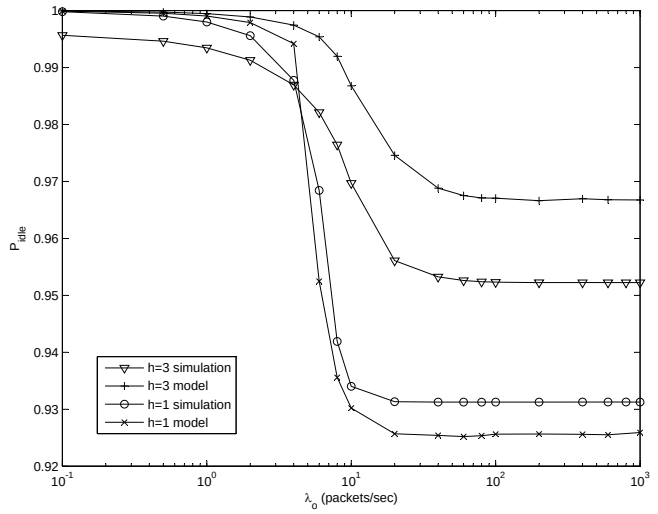

(a)

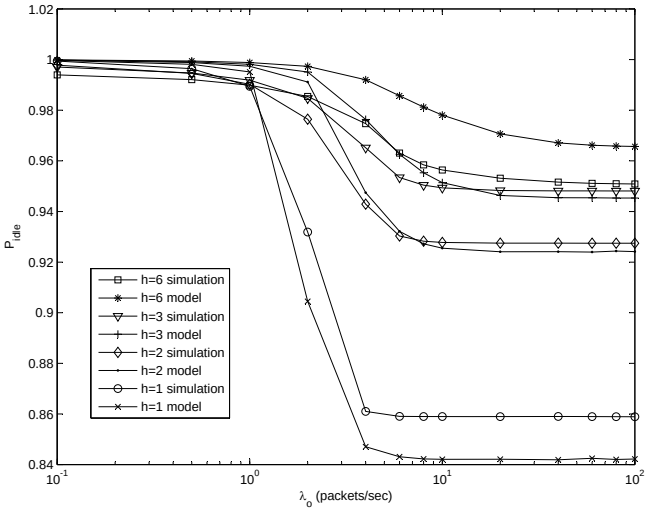

(b)

Figure 3.21: Probability of not setting the NAV, P_{idle}, obtained from analytical model and simulations for: a) 127-node and g) 469-node hexagonal topologies and regular traffic patterns

DATA transmissions. T_{rs} and T_{rc} is observed to be more direct transmissions owing to the increase in the number of contending stations when compared to multi-hop transmissions.

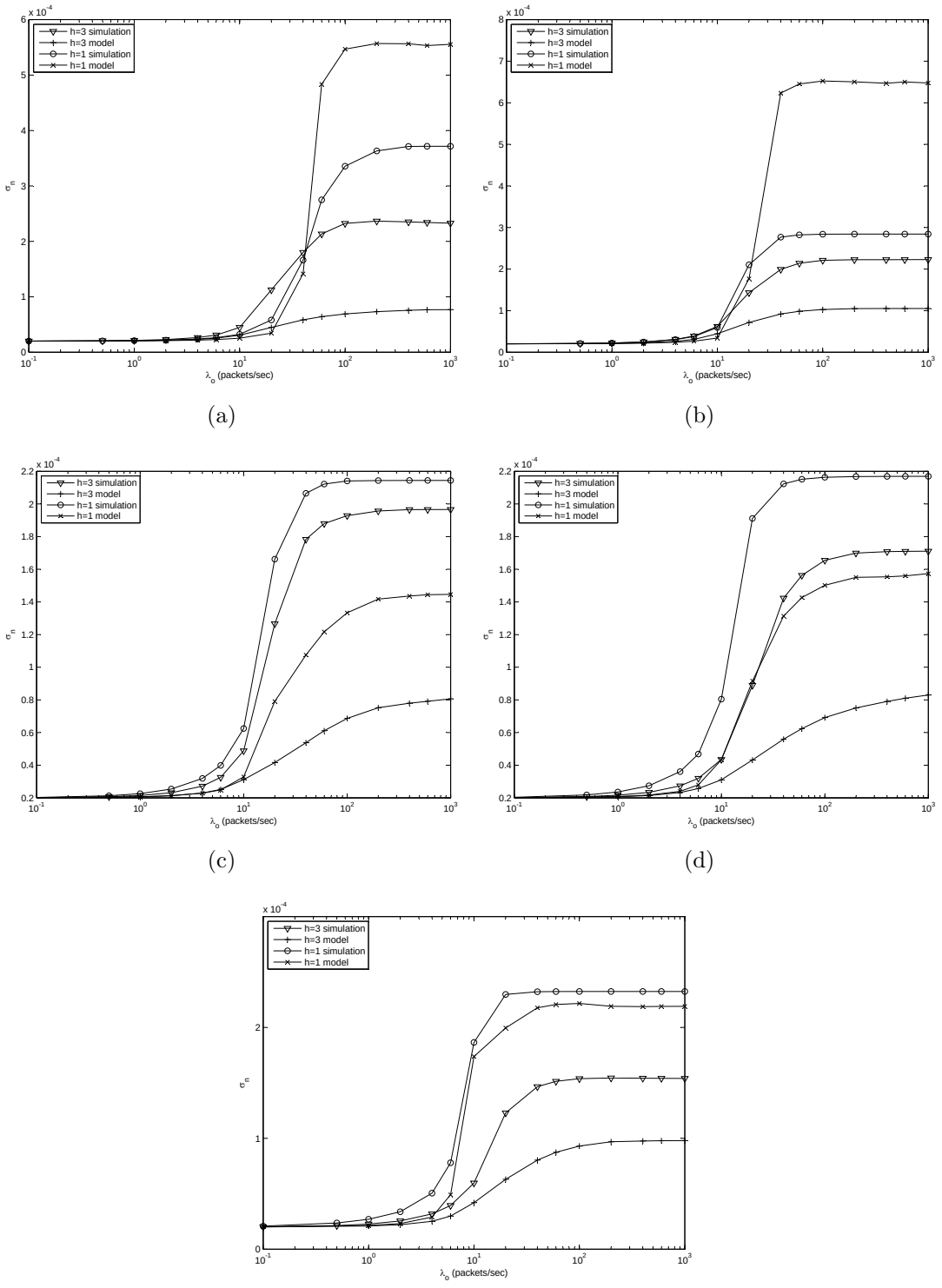

Figure 3.22: The average value of slot duration, $\bar{\sigma_n}$, obtained from analytical model and simulations for: a) 10-node, b) 20-node, c) 50-node, d) 100-node, e) 200-node random topologies and random traffic patterns

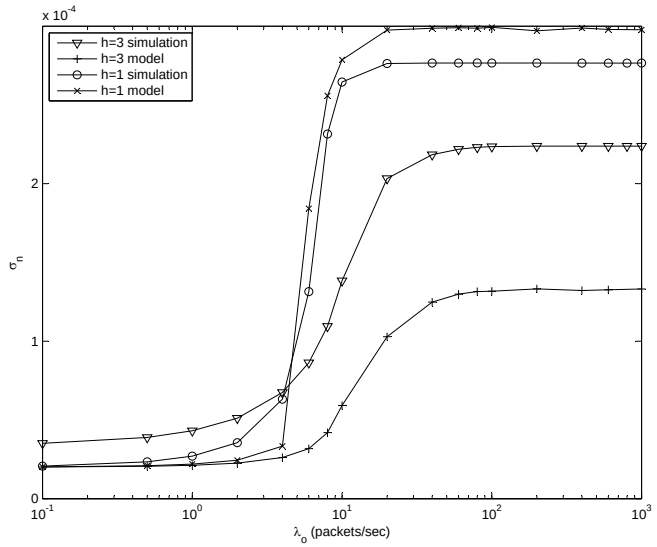

(a)

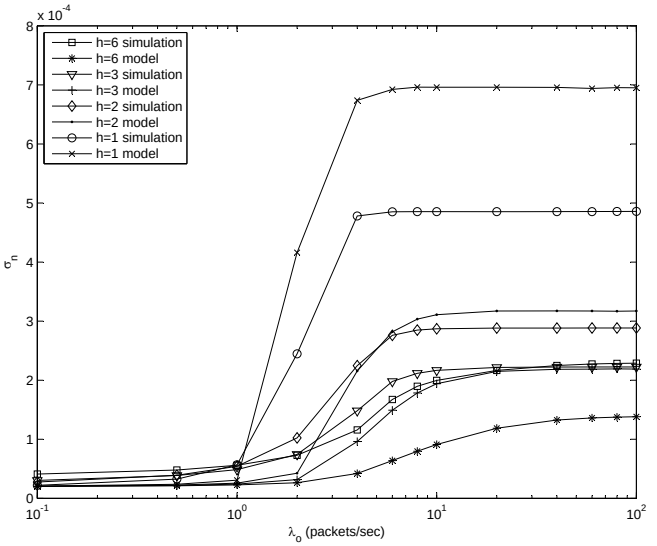

(b)

Figure 3.23: The average value of slot duration, $\bar{\sigma_n}$, obtained from analytical model and simulations for: a) 127-node and g) 469-node hexagonal topologies and regular traffic patterns

3.5.5 Effect of contention window size

The effect of contention window size on the probability of transmission and probability of collision is shown in Fig. 3.24 for the 469-node hexagonal topology. The contention window takes the values $W_0 = \{32, 64, 128\}$. The analytical model is quite good in incorporating the effect of contention window size in calculation of p and τ.

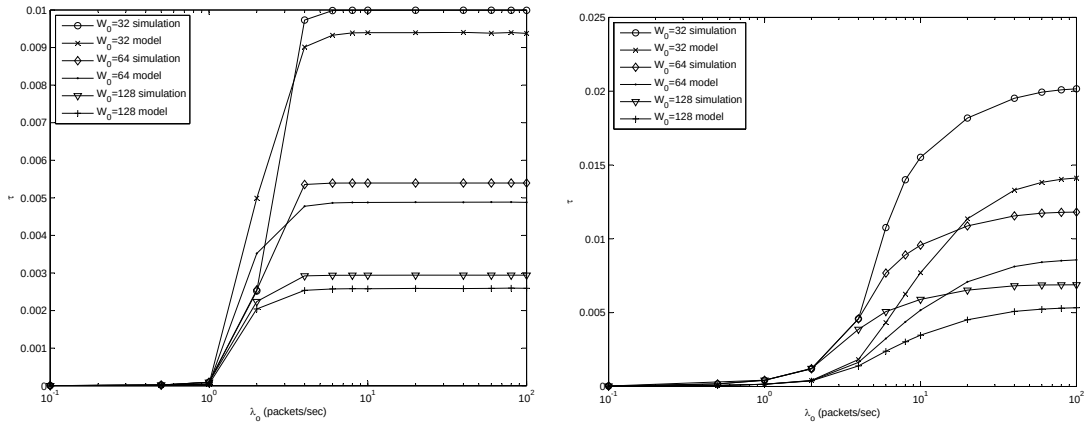

(a) (b)

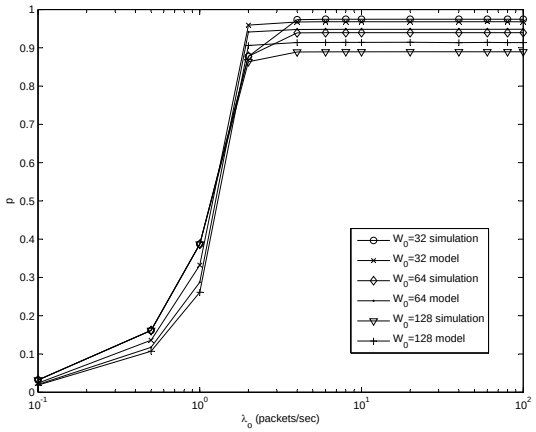

(c)

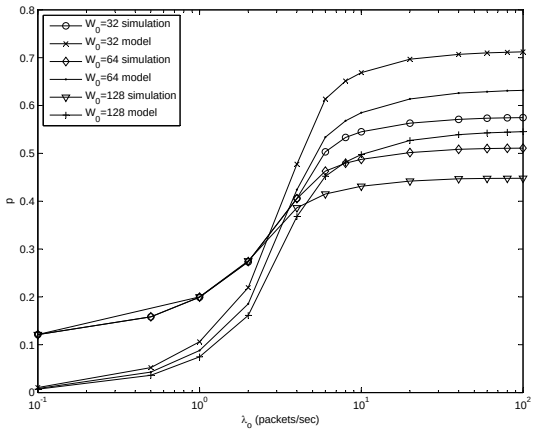

(d)

Figure 3.24: Effect of contention window size, obtained from analytical model and simulations, for the 469-node hexagonal topology: a) τ for $h = 1$, b) τ for $h = 6$, c) p for $h = 1$, d) p for $h = 6$.

Contention window size affects τ and p for moderate-to-heavy traffic loads. τ decreases significantly for direct transmissions and multi-hopping as the minimum contention window size, W_0 is increased, because an increased W_0 implies

longer backoff intervals and less transmission. τ and W_0 behave inversely proportional, where doubling W_0 has an effect of halving τ for direct transmissions. For multi-hop transmissions, the effect of W_0 on τ is significant but not as much as the effect for direct transmissions. Increasing W_0 also decreases p. For direct transmissions, doubling W_0 has an effect of doubling $1 - p$, whereas the effect is not so much for multi-hop transmissions again.

3.5.6 Effect of DATA packet size

The effect of DATA packet size on the probability of transmission and probability of collision is shown in Fig. 3.25 for the 469-node hexagonal topology. The DATA packet takes the values $DATA = \{500, 1000, 2000\}$ bytes plus 72 header bytes.

The DATA packet size has no impact on τ and p for heavy traffic loads, whereas $DATA = 1000$ bytes is observed to result in lower τ and p under low-to-moderate traffic loads.

3.5.7 Effect of maximum retry count

The effect of maximum retry count on the probability of transmission and probability of collision is shown in Fig. 3.26 for the 469-node hexagonal topology. The short retry count (SRC) takes the values $SRC = \{3, 7\}$, whereas the long retry count (LRC) is kept constant. Increasing SRC decreases τ significantly for heavy traffic loads, where the effect is observed to be more with direct transmissions compared to multi-hop transmissions. This is due to the high contention of direct transmissions under heavy traffic loads, which is relieved by the exponentially increased contention window size that is used most of the time with $SRC = 7$. Also, increasing SRC decreases p for heavy traffic loads, due to the exponentially increased contention window size that is used most of the time with $SRC = 7$.

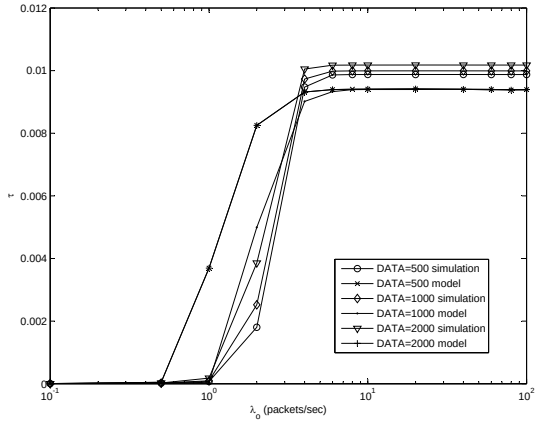

(a)

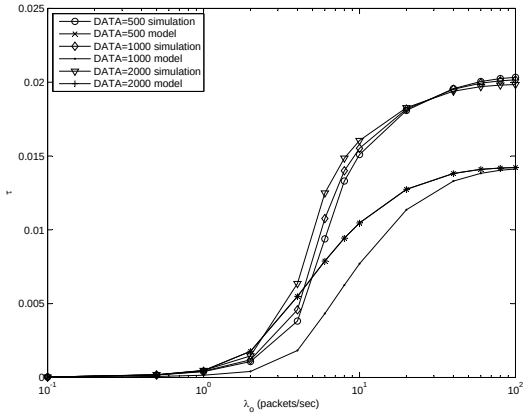

(b)

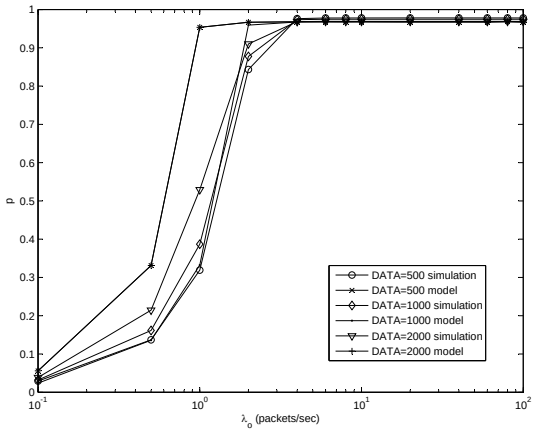

(c)

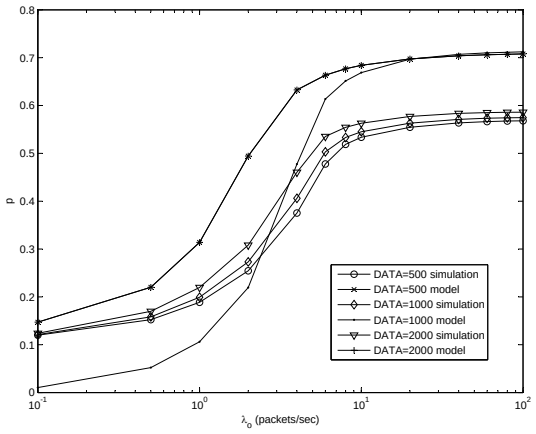

(d)

Figure 3.25: Effect of DATA packet size, obtained from analytical model and simulations, for the 469-node hexagonal topology: a) τ for $h = 1$, b) τ for $h = 6$, c) p for $h = 1$, d) p for $h = 6$.

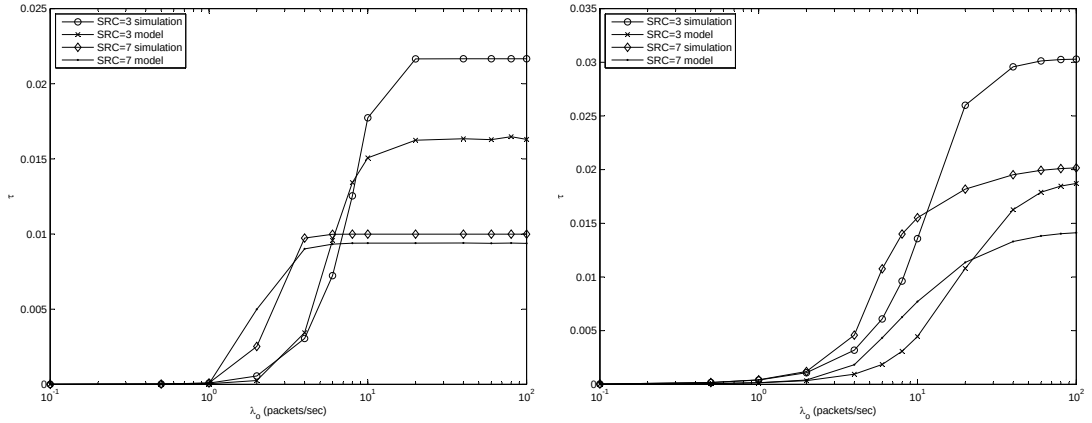

(a) (b)

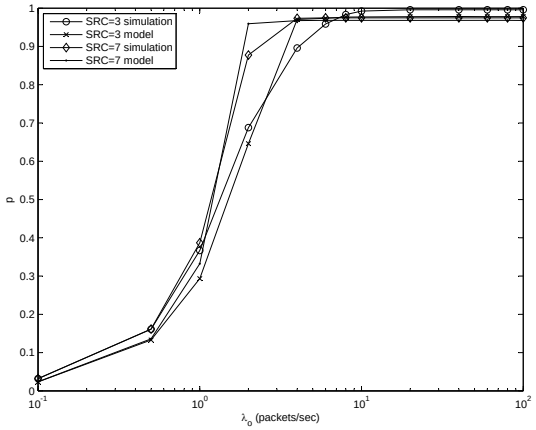

(c)

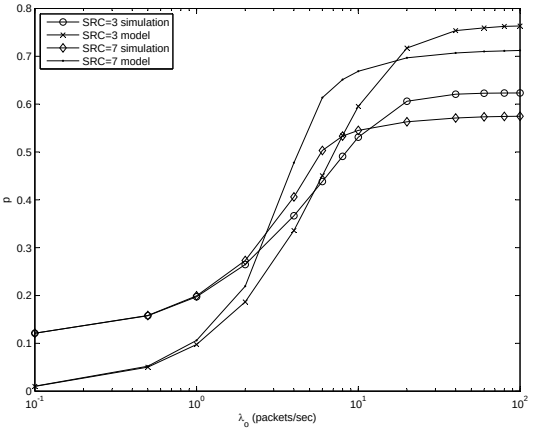

(d)

Figure 3.26: Effect of maximum retry count, obtained from analytical model and simulations, for the 469-node hexagonal topology: a) τ for $h = 1$, b) τ for $h = 6$, c) p for $h = 1$, d) p for $h = 6$.

3.6 Conclusions

An analytical IEEE 802.11 DCF that characterizes a node's behavior in multi-hop networks, which consider hidden terminals, provides fairly accurate results

for large range of traffic loads and works for any given two-dimensional topology and traffic pattern is developed in this chapter. Performance of this model is investigated under different routing strategies. The analytic results obtained via the IEEE 802.11 DCF model supported by simulations, show that the analytical DCF model works fairly well for a large range of traffic loads and networks. It is shown that the analytical DCF model is accurate in predicting the probability of collision, probability of transmission and NAV setting probabilities over a wide range of scenarios. Extensive numerical studies show that the accuracy of all the analytical model in predicting these metrics degrades with the irregularity of the topology and traffic pattern due to the averaging of probability of collision, which is used in developing the DCF model.

We believe that this is also the first study in the literature that provides a quantitative analysis to find the traffic load at which the IEEE 802.11 DCF protocol fails in multi-hop wireless networks for a given set of physical and MAC layer parameters, as opposed to simulation based studies [63, 64].

In this chapter, an analytical IEEE 802.11 DCF model is introduced, which is used for a cross-layer analysis of effect of routing on the goodput and throughput performance of multi-hop wireless networks in the following chapter.

Chapter 4

Goodput and Throughput Analysis of IEEE 802.11 DCF

We present a goodput and throughput analysis for IEEE 802.11 based multi-hop wireless networks that considers carrier sensing, hidden terminals, network allocation vector, intra-path and inter-path interferences, exponential backoff, finite retry limit, finite interface queue buffer sizes, packet drops, overhearing of nodes, etc., and accurately works for a large range of traffic loads.

We are concerned with the average node goodput, which is defined as the *number of data bits per second successfully delivered to the destination, averaged over the all nodes in the wireless network*. We introduce a method for calculation of the average node goodput in an arbitrary network with arbitrary source destination pairs and traffic loads. The average node goodput and throughput of a IEEE 802.11 DCF based multi-hop wireless network is calculated by using the analytical IEEE 802.11 DCF model introduced in Chapter 3. The overhead in IEEE 802.11 mainly comes from backoff, deference, MAC and PHY layer header, management frames and control frames and retransmissions [6].

The primary contribution of this chapter is the introduction of an analytical framework for calculation of goodput and throughput in IEEE 802.11 DCF based multi-hop wireless networks that,

- includes the random access nature of nodes by including the model of the IEEE 802.11 DCF nodes in multi-hop networks,
- models interference of simultaneous transmissions of both different paths and different links of the same path,
- allows paths to cross each other.

The secondary contribution is the demonstration of the effect of routing strategy on the goodput and throughput performance of multi-hop wireless networks. Although multi-hop wireless networks are shown to have limited capacity [64,80,81], their usage may become inevitable in some applications and possible methods that increase the capacity, throughput or goodput should be investigated thoroughly.

An introduction to the goodput and throughput analysis is given next together with a literature review. A theoretical framework to evaluate the goodput and the throughput performance of IEEE 802.11 DCF based networks is introduced in Sec. 4.2 and in Sec. 4.3. Finally, analytical and simulation results are presented in Sec. 4.4.

4.1 Literature Review

In a wireless network of nodes with identical and omni-directional ranges, going from a single hop to 2 hops halves the goodput and throughput of a flow because only one of the two hops can be active at a time. Thus, increasing the hop count from a source to destination is expected to decrease the goodput and thoughput

of the corresponding flow. On the other hand, from a network view of point, the goodput and throughput performance of a network tends to increase due to spatial reuse of the spectrum. Moreover, goodput and throughput performance is vulnerable to medium access control (MAC) related issues such as carrier sensing, collisions, retransmissions, etc [6]. Thus, the inspection of the effect of routing on goodput and throughput performance requires an analysis incorporating an exact MAC behavior.

Despite the fact that random access techniques are pointed out to be suitable to the distributed nature of multi-hop wireless networks [4,12], first analysis based studies that investigate the performance of general multi-hop wireless networks adopt the perfect scheduling and routing assumptions [80, 82–89] in order to simplify the analyzes conducted. The basic question of how multi-hop routing affects the capacity performance of wireless networks has been investigated in these studies mostly under the title of the effect of transmission power. Under a perfect scheduling and routing assumption, capacity performance is shown to increase by multi-hop routing in [12,80,85] and by direct transmissions in [87,90] on the other hand.

The paradoxical effects of power control on the capacity of wireless networks is pointed out in [91]. Through analytic manipulations, the authors concluded that i) under optimum routing and link scheduling, network capacity is increased under the settings of maximal transmission power, ii) when the optimum link selection assumption is relaxed and medium access is done with carrier sensing, higher transmission power for one-hop transmissions decreases network capacity, iii) when optimum routing assumption is replaced with minimum-hop-count routing, then a paradox exists in practice on whether to use higher transmission power to increase network capacity. Although some reasoning is given for the effects of transmission power on capacity under carrier sensing and multi-hop

routing, no analytical model is given and results are obtained by a TDMA simulator that considers exponential backoff and carrier sensing but does not model the MAC properties such as collisions, retransmissions, packet drops. Hence, although the simulation results support the conclusions of the study given above, this study lacks a comprehensive understanding of under which conditions and how transmission power changes capacity, with an overall conclusion of a paradox for the carrier-sense and multi-hop networks.

Some or all features of a random access medium access protocol is used in order to investigate the throughput of IEEE 802.11 DCF based multi-hop networks through simulations in [81, 90, 91] and through analysis in [8, 67, 73, 74, 92–94], which are based on simplified assumptions, owing to the comparable complexity increase when switching from single-hop to multi-hop network architecture. The node throughput is investigated in [8] and in [67, 94] under unsaturated and saturated traffic loads respectively, where hidden terminal effect is not considered. Moreover, [67] assumes that each node is either relay or source. The analysis in [92] calculates the achievable end-to-end path throughput in a network, under traffic loads where the source node is saturated. This analysis accounts for intra-path interference and does not take into account the inter-path interference and its capability is limited to networks where other flows do not intersect the intended path, which restricts its applicability for realistic networks. Thus, this analysis considers only a small portion of hidden terminals that are on the intended path. An analytical model that considers hidden terminal effect in unsaturated networks is derived in [93] for calculation of bandwidth that can be utilized along a path without breaking the QoS requirements of existing traffic in multi-hop IEEE 802.11 networks. The hidden terminal problem is included in the throughput analysis of IEEE 802.11 in [73] and [74], where only 3-node and string topologies are considered, respectively. To the best of our knowledge, there exists no analytical model for calculation of throughput in multi-hop wireless networks that works for arbitrary topologies and large range of traffic

loads while considering hidden terminals, with no assumption on paths and node functionalities.

There are a few studies for analytical evaluation of goodput in wireless networks. Analytical models for goodput in single IEEE 802.11 based wireless local area networks are proposed in [6, 95]. It is shown in [6] that the overhead in goodput of a IEEE 802.11 based network mainly comes from backoff, deference, MAC and PHY layer header, management frames and control frames and retransmissions. To the best of our knowledge there are no analytical models for calculation of goodput in multi-hop wireless networks, which can be used for investigation of the effect of routing.

The dependency of the throughput on traffic load, which is highlighted in [90], is revisited with many studies that simply divided the problem to calculation of throughput under either saturated [67, 73, 74, 92, 94] or unsaturated traffics [8, 93]. An analysis that works accurately for any traffic load and that shows the dependency of throughput on traffic load does not exist up to our knowledge.

4.2 Proposed Goodput Model

In this section, we introduce an analytical goodput model for calculation of the average node goodput and the average network goodput in arbitrary networks with arbitrary source destination pairs and traffic loads. The assumptions given in Sec. 3.4.1 are adopted for the analytical goodput and throughput models.

There are several challenges to take care of during this calculation in a multi-hop network such as

1. parallel transmissions over different paths may take place,

2. parallel transmissions over the same path may take place,

3. packet arrival rates shape the goodput for light traffic loads, whereas MAC specific parameters (such as backoffs, interframe space times, data rates or packet durations) determine the goodput for heavy traffic loads,

4. dropped packets due to finite interface queue buffer size at the PHY layer and dropped packets due to finite retry count at the MAC layer do affect the end-to-end network goodput.

Let us denote a path from source node k to destination node l by γ_{kl}. Also denote the set of paths with source node k by Γ_k.

Definition 1. ***Inter-successful-reception time*** *over the route γ_{kl} is the time between two successive successful DATA packet receptions by the destination node l from the source node k. The inter-successful reception time over the route γ_{kl} is denoted by $\Delta T(\gamma_{kl})$.*

Definition 2. ***Node Goodput*** *of node i, denoted by $G(i)$, is the rate at which DATA frames are successfully delivered by source node i to the network layer at the destination nodes of the paths in the set Γ_i.*

In calculation of node goodput, the bits of retransmissions are not counted in the numerator, but counted as a cost in time in the denominator. Node goodput of node i is calculated by the following equation,

$$G(i) = \frac{b_{DATA}}{\Delta T(i)}, \tag{4.1}$$

where b_{DATA} is the number of bits in the DATA frame and $\Delta T(i)$ is the average of inter-successful-packet reception time of node i averaged over set Γ_i, which is the set of all routes originating from node i. $\Delta T(i)$ is given by

$$\Delta T(i) = \frac{1}{|\Gamma_i|} \sum_{j \neq i : j \in \Gamma_i} \Delta T(\gamma_{ij}). \tag{4.2}$$

For a node to deliver one DATA packet to the network layer of a destination node j, a time of $\Delta T(\gamma_{ij})$ is required. And for a node to deliver one DATA packet to the destination, a total time of $\Delta T(i)$ is required on the average.

Definition 3. ***Network Goodput****, denoted by G_n, is the total rate at which DATA frames are successfully delivered by all nodes in the network to the network layer at the destination nodes.*

Network goodput is given by,

$$G_n = \sum_{i \in V} G(i), \tag{4.3}$$

where V is the set of all nodes in the multi-hop wireless network. The summation over all node goodputs provides a goodput analysis where parallel transmissions in the wireless network are taken into account.

Definition 4. ***Average Node Goodput****, denoted by $\bar{G}$, is the average rate at which DATA frames are successfully delivered by source node i to the network layer at the destination nodes of the paths in the set Γ_i, averaged over all nodes $i \in V$.*

Finally, the average node goodput is given by,

$$\bar{G} = \frac{1}{|V|} \sum_{i \in V} G(i), \tag{4.4}$$

where $|V|$ is the number of all nodes in the multi-hop wireless network.

The rest of this section is devoted to calculation of inter-successful-reception time under both unsaturated and saturated traffic loads.

4.2.1 Inter-successful-reception time

One successfully received packet by the destination of an h-hop path γ_{ij} takes $\Delta T(\gamma_{ij})$ time. This time includes the time spent for dropped packets due to finite interface queue buffer size at the PHY layer and dropped packets due to finite retry count at the MAC layer, which degrade the node and network goodputs. $\Delta T(\gamma_{ij})$ is simply the time required for all necessary successful/failure

transmissions over the first hop plus the time required for the final successful transmission to proceed until new transmissions take place in the first hop, i.e. until parallel transmissions over the same path γ_{ij} become independent from the transmission of the successful packet in question. This way, a goodput analysis that takes care of parallel transmissions over the same path is provided.

Calculation of the time required for all necessary successful/failure transmissions over the first hop depends either on arrival rates under light traffic loads or on MAC specific parameters under heavy traffic loads. In order to calculate the time spent over first hop for one successful packet reception at the destination, we first define the times required for one successful and dropped transmission over a link and give the calculations. Afterwards, the definitions regarding the number of successful/failure transmissions over the first hop is given and the required quantities are calculated. Note that for one successful packet to be finally received at the destination of path γ_{ij} with $h > 1$, more than one successful transmissions may take place at the first hop if P_{ifq} or p is nonzero, since some of these successful packets are dropped at the IFQ or the link. The IEEE 802.11 DCF mechanism retransmits a packet for a finite number of times and drops the packet after M retries, thus the packets counted at the first hop of transmission are different from the successfully received packet by the final destination (except the single successful transmission at the first hop), but time spent for these packets are counted while computing the inter-successful-reception time. This way, the effect of dropped packets are included in the goodput calculations, giving us valuable information on how dropped packets degrade the goodput.

Let us denote the duration over a link for one successful transmission by T_{succ+} and for a dropped packet by T_{drop+}. One successful transmission over a link, includes the retransmissions that is less than the maximum retry limit M and one successful transmission. T_{succ+} and T_{drop+} include the time spent for control packets, idle times due to backoff mechanisms and interframe spaces,

given by:

$$\begin{aligned} T_{succ+} &= \bar{n}_M(DIFS + T_{RTS} + SIFS + T_{CTS} + EIFS) \\ &\quad + T_{retrybackoff} \\ &\quad + DIFS + T_{RTS} + T_{CTS} + T_{DATA} + T_{ACK} + 3SIFS \\ &\quad + T_{succbackoff}, \\ T_{drop+} &= M(DIFS + T_{RTS} + SIFS + T_{CTS} + EIFS) \\ &\quad + T_{dropbackoff}, \end{aligned} \tag{4.5}$$

where $\bar{n}_M$ is the average number of retries calculated as follows:

$$\bar{n}_M = \sum_{i=0}^{M-1} ip^i(1-p) + Mp^M. \tag{4.6}$$

$T_{succbackoff}$ is the average duration of backoff after one successful transmission over a link and $T_{dropbackoff}$ is the average duration of backoff during one dropped packet over a link due to exceeding retry count over a link, that are given by

$$\begin{aligned} T_{retrybackoff} &= \sum_{0}^{\bar{n}_M} \frac{W_i}{2}\bar{\sigma}, \\ T_{succbackoff} &= \frac{W_0}{2}\bar{\sigma}, \\ T_{dropbackoff} &= \sum_{0}^{M-1} \frac{W_i}{2}\bar{\sigma}. \end{aligned} \tag{4.7}$$

The parameters $p, \bar{\sigma}$ and $P_{ifq}(i)$ for node i, which are used for the calculation of inter-successful-reception time, are obtained by the analytical IEEE 802.11 DCF model introduced in Chapter 3.

For the calculation of the average node goodput, let us define $N_{succ}(\gamma_{ij}, 1)$ as the number of successful transmissions on the first hop, $N_{drop}(\gamma_{ij}, 1)$ as the number of packet drops that take place on the first hop and $N_{dropIFQ}(\gamma_{ij}, 1)$ as the number of packet drops at the IFQ at the first node of the h-hop path γ_{ij}, node i, for a single successful DATA packet to be received by the destination. Each h-hop path γ_{ij} consists of nodes $\{i \equiv x_0(\gamma_{ij}), x_1(\gamma_{ij}), ..., x_{h-1}(\gamma_{ij}), j \equiv x_h(\gamma_{ij})\}$ illustrated in Fig. 4.1. For one successful transmission over the first hop to reach

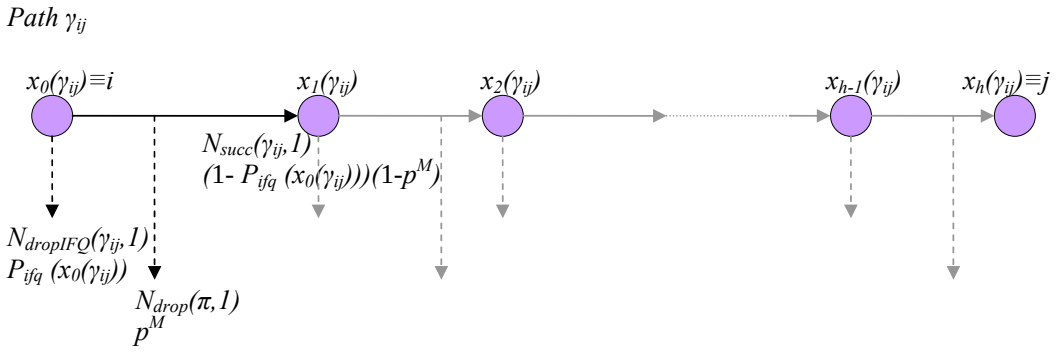

Figure 4.1: Illustration of number of successful/dropped packets over first hop of the h-hop path γ_{ij}: $N_{succ}(\gamma_{ij},1)$, $N_{drop}(\gamma_{ij},1)$ and $N_{dropIFQ}(\gamma_{ij},1)$

the final destination, the DATA packet should be transmitted successfully over the rest $h-1$ hops with probability $(1-p^M)^{h-1}$ and should not be dropped at the interface queues of nodes $\{x_1(\gamma_{ij}), x_1(\gamma_{ij}), ..., x_{h-1}(\gamma_{ij})\}$. Thus, the probability that one successful transmission over the first hop reaches the final destination is $(1-p^M)^{h-1}\prod_{j=1}^{h-1}(1-P_{ifq}(x_{h-j}(\gamma_{ij})))$, and the number of successful transmissions over the first hop needed for one successful reception at the final destination is the reciprocal of this probability, giving us $N_{succ}(\gamma_{ij},1)$, given by

$$N_{succ}(\gamma_{ij},1) = ((1-p^M)^{h-1}\prod_{j=1}^{h-1}(1-P_{ifq}(x_{h-j}(\gamma_{ij}))))^{-1}. \tag{4.8}$$

Since $N_{succ}(\gamma_{ij},1)$ successful transmissions over the first hop take place with probability $1-p^M$ for each packet, the number of dropped packets over the first hop becomes $\frac{p^M}{(1-p^M)}$ times the number of successful transmissions over the first hop, which are dropped with probability p^M due to exceeding maximum retry limit. Hence, $N_{drop}(\gamma_{ij},1)$ is obtained as:

$$N_{drop}(\gamma_{ij},1) = N_{succ}(\gamma_{ij},1)\frac{p^M}{(1-p^M)}. \tag{4.9}$$

A packet at the entry of IFQ of node $x_0(\gamma_{ij})$ reaches the final destination successfully with probability $(1-P_{ifq}(x_0(\gamma_{ij})))X$, where $X = (1-p^M)^h\prod_{j=1}^{h-1}(1-P_{ifq}(x_{h-j}(\gamma_{ij})))$, so $\frac{1}{(1-P_{ifq}(x_0(\gamma_{ij})))X}$ packets should come to the entry of IFQ of node $x_0(\gamma_{ij})$ until one successful reception at the final destination, among these

packets $\frac{1}{X}$ of them enter the IFQ. Thus, the number of dropped packets at the first IFQ, $N_{dropIFQ}(\gamma_{ij},1)$ becomes $\frac{P_{ifq}(x_0(\gamma_{ij}))}{(1-P_{ifq}(x_0(\gamma_{ij})))X}$ leading to

$$N_{dropIFQ}(\gamma_{ij},1) = (P_{ifq}(x_0(\gamma_{ij}))(1-p^M)^h \prod_{j=1}^{h}(1-P_{ifq}(x_{h-j}(\gamma_{ij})))^{-1}. \tag{4.10}$$

The inter-successful-reception time is calculated differently under unsaturated and saturated traffic loads, which is given next.

Unsaturated Traffic

The inter-successful-reception time over the h-hop path γ_{ij} under unsaturated traffic is composed of two terms, the time required at the interface queue of $x_0(\gamma_{ij})$ for accumulation of $N_{succ}(\gamma_{ij},1)$, $N_{drop}(\gamma_{ij},1)$ and $N_{dropIFQ}(\gamma_{ij},1)$ packets plus the time required for a single successful transmission to proceed over the next hops, excluding the hops where independent intra-path transmissions may take place.

$\Delta T(\gamma_{ij})$, the inter-successful-reception time over the h-hop path γ_{ij} under unsaturated traffic depends on the arrival rate of packets to the first node of path γ_{ij}. One successful reception at the destination costs $N_{succ}(\gamma_{ij},1)$ successful transmissions and $N_{drop}(\gamma_{ij},1)$ dropped packets at the first hop, and $N_{dropIFQ}(\gamma_{ij},1)$ packet drops at the interface queue of the first node of the path γ_{ij}. Hence, under unsaturated traffic, time required over first hop is equal to at least the duration required for $N_{succ}(\gamma_{ij},1)+N_{drop}(\gamma_{ij},1)+N_{dropIFQ}(\gamma_{ij},1)$ packets to arrive at the first IFQ, which is $\frac{1}{\lambda_t}(N_{succ}(\gamma_{ij},1)+N_{drop}(\gamma_{ij},1)+N_{dropIFQ}(\gamma_{ij},1))$.

The time required over the rest of the hops is composed of the duration of a successful transmission plus the waiting time at the interface queues over the next hops at which parallel intra-path transmissions (parallel to the transmissions of

first hop) can not occur. The independent hops where parallel intra-path transmissions may occur is dependent on the geometry of nodes and carrier sensing range and transmission range of transmissions. For a linear path with equal hop lengths and equal carrier sensing range and transmit ranges, the transmissions over the second and third hops- if these hops exist- is dependent on the transmission over the first hop, whereas parallel intra-path transmissions may occur at the rest of the hops. In order to simplify the goodput analysis, we assume that the dependent intra-path transmissions occur at the second and third hops of path γ_{ij} on the average.

As a result, the calculation of the inter-successful-reception time, $\Delta T(\gamma_{ij})$, is composed of the time required for transmissions over the first hop plus the time required for one successful transmission over the second and third hops and waiting times at the interface queues of nodes $x_1(\gamma_{ij})$ and $x_2(\gamma_{ij})$ of path γ_{ij}. Thus, $\Delta T(\gamma_{ij})$ under unsaturated traffic becomes

$$\begin{aligned}\Delta T(\gamma_{ij}) &= min(h-1,2)T_{succ+} \\ &+ \sum_{k=1}^{min(h-1,2)} E[T_W](x_k(\gamma_{ij})) \\ &+ \frac{1}{\lambda_t}(N_{succ}(\gamma_{ij},1) + N_{drop}(\gamma_{ij},1) + N_{dropIFQ}(\gamma_{ij},1)),\end{aligned} \tag{4.11}$$

where $E[T_W](k)$ is the expected waiting time at the IFQ of node k. The $\Delta T(\gamma_{ij})$ is obtained by addition of $min(h-1,2)T_{succ+}$ to the time required over first hop, which corresponds to time required for successful transmission over rest of the hops and addition of $\sum_{k=1}^{min(h-1,2)} E[T_W](x_k(\gamma_{ij}))$, which is the time spent waiting at the queue of next IFQs. The calculation of $E[T_W]$ of an M/G/1/K queue is given in Appendix B.

Saturated Traffic

The inter-successful-reception time over the h-hop path γ_{ij} under saturated traffic is composed of two terms, the time required to send $N_{succ}(\gamma_{ij},1)$ and $N_{drop}(\gamma_{ij},1)$

packets over the first hop plus the time required for a single successful transmission to proceed over the next hops, excluding the hops where independent intra-path transmissions may take place. $\Delta T(\gamma_{ij})$ under saturated load becomes

$$\begin{aligned}\Delta T(\gamma_{ij}) &= min(h-1,2)T_{succ+} \\ &+ \sum_{k=1}^{min(h-1,2)} E[T_W](x_k(\gamma_{ij})) \\ &+ N_{succ}(\gamma_{ij},1)T_{succ+} + N_{drop}(\gamma_{ij},1)T_{drop+},\end{aligned} \tag{4.12}$$

Under saturated traffic, since IFQ becomes never empty, the time required to sent $N_{succ}(\gamma_{ij},1) + N_{drop}(\gamma_{ij},1)$ packets over the first hop dominates the time required over first hop, which is $N_succ(\gamma_{ij},1)T_{succ+} + N_{drop}(\gamma_{ij},1)T_{drop+}$. The required time over the rest of the hops to transmit the successful packet to the destination is obtained by an addition of duration of $min(h-1,2)T_{succ+} + \sum_{k=1}^{min(h-1,2)} E[T_W](x_k(\gamma_{ij}))$.

Combining the results in Equations (4.11) and (4.12), the inter-successful-reception time over the h-hop path γ_{ij}, $\Delta T(\gamma_{ij})$, becomes

$$\begin{aligned}&\Delta T(\gamma_{ij}) = min(h-1,2)T_{succ+} \\ &+ \sum_{k=1}^{min(h-1,2)} E[T_W](x_k(\gamma_{ij})) \\ &+ max(\frac{1}{\lambda_t}(N_{succ}(\gamma_{ij},1) + N_{drop}(\gamma_{ij},1) + N_{dropIFQ}(\gamma_{ij},1)), \\ &N_{succ}(\gamma_{ij},1)T_{succ+} + N_{drop}(\gamma_{ij},1)T_{drop+}).\end{aligned} \tag{4.13}$$

Having found the inter-successful-reception time over path γ_{ij}, the node goodput, the network goodput and the average node goodputs are obtained by Equations (4.1), (4.3) and (4.4), respectively.

4.3 Throughput Model

Definition 5. ***Average node throughput*** *is the number of bits successfully transmitted per second by a node averaged over all nodes in the network.*

The average node throughput is the rate of successful delivery of packets at the link layer, thus any retransmission increases the average node throughput.

The calculation of average node throughput is adopted from the IEEE 802.11 DCF based analyzes for single-hop networks [7,8] and for multi-hop networks [8], and is given by:

$$S = \frac{\tau(1-p)b_{DATA}}{\bar{\sigma_n}}, \tag{4.14}$$

where b_{DATA} is the number of bits of DATA packet including headers, τ is the probability of transmission, p is the collision probability and $\bar{\sigma_n}$ is the average slot duration calculated in Equation (3.3).

4.4 Numerical Results

Node goodput and node throughput performance of routing strategies are studied for different topologies deployed in a fixed area: a hexagonally placed 127-node regular topology with $h = \{1, 3\}$; a hexagonally placed 469-node regular topology with $h = \{1, 2, 3, 6\}$; and 32 randomly generated topologies (10 with 10, 10 with 20, 5 with 50, 4 with 100 and 3 with 200 nodes) with $h = \{1, 3\}$ are compared through analysis and simulations. The effects of contention window size, DATA packet size and maximum retry count on average node goodput and throughput are investigated for the 469-node hexagonal topology. For the hexagonal topologies, source-destination pairs are chosen so that all possible linear paths carry traffic, while for the random topologies all source destination pairs that have a three-hop path in between are chosen. The hexagonal topology is homogeneous

in topology and traffic distribution, whereas the random topologies have no homogeneity. The simulations are conducted using Network Simulator 2, version ns-allinone-2.34 [79]. The parameters used for both the analytical model and the simulations are the same as the parameters listed in Table 3.2 in Chapter 3.

4.4.1 Average node goodput

The average node goodput computed by the analytical model and simulations for random topologies of size 10, 20, 50, 100 and 200 in Fig. 4.2, and hexagonal topologies of sizes 127 and 469 nodes are plotted in Fig. 4.3. Average node goodput in simulations is calculated by dividing the total number of bits of DATA frames successfully received by the network layers of all destinations by the simulation duration times the total number of nodes in the wireless network.

The goodput increases under light traffic and decreases as the traffic increases. An error of up to 50% is observed during the moderate traffic rates. The error stems from misleading DCF model calculations for a small interval of moderate traffic loads. The error is especially large for the 10-node and 20-node topology case where the error due to averaging operations of the DCF model is large. The results show that under light traffic, goodput is independent of the routing strategy whereas goodput is maximized by direct transmissions for heavy traffic loads. For moderate traffic rates, the optimum routing strategy that maximizes goodput depends on the network density. Among the networks considered in this study, for the 200-node random network, the 127-node and 469-node hexagonal networks, goodput increases with routing for moderate traffic loads. For the 200-node random network goodput is increases up to 50%, for the 127-node hexagonal topology goodput is increased more than twice and for the 469-node hexagonal topology goodput is increased up to six times by multi-hopping for moderate traffic rates. On the other hand, goodput is increased by direct transmission for heavy traffic loads. Goodput that tends to vanish to zero by multi-hopping by

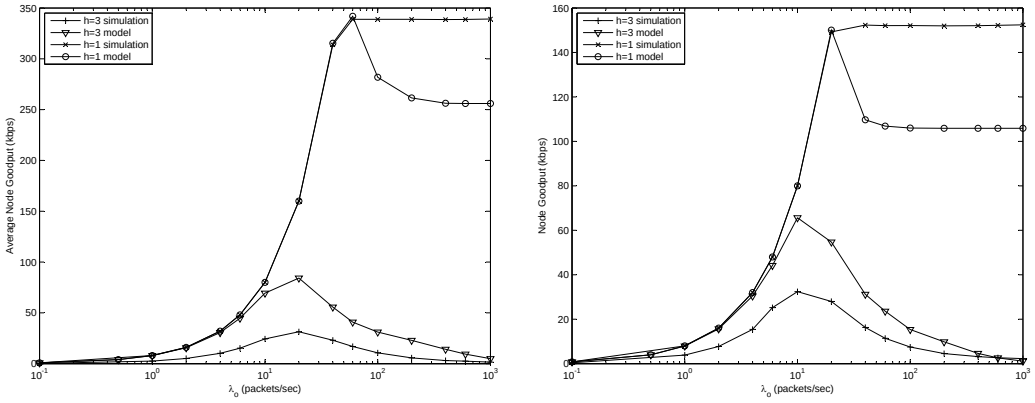

(a)

(b)

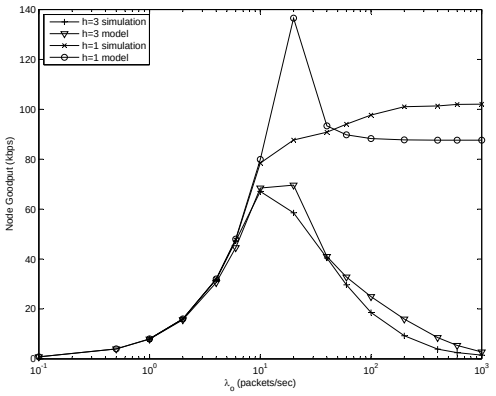

(c)

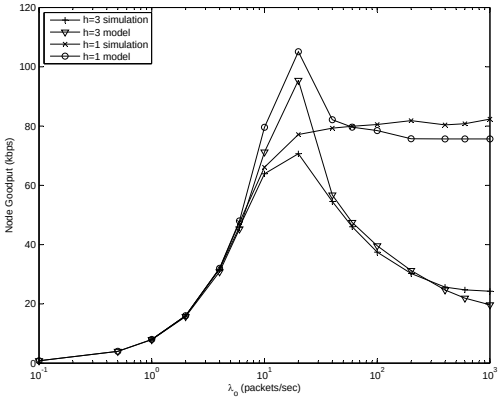

(d)

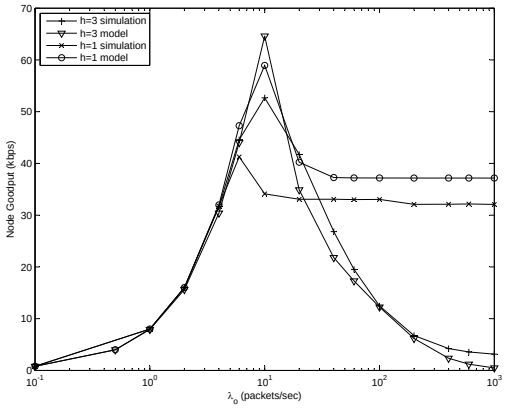

(e)

Figure 4.2: Average node goodput obtained from analytical model and simulations for a) 10-node, b) 20-node, c) 50-node, d) 100-node, e) 200-node random topologies and random traffic patterns

increased traffic loads, is kept constant at a rate of about 100*kbps* for the 50-node random topology, at about 80*kbps* for the 100-node random topology, at about 40*kbps* for the 200-node random topology, at about 25*kbps* for the 127-node

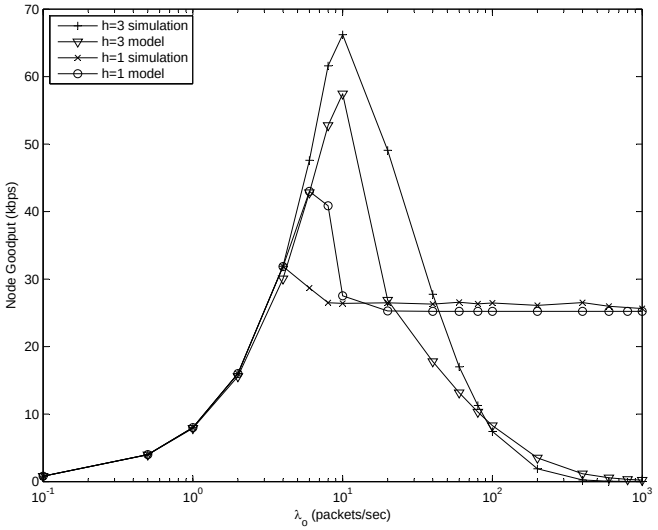

(a)

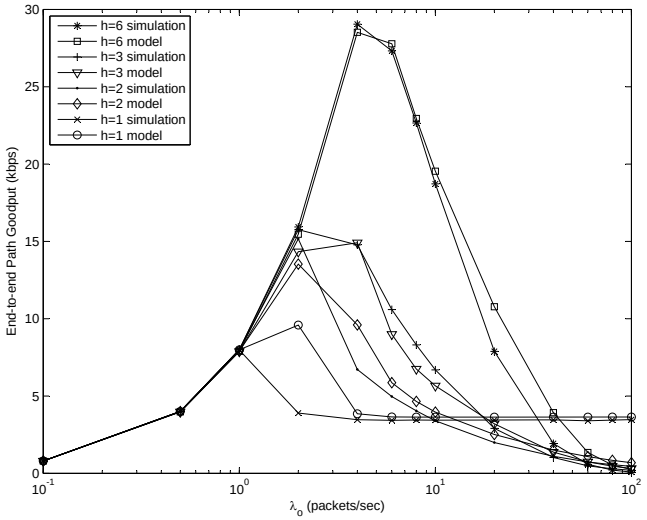

(b)

Figure 4.3: Average node goodput obtained from analytical model and simulations for a) 127-node and d) 469-node hexagonal topologies and regular traffic patterns

hexagonal topology and at about $5kbps$ for the very dense 469-node hexagonal topology (at which 126 nodes share the same channel).

4.4.2 Average node throughput

The average node throughput computed by the analytical model and simulations for random topologies of size 10, 20, 50, 100 and 200 are plotted in Fig. 4.4,

and for hexagonal topologies of size 127 and 469 nodes are plotted in Fig. 4.5.

Average node throughput in simulations is calculated by dividing the total

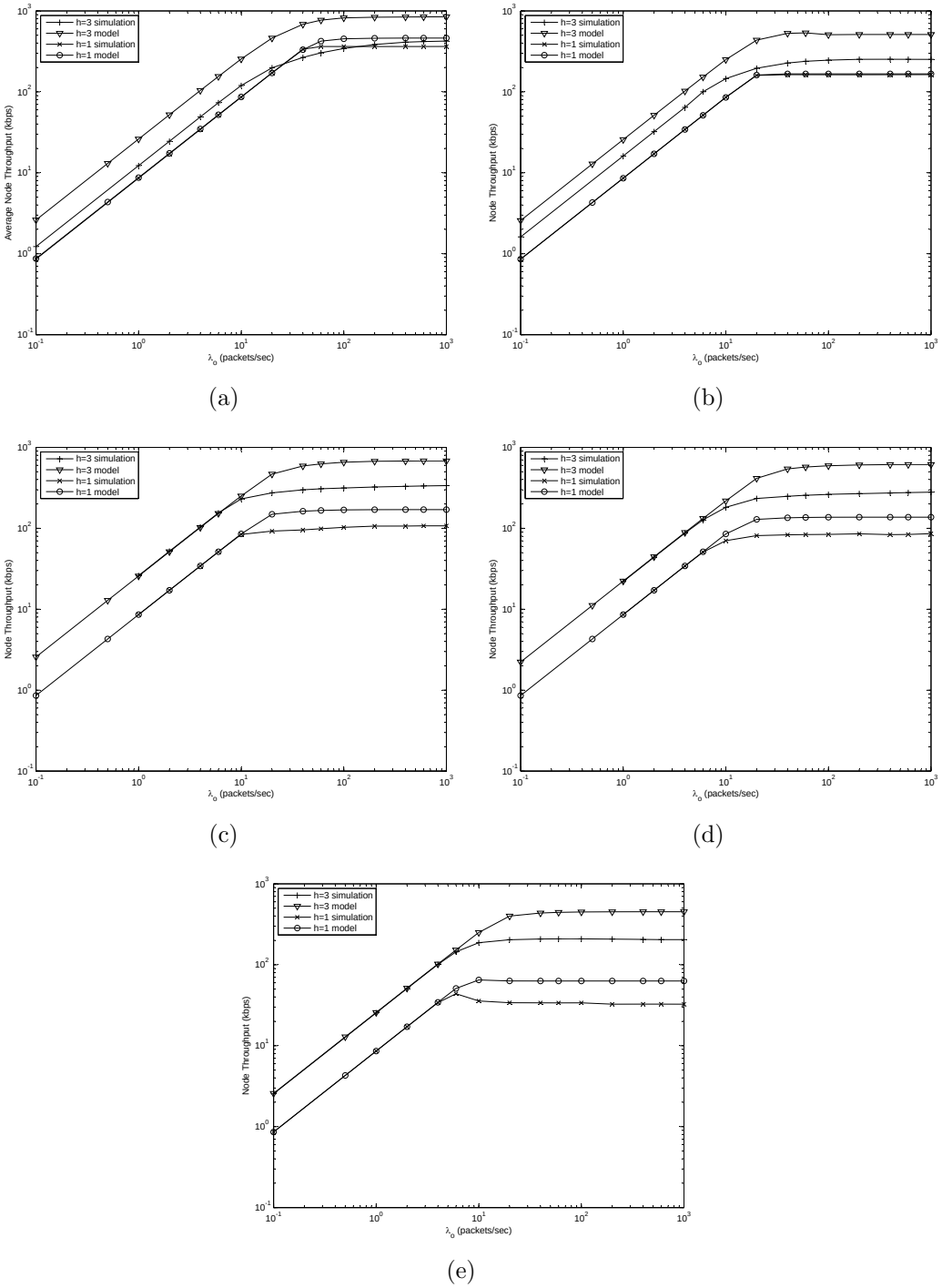

Figure 4.4: Average node throughput obtained from analytical model and simulations for a) 10-node, b) 20-node, c) 50-node, d) 100-node, e) 200-node random topologies and random traffic patterns

number of bits of DATA frames successfully received by the link layers of all

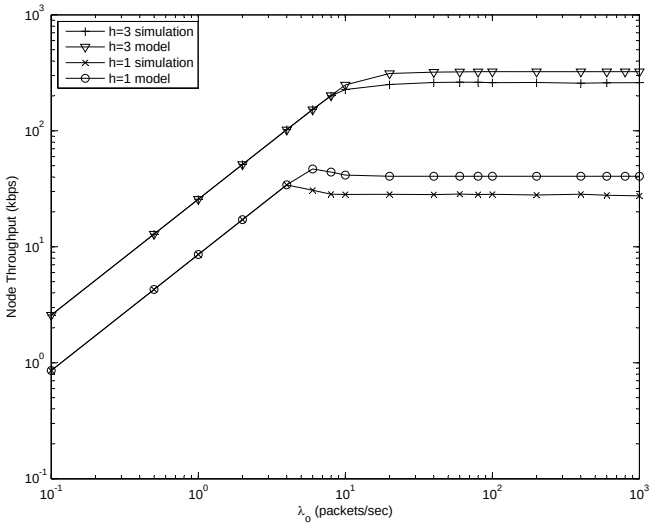

(a)

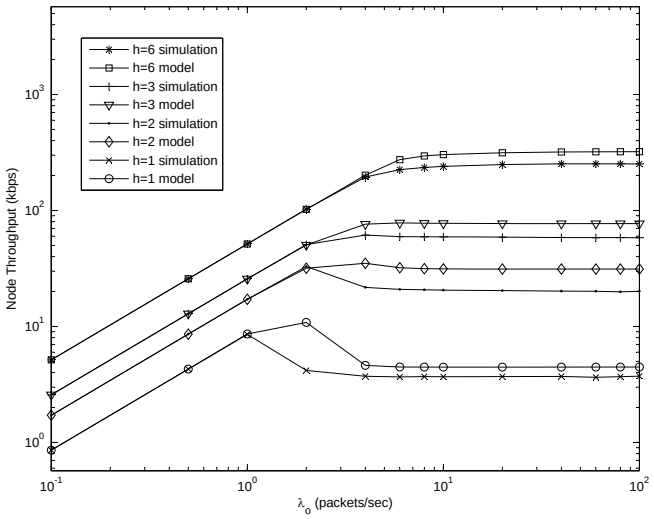

(b)

Figure 4.5: Average node throughput obtained from analytical model and simulations for a) 127-node and d) 469-node hexagonal topologies and regular traffic patterns

nodes by the simulation duration times the number of nodes in the wireless network.

Average node throughput is observed to increase with increasing traffic load until it becomes constant at heavy traffic loads, where packets are retransmitted/dropped due to increased congestion. The most important observation is that, throughput is increased for multi-hopping for large networks, except the

10-node network for moderate traffic loads. The saturation traffic load decreases for increased network size.

The accuracy of the analytical throughput model is observed to be quite well for large networks, where errors exists at throughput calculation for heavy traffic loads. The accuracy is observed to degrade for the 10-node random network, where direct transmissions may become more throughput efficient due to edge effects. This is a parallel result with the capacity related study [87], where direct transmissions is shown to increase capacity for networks of sizes up to 10 nodes.

4.4.3 Effect of contention window size

The effect of contention window size on the average node goodput and throughput is shown in Fig. 4.6 for the 469-node hexagonal topology. The contention window takes the values $W_0 = \{32, 64, 128\}$. Increasing minimum contention window size, W_0, is observed to increase both goodput and throughput for direct transmissions, and has almost no effect for multi-hop transmissions. Recall from Fig. 3.24 that, increasing W_0 decreases τ and increases $1 - p$. It turns out that the change in the amount of these MAC parameters resulting from variations of W_0, affects goodput and throughput values obtained for direct transmissions, and has no effect for multi-hop transmissions.

4.4.4 Effect of DATA packet size

The effect of DATA packet size on the average node goodput and throughput is shown in Fig. 4.7 for the 469-node hexagonal topology. The DATA packet size takes the values $DATA = \{500, 1000, 2000\}$ bytes plus 72 header bytes. Increasing the DATA frame size increases average node goodput and throughput

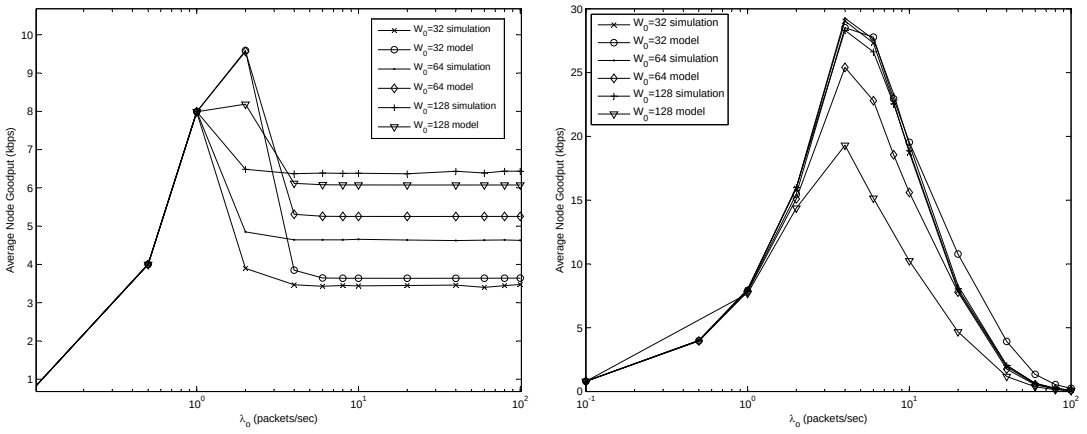

(a) (b)

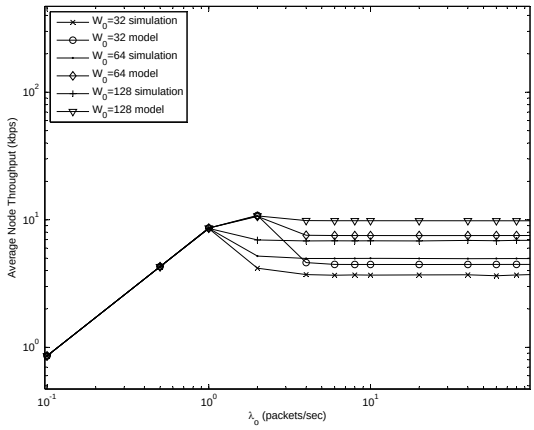

(c)

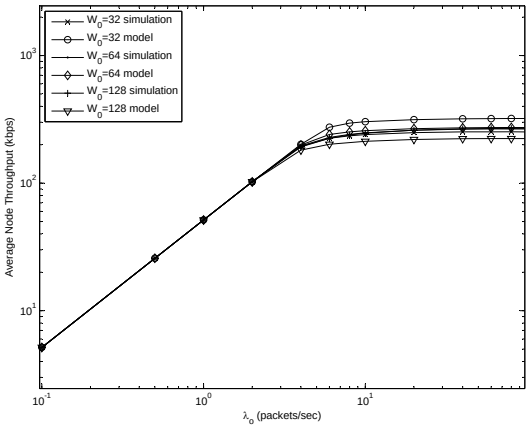

(d)

Figure 4.6: Effect of contention window size, obtained from analytical model and simulations, for the 469-node hexagonal topology: a) average node goodput for $h = 1$, b) average node goodput for $h = 6$, c) average node throughput for $h = 1$, d) average node throughput for $h = 6$.

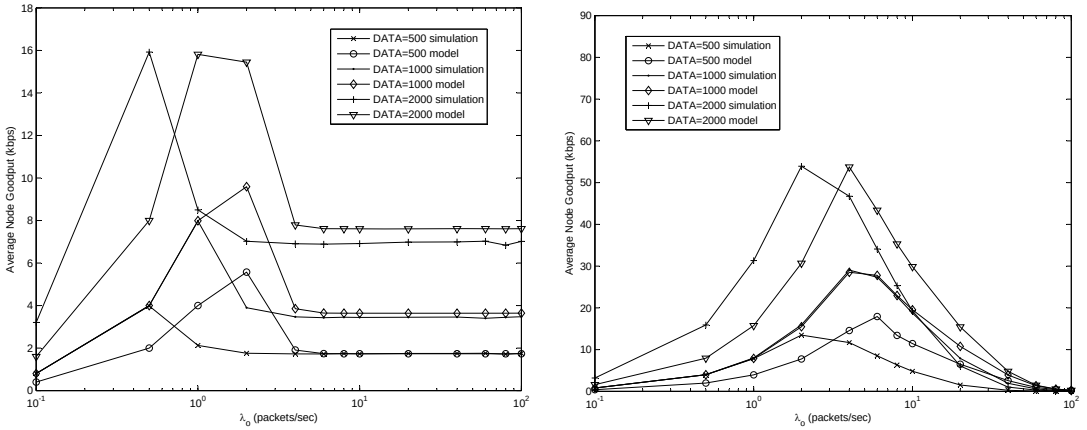

(a) (b)

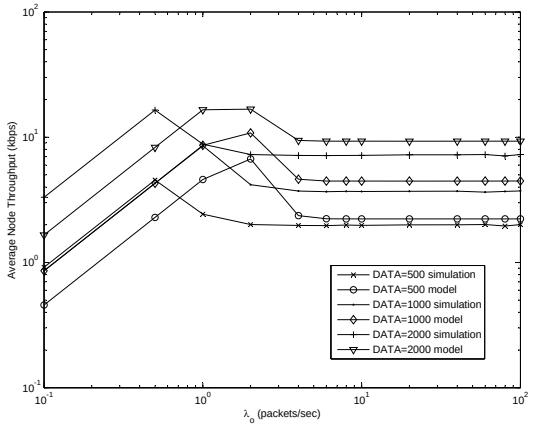

(c)

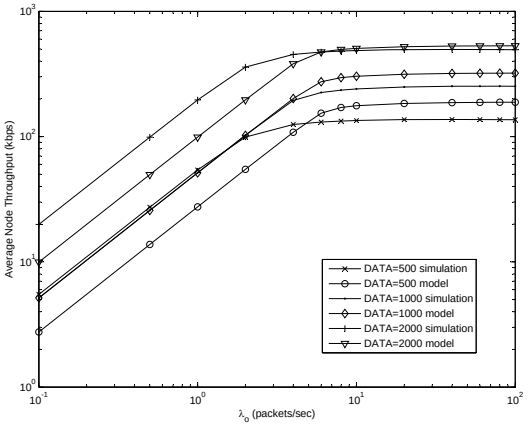

(d)

Figure 4.7: Effect of DATA packet size, obtained from analytical model and simulations, for the 469-node hexagonal topology: a) average node goodput for $h = 1$, b) average node goodput for $h = 6$, c) average node throughput for $h = 1$, d) average node throughput for $h = 6$.

significantly for heavy traffic loads. This shows that the effect of DATA frame size on inter-successful-reception time is negligible.

4.4.5 Effect of maximum retry count

The effect of maximum retry count on the average node goodput and throughput is shown in Fig. 4.8 for the 469-node hexagonal topology. The short retry count, SRC, takes the values $SRC = \{3, 7\}$ while the long retry count, LRC, is kept constant. Increasing SRC results with an increased average node goodput and throughput for heavy traffic loads with both direct transmissions and multi-hop transmissions, whereas the effect is not as significant as the effect of contention window and DATA frame size. This is due to the exponentially increased contention window size that is used most of the time with $SRC = 7$.

4.5 Conclusions

In this chapter we introduce a method for calculation of average node goodputs and the average node throughput in a 802.11 DCF based multi-hop wireless network with arbitrary source destination pairs and traffic loads. The goodput calculation considers the performance degradation due to packet drops that occur because of interface queue buffer overflow at the PHY layer and because of finite retry count at the MAC layer.

The goodput and throughput performance of IEEE 802.11 multi-hop networks under various routing strategies is investigated. The analytic results obtained via the IEEE 802.11 DCF model introduced in Chapter 3 and the analytic goodput model, supported by simulations, show that selection of routing strategy based on the traffic load increases goodput significantly. Under light traffic, arrival rate of packets is responsible for most of the inter-successful-reception time

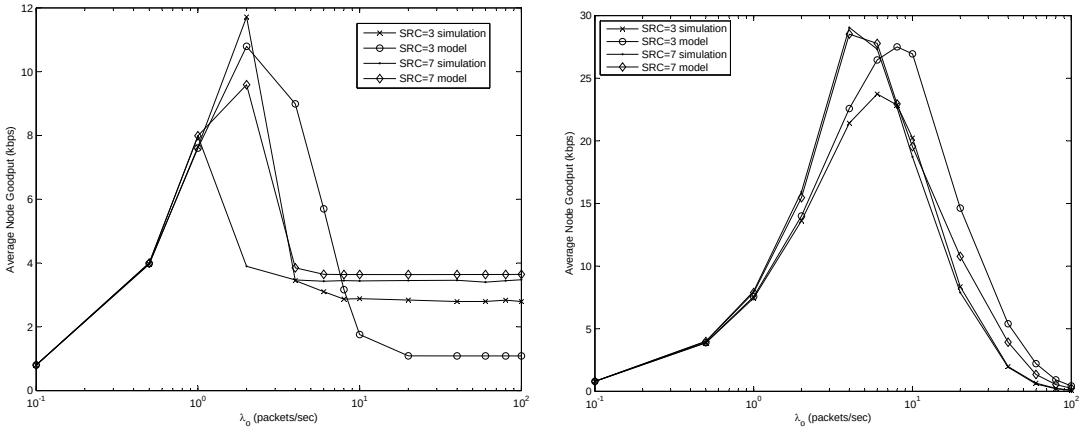

(a)

(b)

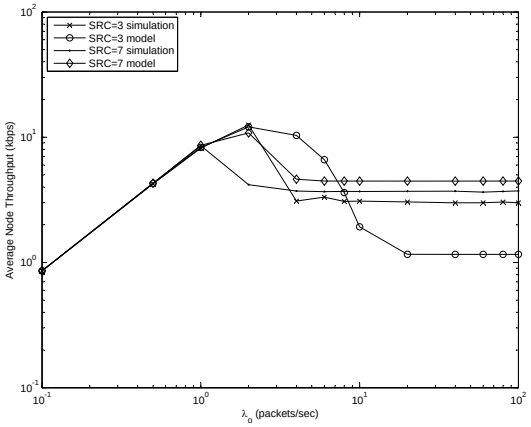

(c)

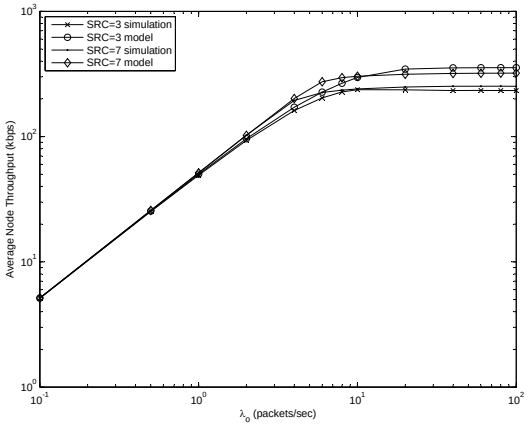

(d)

Figure 4.8: Effect of maximum retry count, obtained from analytical model and simulations, for the 469-node hexagonal topology: a) average node goodput for $h = 1$, b) average node goodput for $h = 6$, c) average node throughput for $h = 1$, d) average node throughput for $h = 6$.

consumed, making any routing strategy equivalently optimum. Under moderate traffic, parallel concurrent transmissions dominate and multi-hop transmissions become more advantageous. At heavy traffic, multi-hopping results with excessive traffic congestion due to increased packet collisions, where the inter-successful-reception time goes to infinity, and direct transmissions increase goodput. It is also shown that the increasing the contention window size, the DATA packet size and maximum retry limit result in significant increases in goodput and throughput, whereas the impact of maximum retry limit is smaller.

We also demonstrate that under the IEEE 802.11 DCF protocol, goodput and throughput behave differently in multi-hop networks. We show through analysis and simulations that:

1. Node throughput is network density dependent. Direct transmissions, i.e. high transmission power, increases node throughput in small networks. Multi-hop transmissions, i.e. low transmission power, increases node throughput in large multi-hop networks.

2. Node goodput, on the other hand, is not only network dependent but also traffic load dependent. Multi-hop transmissions increases node goodput in dense networks under moderate traffic loads, else direct transmissions increase node goodput.

3. Under heavy traffic rates, goodput performance drops extremely with multi-hop transmissions, whereas throughput performance is constant. The reason behind this diverse behavior is that goodput is the rate achieved by the network layer, where only successfully received packets by the final destinations increase the goodput. On the other hand, throughput is the rate achieved by the link layer, where any successful transmission at a link increases throughput.

Goodput behaves different than throughput in multi-hop wireless networks and we argue that it is important to investigate the techniques that optimize goodput performance. As a result we show that, optimum selection of a routing strategy increases goodput considerably in multi-hop wireless networks.

Goodput results obtained by the analytical model over a large range of traffic loads and observing the asymptotic behavior as traffic load goes to infinity, show that for typical networks high transmission power increases goodput, i.e. direct transmission increases goodput, and goodput degrades as the hop number increases. The analytical goodput and throughput model presented in this chapter is the first analytical effort to bring extensions to the effects of power control on the goodput and throughput performance of wireless networks. The optimum link scheduling and optimum routing assumptions of capacity related studies are relaxed in this dissertation by not only a simplistic carrier sensing assumption but also a comprehensive modelling of IEEE 802.11 DCF in multi-hop networks, which takes carrier sensing, hidden terminals, intra-path and inter-path interferences, exponential backoff, finite retry limit, finite interface queue buffer sizes, packet drops, overhearing of nodes etc. into account.

After investigation of the effect of routing on the goodput and throughput performance of multi-hop wireless networks in this chapter, the effect of routing on the energy performance is investigated in the following chapter.

Chapter 5

Energy Analysis of IEEE 802.11 DCF

Recall that the problem investigated in this dissertation is to determine the routing strategy that increases energy and/or goodput/throughput performance in multi-hop wireless networks where MAC contention -specifically the IEEE 802.11 DCF- is considered. Having developed an analytical model for the IEEE 802.11 DCF in multi-hop networks, the next step is investigation of the effect of routing strategy on energy performance in multi-hop wireless networks, which is the subject of this chapter.

Cross-layer design of energy-efficient routing protocols is shown to play a dominant role in reducing power consumption [21, 30–33]. Contention at the MAC layer and the relaying strategy used by the routing protocol at the network layer are expected to affect each other and energy-efficiency. Under transmit power control, the energy consumed at the PHY layer decreases when switching from direct transmission to multi-hopping, which in turn decreases the number of contending stations within the transmission range. A decreased number of contending stations implies less contention, a decreased number of collisions,

retransmissions, backoff and freezing mechanisms at the MAC layer, and less overhearing, which decrease the overall energy consumption. On the other hand, multi-hopping requires successful transmissions at all hops of the path and energy is lost when packet is lost at some hop. The relaying strategy used by the routing protocol at the network layer has impacts on MAC layer parameters, affecting energy-efficiency. Thus, for energy-efficient selection of routes, the behavior of MAC layer should be carefully contemplated.

Studies related to energy-efficient routing given in the next section reveal that the optimum energy-efficient routing strategy depends on the relative ratios of energy consumed during transmission, reception and processing overhead. But, the impact of contention at the MAC layer on energy-efficiency, which results in collisions and retransmissions, and energy cost of overhearing by the neighboring nodes, has not been considered so far in the decision of routing strategy in multi-hop wireless networks. In this chapter, we propose a comprehensive energy model which finds out the energy consumption for successfully delivering one bit of data to its destination in a multi-hop wireless network considering carrier sensing, collisions, freezing mechanism in backoff and extra energy consumption due to overhearing.

There have been efforts on evaluating the energy consumption performance of IEEE 802.11 DCF in single-hop networks but none for multi-hop networks, due to the lack of an analytical model for IEEE 802.11 DCF that considers hidden terminals and works for various large topologies where an energy analysis is meaningful.

The energy consumption analysis in IEEE 802.11 DCF based multi-hop wireless networks is built on top of the DCF model developed in the previous and has the same primary features as the IEEE 802.11 DCF model. So that the energy model

- considers hidden terminals,
- provides fairly accurate results for large range of traffic loads,
- works for any given two-dimensional topology,
- increases the accuracy and scalability of the analytical model by joint use of fixed and variable slots
- allows each node to be both source and/or relay.

We begin this chapter by a literature review of studies, which are grouped into two subcategories: studies related to energy-efficient routing, and studies incorporating analytical modelling efforts of energy in IEEE 802.11 DCF based wireless networks. Energy consumption analysis that is based on EPB metric is given in Sec. 5.2.2. Computed analytical results and simulation results are given next, followed by conclusions.

5.1 Literature Review

In this section, an overview of studies that investigate the effect of routing on energy performance in multi-hop wireless networks is followed by a literature review of energy models that incorporate IEEE 802.11 DCF.

5.1.1 Effect of routing on energy performance

Many minimum-energy routing protocols consider solely the energy consumption at the amplifier due to transmission, ignoring the energy consumed at the transmitter and receiver circuitry for the reception and processing of the packets. For example, the Minimum Total Transmission Power Routing Protocol (MTPR)

selects the route with minimum sum of link transmission powers, favoring multi-hop paths [14, 15].

However signal processing associated with packet transmission and reception, and even hardware operation in the standby mode, consumes non-negligible energy as well [34]. Moreover, many cross-layer communication techniques that reduce transmit power require a significant amount of signal processing. Although it is widely assumed that the energy required for this processing is small and continues to decrease with ongoing improvements in hardware technology [35], the results in [34] suggest that these energy costs are still significant.

Studies that have considered energy consumption due to reception and processing at nodes have shown that routing through multiple short-hops is not always more energy-efficient than longer hops, favoring direct hop transmission [36–40].

The optimum number of hops in a chain network where only the end node is transmitting to the sink is studied in [36]. The optimum number of hops is shown to be dependent on the ratio of energies consumed for transmission and relaying overhead, and total distance from source to sink. These results are extended in [37] and the optimum one-hop transmission distance for different rates of energies consumed for transmission and relaying overhead for randomly distributed location of nodes. The optimum one-hop transmission distance determines the number of hops that are required to reach the destination.

In [38], a chain where all nodes are senders is taken into account, and it is shown that the optimum spacing between nodes should follow a decreasing trend towards the sink, contrary to [37] that suggests a constant optimum spacing. This is a consequence of the fact that, when each node in the chain generates traffic, the nodes closer to the sink are exposed to more relay traffic consuming more

power. Hence, compensation of this additional energy consumption is possible by a decreased spacing toward the sink node.

The energy-efficient routing strategy among single-hop and two-hop transmissions in a three-node basic network is studied in [39], as a function of the angle between the nodes. The results of this study also reveal that the energy-efficient routing strategy among direct transmission and multi-hopping depends on the ratio of transmission energy to the relaying overhead.

A comparison of energy-efficiency of direct transmission with minimum-transmission-energy (MTE) routing protocol is made in [38] for a randomly distributed nodes in a large network and it is shown that MTE performs worse than direct transmission when transmission energy is on the same order as receive energy, which occurs when transmission distance is short and/or the radio electronics energy is high.

A discussion of disadvantages multi-hop routing, called as short-hop routing, are given in [42, 96]. The reasons why short-hop routing is not as beneficial as it is regarded in the literature are listed for providing an insight to the problem. Additional to the relative values of reception and transmission, it is pointed out interference, end-to-end reliability, sleep modes, traffic accumulation, etc. are some of the factors that work against short-hop transmissions.

The problem of routing is considered in [97] for large wireless networks of randomly distributed nodes with Rayleigh fading channels. It is shown that routing over many short hops is not as advantageous in a Rayleigh network as it is for the networks that are based on the geometric deterministic disc model.

5.1.2 Energy models for the IEEE 802.11 DCF

The energy consumption of IEEE 802.11 network interface cards is measured experimentally on a simple scenario with one station performing as the transmitter and the other as the receiver in [98–101]. None of these studies include the energy consumption due to contention which is the nature of the DCF protocol.

The authors in [102] have proposed mathematical models to analyze energy consumption of some MAC protocols including IEEE 802.11 in single-hop networks and showed that MAC protocols that aim to reduce the number of contentions reduce energy consumption. The analysis ignores binary exponential backoff mechanism and hence does not model the IEEE 802.11 DCF protocol accurately. The authors in [103] analyzed energy consumption of IEEE 802.11 WLANs based on the p-persistent CSMA scheme and obtained the theoretical performance bounds of energy consumption by deriving the optimum p values that minimizes the energy consumption. Energy consumption is observed to be more for higher number of contending stations and larger packet sizes. The analysis in [103] is based on basic access scheme and saturated traffic conditions and approximates the binary exponential backoff technique of IEEE 802.11 DCF by the p-persistent model.

In [68] and [104] analytic models which characterize IEEE 802.11 MAC energy consumption in a single-hop network under saturated traffic conditions are proposed. The retry limit is assumed to be finite in [68] and infinite in [104]. Both models consider the binary exponential backoff and account for the IEEE 802.11 DCF protocol by encapsulating the carrier sensing, collisions, and freezing mechanism in backoff. In [68], the effects of transmission rate, packet size, different power consumption rates for transmit, receive and idle modes on energy efficiency in case of RTS/CTS exchange are investigated. It is shown that the power consumption in receive and idle modes is responsible for most of the energy consumed whereas the transmit energy has little impact, and energy consumption

is shown to be more for higher number of contending stations and larger payloads. In [104], the effects of using basic access or RTS/CTS exchange, transmission rate, contention window size, and packet size are investigated and shown that energy consumption is more for basic access (as opposed to RTS/CTS exchange), for higher number of contending stations, lower data rates and lower contention window sizes.

Despite the various studies conducted on energy-efficiency of IEEE 802.11 DCF based single-hop networks [68,98–104], the energy consumption of the IEEE 802.11 DCF protocol in a multi-hop wireless network is not mathematically modelled so far. The underlying reason is that there is no existing analytical model for IEEE 802.11 DCF in large scale multi-hop wireless networks.

5.2 Proposed Energy Model

In this section, we propose an energy model which finds out the energy consumption for successfully delivering one bit of DATA to its destination in a IEEE 802.11 based multi-hop network considering carrier sensing, collisions, freezing mechanism in backoff and energy consumption due to overhearing.

5.2.1 Assumptions

The assumptions given in Sec. 3.4.1 are adopted for the energy model. In this chapter, we additionally assume that the PHY layer may be in transmit, receive, idle or sleep mode and denote the power consumed by Pwr_{tx}, Pwr_{rx}, Pwr_{idle} and Pwr_{sleep}, respectively. We neglect the power consumption in the sleep mode.

5.2.2 Energy per bit

The total energy cost of transmitting one successful bit over a path is called *Energy Per Bit (EPB)* and is given by

$$EPB = E_{tx} + E_{rx} + E_{overhear} + E_{idle}, \tag{5.1}$$

where E_{tx} (E_{rx}) is the total energy per bit consumed by all path nodes for transmitting (receiving), $E_{overhear}$ is the total energy per bit consumed by all path and neighbor nodes while overhearing, i.e., receiving packets intended for other nodes, and E_{idle} is the energy spent during idle modes of the transceiver. Path nodes are the source and destination nodes plus any relay nodes in between. Neighboring nodes are the nodes inside the union of transmission areas of all path nodes, excluding the path nodes. The path nodes consume energy while transmitting/receiving and overhearing; and the neighbor nodes consume energy while overhearing. Inclusion of the energy spent during idle mode corresponds no sleeping regime and exclusion of it corresponds to a perfect sleeping regime adapted in the wireless network.

EPB is calculated by considering the energy consumed by a DATA packet and any related control packets, collisions, retransmissions and packet drops due to that specific DATA packet. For a single successful DATA packet to be received by the destination, a total of N_{succ} successful transmissions and N_{drop} packet drops take place on the average, over an h-hop path. Let us denote a path from source node k to destination node l by γ_{kl}. Also denote the set of all paths in the network by Γ. Each h-hop path γ_{kl} consists of nodes $\{k \equiv x_0(\gamma_{kl}), x_1(\gamma_{kl}), ..., x_{h-1}(\gamma_{kl}), l \equiv x_h(\gamma_{kl})\}$. N_{succ} and N_{drop} are obtained by averaging the total number of successful/failed transmissions over all h-hop paths $\gamma_{kl} \in \Gamma$:

$$N_{succ} = \frac{1}{|\Gamma|} \sum_{\gamma_{kl} \in \Gamma} \{\sum_{i=0}^{h-1} ((1-p^M)^i \prod_{j=1}^{i} (1 - P_{ifq}(x_{h-j}(\gamma_{kl}))))^{-1}\}, \tag{5.2}$$

$$N_{drop} = N_{succ} \frac{p^M}{(1-p^M)}.$$

Let us denote the duration where transmit or receive energy is spent over a link for one successful transmission by T_{succ} and for a dropped packet by T_{drop}:

$$T_{succ} = \bar{n}_M T_{RTS} + T_{CTS} + T_{DATA} + T_{ACK},$$

$$T_{drop} = M T_{RTS}.$$

$\bar{n}_M$ is the average number of retries and is calculated in Equation (4.6).

T_{busy} denotes the total time duration where transmit or receive energy is spent over an h-hop path which is given by

$$T_{busy} = N_{succ} T_{succ} + N_{drop} T_{drop}.$$

E_{tx} and E_{rx} are given by

$$E_{tx} = \frac{1}{b_{DATA}} Pwr_{tx} T_{busy},$$
$$E_{rx} = \frac{1}{b_{DATA}} Pwr_{rx} T_{busy}.$$

A specific transmission flowing through an h-hop path consumes no additional energy at an overhearing node if the NAV of the overhearing node is already set. Recalling that P_{idle} is a conditional probability conditioned on the event that the node is carrier sensing with zero NAV, and noting that the probability that a node is carrier sensing with zero NAV is $1-\tau$, the unconditional probability that NAV of a node is not set becomes $(1-\tau)P_{idle}$. Since the number of overhearing nodes is $n-2$, excluding the transmitter and receiver, we have $(n-2)(1-\tau)P_{idle}$ overhearing nodes with zero NAV. Thus, we obtain

$$E_{overhear} = \frac{(n-2)(1-\tau)P_{idle} Pwr_{rx} T_{busy}}{b_{DATA}}.$$

5.2.3 Idle energy per bit

In this section, we find out the idle energy consumption for successfully delivering one bit of DATA to its destination in a IEEE 802.11 based multi-hop network.

Idle energy is consumed during idle waiting, carrier sensing, backoff and freezing mechanism in backoff in case no sleeping regime is employed. The total idle energy cost of transmitting one successful bit over a path is denoted by E_{idle}.

In order to compute the idle energy dissipated per bit, the time duration necessary for successful reception of one frame by the destination is required. This is the average inter-successful-reception time, denoted by $\bar{\Delta T}$ and calculated as

$$\bar{\Delta T} = \frac{1}{|V|} \sum_{i \in V} \Delta T(i).$$

where $\Delta T(i)$ is obtained in Equation (4.2).

Path nodes dissipate transmission and reception power, and neighbor nodes dissipate reception power for T_{busy} duration until a frame is successfully received by the destination. Recall that the number of overhearing nodes is $(n-2)(1-\tau)P_{idle}$. Thus, during ΔT, the time that each node remains idle is approximately $\Delta T - T_{busy}\{2 + (n-2)(1-\tau)P_{idle}\}$. E_{idle} is given by

$$E_{idle} = \frac{Pwr_{idle}}{b_{DATA}}(\bar{\Delta T} - T_{busy})\{2 + (n-2)(1-\tau)P_{idle}\}.$$

Note that the calculation of EPB stated above requires calculation of the following IEEE 802.11 MAC parameters in a multi-hop wireless network: $p, P_{idle}, \tau, P_{ifq}, T_{rs}$ and T_{rc}, that are obtained in Chapter 3.

5.3 Numerical Results

Energy consumption of direct transmission and multi-hopping are compared using the analytical energy model developed for IEEE 802.11 DCF based wireless networks. The model is applied to several random topologies deployed in a fixed area consisting of 10, 20, 50, 100 and 200 nodes and to hexagonal 127-node and 469-node regular topologies. The effects of contention window size, DATA packet

Table 5.1: Power consumption values used for both the analytical model and simulation runs.

Pwr_{tx}	$1.425 + 0.25h^{-\eta}$ W
Pwr_{rx}	1.425 W
Pwr_{idle}	1.319 W

size and maximum retry count on energy consumption are investigated for the 469-node hexagonal topology. Each path is traversed either by direct transmission or by multi-hopping. In case of multi-hopping, transmission power is reduced so as to reach the next hop. For the hexagonal topology, source-destination pairs are chosen so that all possible linear paths carry traffic, while for the random topologies all source destination pairs that have a three-hop path in between are chosen. The hexagonal topology is homogeneous in topology and traffic distribution, whereas the random topologies have no homogeneity. The simulations are conducted using Network Simulator 2, version ns-allinone-2.34 [79]. The parameters used for both the analytical model and the simulations are the same with the parameters listed in Table 3.2. Energy specific parameters are listed in Table 5.1. The power consumption values of transmit, receive and idle modes of the $2.4GHz$ IEEE 802.11b Wavelan card are adapted [105].

5.3.1 Total EPB

We first assume that nodes have perfect sleeping mechanisms and hence the energy spent in idle mode is neglected. The average EPBs computed by the analytical model and simulations for random topologies of size 10, 20, 50, 100 and 200 nodes are plotted in Fig. 5.1 as a function of the average packet generation rate λ_o. The results show that the energy model is quite well in predicting the EPB for a random multi-hop networks. The model predicts the energy consumption fairly well for a wide range of traffic loads. The error observed for random topologies stems from computation of average values for p and geometry related variables in order to come up with a computationally tractable analytical model.

As the number of nodes in the network increases, more energy-efficient three-hop-path alternatives emerge and EPB difference between $h = 1$ and $h = 3$ increases under moderate traffic. At heavy traffic load, EPB with multi-hopping increases sharply due to heavy collisions and increased number of retransmissions, and high offered traffic load make the network unstable.

It is observed that EPB increases as the node density is increased due to increased receive energy consumption by increased number of overhearing nodes. Furthermore, multi-hopping ($h = 3$) becomes more energy-efficient than direct transmission ($h = 1$) at moderate traffic loads as the number of nodes and hence the density increases. This is due to the fact that denser networks allow more energy-efficient multi-hop paths.

Since the numerical solution of the analytical model requires substantially long computation times, we used hexagonal topologies with 127 and 469 nodes in order to study larger networks since the symmetric nature of this topology simplifies calculations. EPB computed by the analytical model and simulations for the hexagonal topologies as a function of the packet generation rate λ_o are shown in Fig. 5.2. The error is less compared to random topologies due to the homogeneity of the hexagonal topology and traffic. It is observed that multi-hopping is significantly more energy-efficient than direct transmission under light-to-moderate traffic for the dense and regular hexagonal topology. More discernible energy savings with $h = 6$ is due to the availability of many multi-hop paths with equal hop lengths.

Previous studies on minimum-energy routing consider solely the energy consumption at the amplifier due to transmissions and it is stated in these studies that multi-hop paths are more energy-efficient [14,15]. Based on our results, this statement is valid only for low-to-moderate traffic loads and for dense topologies where more energy-efficient alternative multi-hop paths exist. Consideration of MAC contention changes the optimum routing strategy to direct transmission

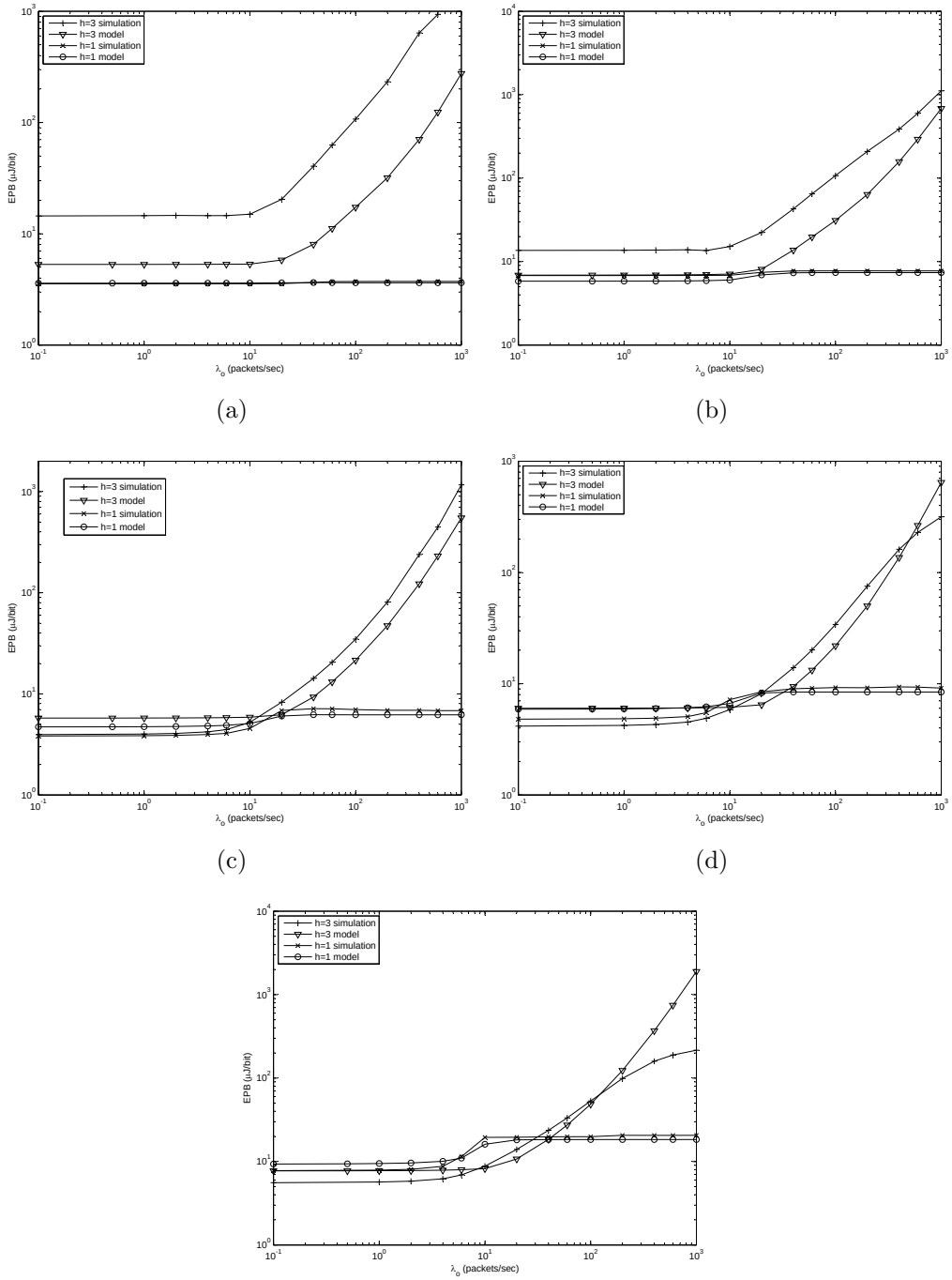

Figure 5.1: EPB obtained from analytical model and simulations without inclusion of energy consumed in the idle mode for a) 10-node, b) 20-node, c) 50-node, d) 100-node, e) 200-node random topologies and random traffic patterns

at heavy traffic loads, reducing the energy consumption by $400\% - 500\%$ for random topologies and by 2-orders of magnitude for the hexagonal topology and the energy saving increases as the traffic gets heavier.

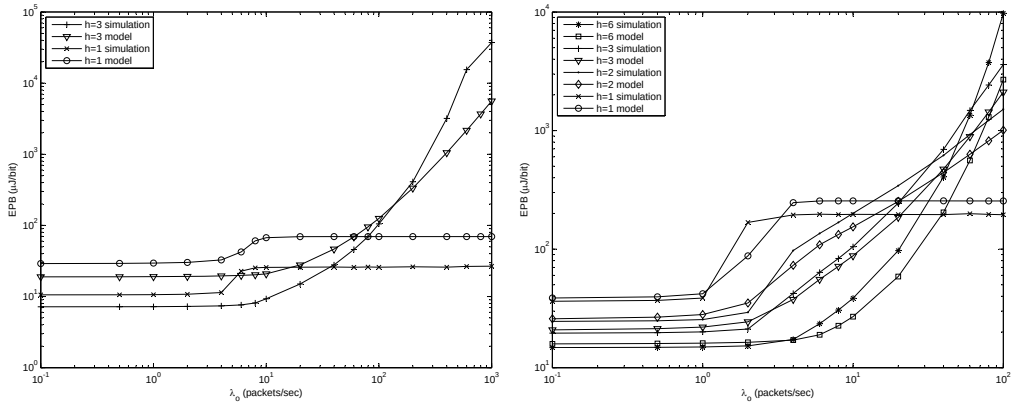

(a) (b)

Figure 5.2: EPB obtained from analytical model and simulations without inclusion of energy consumed in the idle mode for a) 127-node and f) 469-node hexagonal topologies and regular traffic patterns

5.3.2 Effect of idle energy and sleeping mechanism

EPB with the inclusion of power consumption in the idle mode is plotted in Fig. 5.3 for the random topologies and in Fig. 5.4 and hexagonal topologies, which corresponds to the energy consumption where the transceiver never enters the sleep mode. Consideration of idle energy makes any routing strategy equivalently energy-efficient for light traffic loads. For moderate and heavy traffic loads, EPB exhibits a similar behavior as the case of perfect sleep management shown in Fig. 5.1.

5.3.3 Components of EPB

The components of EPB, namely, idle, overhear, transmit and receive energies per bit for the hexagonal topology are shown in Fig. 5.5 for direct transmission ($h = 1$) and for multi-hopping with $h = 6$ as the traffic load changes. It is observed that idle and receive energy during overhearing are responsible for most of the energy consumed, especially at light traffic loads. Energy spent during transmission and reception at the intended receiver constitute a small portion of

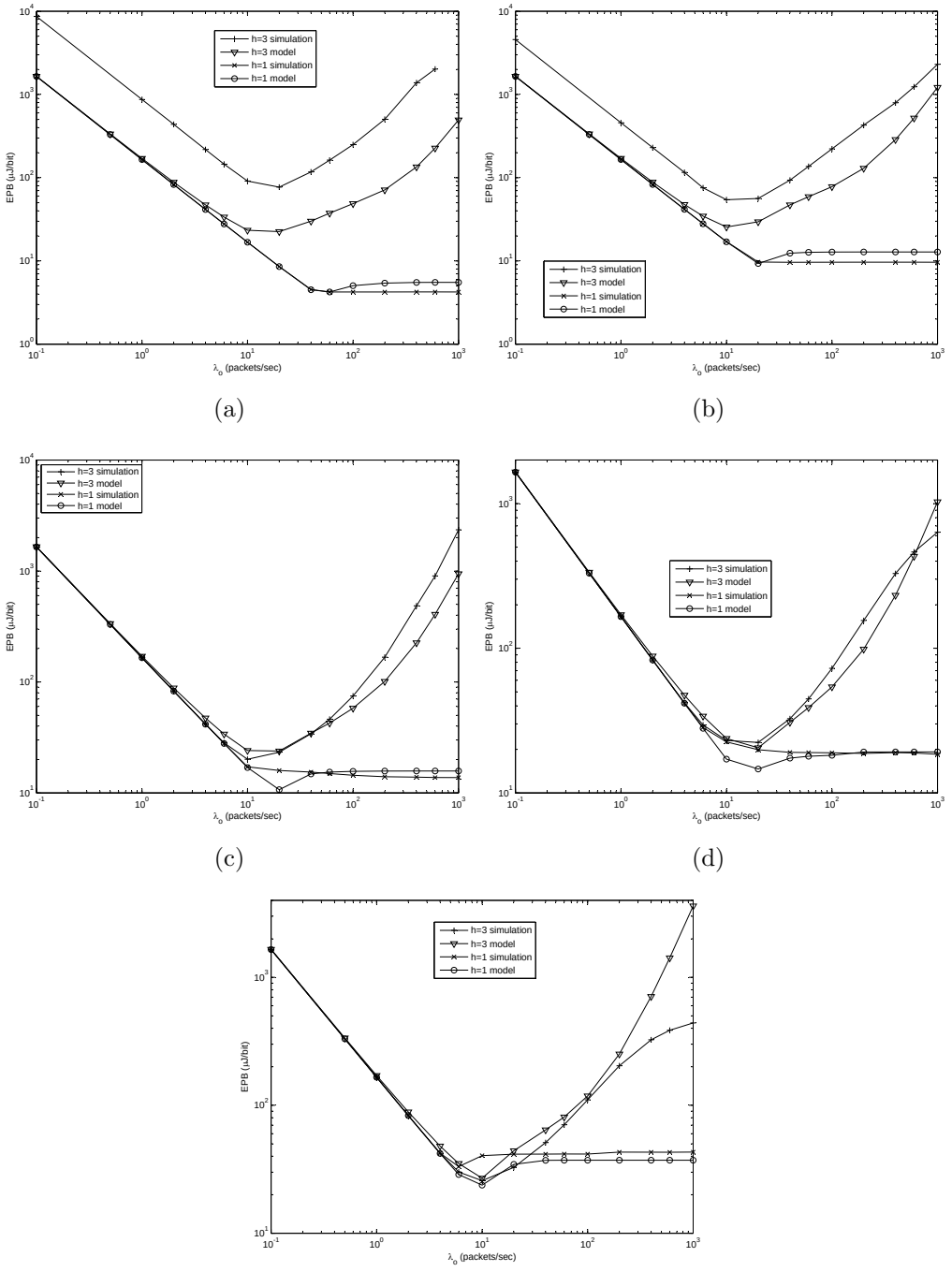

Figure 5.3: EPB obtained from analytical model and simulations with inclusion of energy consumed in the idle mode for a) 10-node, b) 20-node, c) 50-node, d) 100-node, e) 200-node random topologies and random traffic patterns

EPB, about 1% of EPB for direct transmission and about 10% of EPB for $h = 6$ under moderate-to-heavy traffic. It is seen that inclusion of energy expenditure during idle listening, carrier sensing, collisions, freezing mechanism in backoff

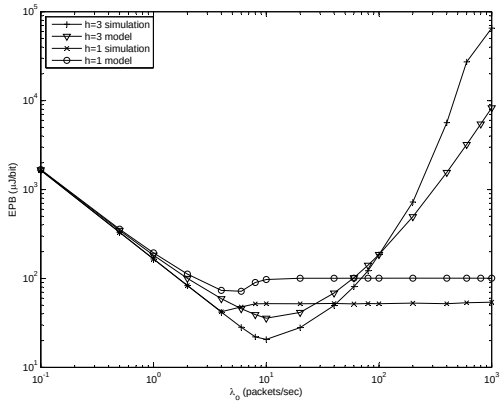

(a)

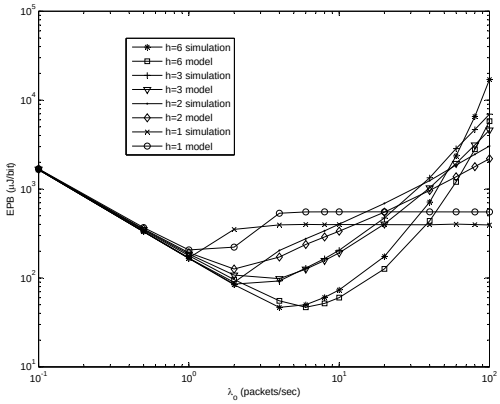

(b)

Figure 5.4: EPB obtained from analytical model and simulations with inclusion of energy consumed in the idle mode for a) 127-node, b) 469-node hexagonal topologies and regular traffic patterns

and extra energy consumption due to overhearing significantly affect the energy consumption.

The components of EPB, namely, idle, overhear, transmit and receive energies per bit for the 200-node random topology are shown in Fig. 5.6 for direct transmission ($h = 1$) and for multi-hopping with $h = 3$ as the traffic load changes.

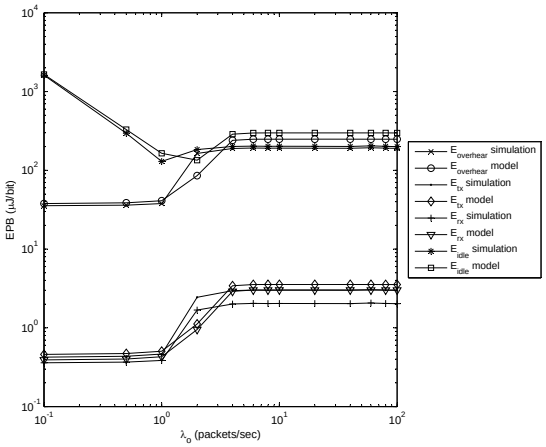

(a)

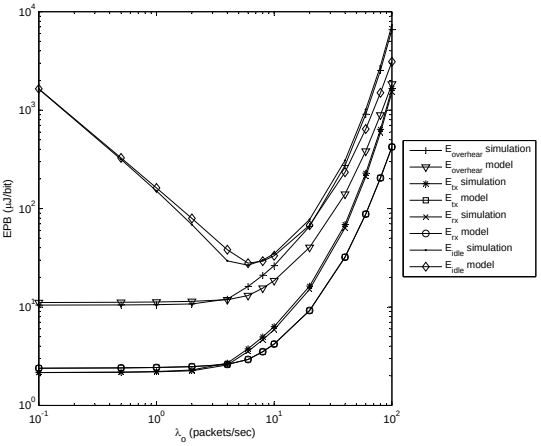

(b)

Figure 5.5: Idle, overhear, transmit and receive energies per bit in the 469-node hexagonal topology for a) direct transmission and b) multi-hopping with $h = 6$

5.3.4 Effect of processing power

The EPB calculated for a processing power of $10\mu J/bit$ at relay nodes is observed to change the optimum hop number in Fig. 5.7. The optimum hop number is different for changing traffic: $h^* = 2$ for $\lambda \leq 2$, $h^* = 3$ for $2 < \lambda \leq 10$, $h^* = 1$ for $10 < \lambda$. The optimum routing strategy for energy-efficient routing is traffic dependent for $P_{process} = 10\mu J/bit$.

The EPB with the inclusion of energy consumption in idle mode versus processing power at relay nodes is plotted for different routing strategies for the hexagonal topology in Fig. 5.8 for $\lambda_o = \{0.5, 4, 60\}$ packets/sec. The results

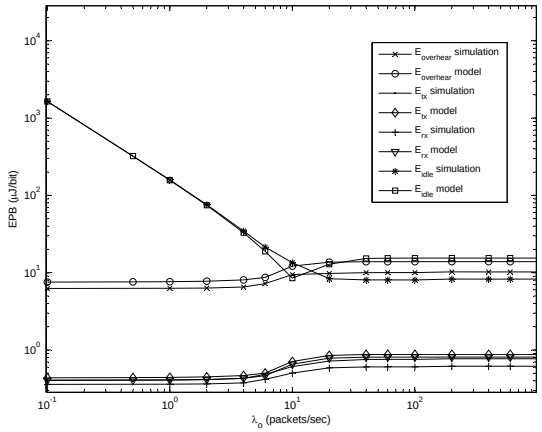

(a)

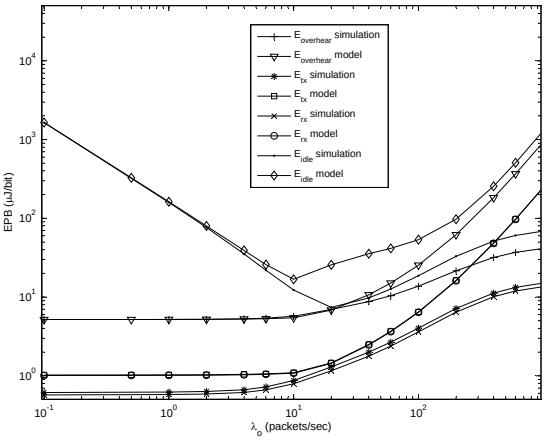

(b)

Figure 5.6: Idle, overhear, transmit and receive energies per bit in the 200-node random topology for a) direct transmission and b) multi-hopping with $h = 3$

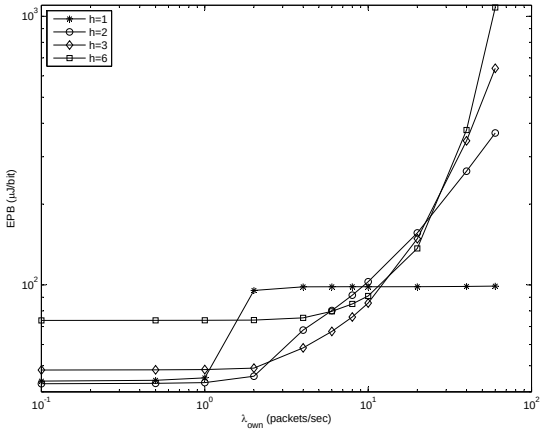

Figure 5.7: EPB of analytical results for $h = \{1, 2, 3, 6\}$ for $P_{process} = 10\mu J/bit$

show that the processing power affects the optimum hop number for energy-efficient routing only under moderate traffic loads. Under moderate traffic loads

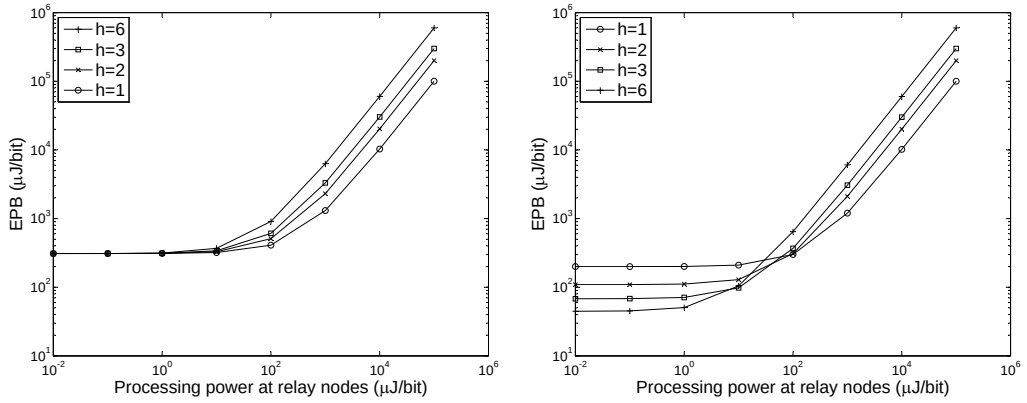

(a)

(b)

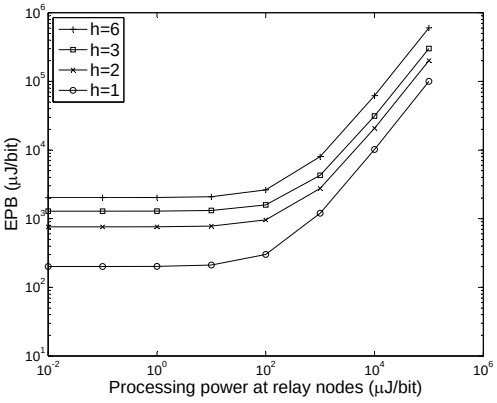

(c)

Figure 5.8: EPB with idle energy versus processing power for a) $\lambda_o = 0.5$, b) $\lambda_o = 4$ and c) $\lambda_o = 60$ packets/sec

$h = 6$ is optimum for low processing power, whereas $h = 1$ becomes more energy-efficient as processing power increases. Meanwhile, under light and heavy traffic $h = 1$ has the highest energy-efficiency independent of the processing power.

5.3.5 Effect of contention window size

EPB with no sleeping regime versus minimum contention window size, $W_0 = \{32, 64, 128\}$, for $h = \{1, 2, 3, 6\}$ and $\lambda_o = \{0.5, 4, 60\}$ packets/sec for the hexagonal topology are shown in Fig. 5.9. EPB is observed to be independent of the minimum contention window size under light traffic loads. Otherwise, increasing the contention window decreases EPB by about up to 50% for $h = \{1, 2, 3\}$ and

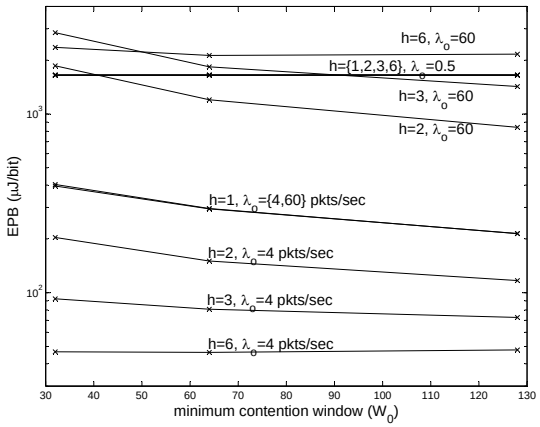

Figure 5.9: EPB with idle energy consumption versus minimum contention window W_0, for $h = \{1, 2, 3, 6\}$ and $\lambda_o = \{0.5, 4, 60\}$ packets/sec

by about 8% for $h = 6$. This result reveals that controlling the contention window size is a successful cross-layer energy-efficiency approach, promising significant energy savings under heavy traffic conditions.

The effect of contention window size on EPB with perfect sleeping regime is shown in Fig. 5.10 for the 469-node hexagonal topology. The contention window takes the values $W_0 = \{32, 64, 128\}$. The contention window size affects EPB under moderate-to-heavy traffic loads with direct transmissions, where the MAC contention is high. The effect is negligible for multi-hop transmissions and becomes noticeable with increasing traffic. Under high contention, changing contention window size from $W_0 = 32$ to $W_0 = 128$ halves the EPB, providing a substantial energy saving.

5.3.6 Effect of DATA packet size

The effect of DATA packet size on EPB with perfect sleeping regime is shown in Fig. 5.11 for the 469-node hexagonal topology. The contention window takes the values $DATA = \{500, 1000, 2000\}$ bytes plus 72 header bytes. The DATA packet

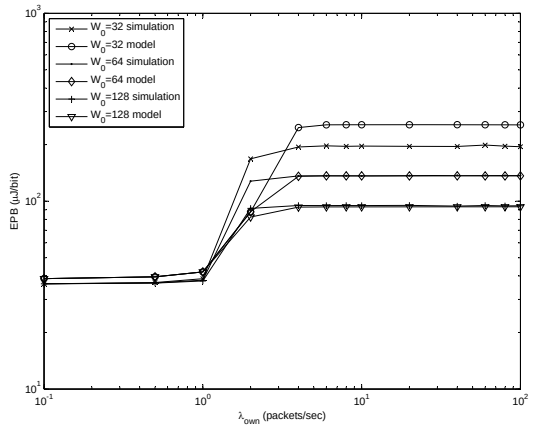

(a)

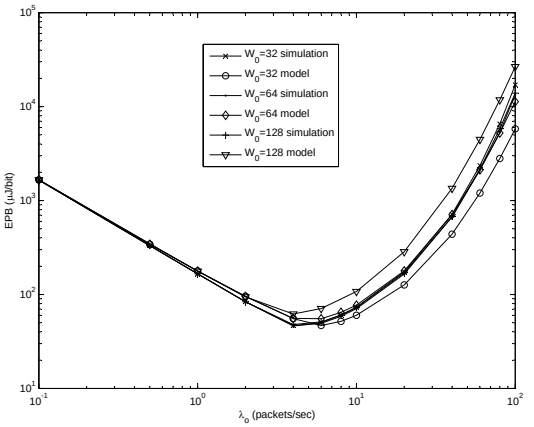

(b)

Figure 5.10: Effect of contention window size, obtained from analytical model and simulations, for the 469-node hexagonal topology: a) EPB for $h = 1$, b) EPB for $h = 6$.

size affects EPB for all traffic loads with both direct transmissions and multi-hopping, so that doubling DATA packet size almost halves the EPB, providing a substantial energy saving.

5.3.7 Effect of maximum retry count

The effect of maximum retry count on EPB with perfect sleeping regime is shown in Fig. 5.11 for the 469-node hexagonal topology. The short retry count (SRC) takes the values $SRC = \{3, 7\}$, whereas the long retry count (LRC) is kept constant. Increasing SRC decreases EPB for heavy traffic loads with direct

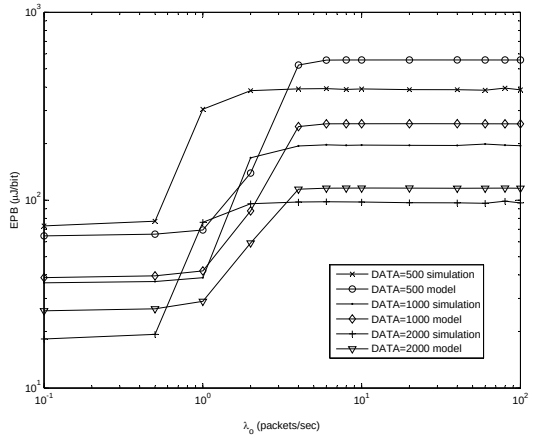

(a)

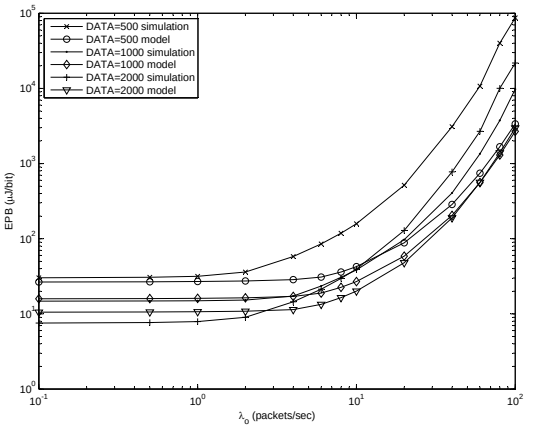

(b)

Figure 5.11: Effect of DATA packet size, obtained from analytical model and simulations, for the 469-node hexagonal topology: a) EPB for $h = 1$, b) EPB for $h = 6$.

transmissions, whereas the effect is negligible with multi-hop transmissions.

5.4 Conclusions

Using the analytical energy model for IEEE 802.11 DCF based wireless networks, it is shown that the model accurately computes the energy expenditure over a wide range of scenarios. The analytic results obtained via the IEEE 802.11 DCF and the energy model, supported by simulations, show that the energy-efficient routing strategy highly depends on the traffic load. Under light traffic, energy

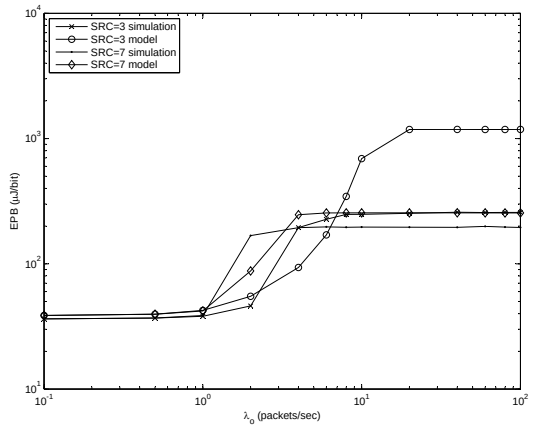

(a)

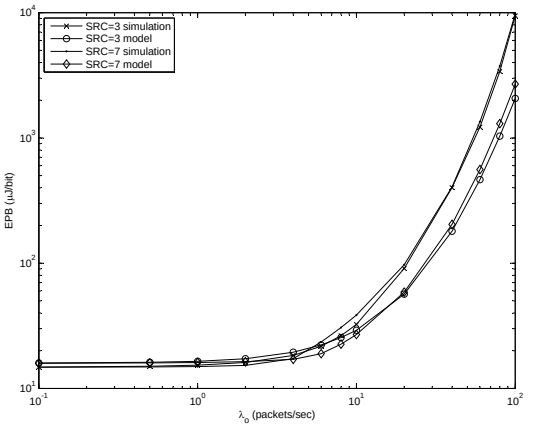

(b)

Figure 5.12: Effect of maximum retry count, obtained from analytical model and simulations, for the 469-node hexagonal topology: a) EPB for $h = 1$, b) EPB for $h = 6$.

spent during idle mode is responsible for most of the energy consumed, making any routing strategy equivalently optimum. Under moderate traffic, energy spent during idle and receive modes dominates and multi-hop transmissions become more advantageous. At heavy traffic, multi-hopping becomes unstable due to increased packet collisions and excessive traffic congestion, and direct transmission becomes more energy-efficient and stable. Our extensive numerical studies show that the accuracy of the analytical model in predicting EPB degrades with the irregularity of the topology and traffic pattern due to the averaging of p, however the general characteristics of the EPB curves and the implications regarding routing are not affected.

The results show that the energy-efficient routing strategy depends not only on the processing power as shown before [37–40], but also depends on the traffic load. It is shown that the dependence on processing power is valid only for a specific range of traffic loads. Previous studies, e.g., [14,15], that consider solely the energy consumption due to transmissions, state that multi-hop paths are more energy-efficient. Our results show that this is valid for low-to-moderate traffic loads with a perfect sleeping regime or for moderate traffic loads with no sleeping regime and dense topologies with more energy-efficient alternative multi-hop paths.

We have also shown the effect of the contention window size, the DATA packet size and maximum retry limit on EPB performance. EPB with perfect sleeping regime is shown to decrease significantly with increasing contention window size, DATA packet size and maximum retry limit.

Transmission power reduction with multi-hopping decreases the number of contending stations in the transmission range, which results in less collisions, retransmissions, backoff and freezing mechanisms at the MAC layer, reducing the energy consumption of multi-hopping for low-to-moderate traffic loads. However, as the traffic increases, MAC layer contentions increase and end-to-end throughput approaches to zero due to heavy packet drops at intermediate hops, resulting in an increase in the energy-per-bit. It is shown through simulations and analytical model that multi-hopping becomes more energy-efficient up to some traffic rate and direct transmission becomes more energy-efficient afterwards. Furthermore, the advantage of multi-hopping is larger for dense and regular topologies. The results show that the energy consumed per bit by direct transmission is more robust in a multi-hop network, because excessive packets are dropped at the interface queues before being transmitted. But in multi-hop routing, packet drops occur at the wireless links, substantially increasing the energy waste especially when the network is congested.

Up to this chapter, we have analyzed the effect of hop-count on goodput, throughput and energy performance of multi-hop wireless networks. Based on the results obtained, an adaptive route selection algorithm is introduced in the next chapter.

Chapter 6

LACAR: A Load-Adaptive Contention-Aware Route Selection Algorithm for Multi-Hop Networks

The goodput and energy performances are shown to be network and traffic dependent in previous two chapters. In this chapter, a cross-layer load-adaptive contention-aware route selection algorithm for multi-hop wireless networks is proposed, which takes MAC contention into account and dynamically changes the routing algorithm according to the network traffic load.

After a literature review of some relevant contention-aware routing algorithms, the proposed route selection algorithm is introduced in Sec.6.2. Simulation results obtained by running the route selection algorithm on two different topologies and are given afterwards, followed by conclusions.

6.1 Literature Review

Different types of routing protocols have been developed for multi-hop wireless networks, which can be categorized into proactive (e.g. DSDV [106]), reactive algorithms (e.g. AODV [107] and DSR [108]). Proactive protocols maintain fresh lists of routes to destinations by periodically distributing routing tables throughout the network, whereas reactive protocols find a route on demand by flooding the network with route request packets. Network performance suffers from amount of data, slow reaction on restructuring and failures with proactive algorithms; and from high latency in route finding and excessive flooding with reactive algorithms. Thus, these protocols may lead to poor routing performance due to the network congestion within certain area of the wireless networks.

Several congestion-aware routing protocols have been investigated [109–112] to enhance the network performance. The Dynamic Load-Aware Routing (DLAR) [109] and the Load- Balanced Ad-hoc Routing (LBAR) [110] schemes consider the number of interfering routes around a node in order to determine if the node should be selected as a forwarding node within the route. The routing with Minimum Contention time and Load balancing (MCL) [111] algorithm determines its route selection criterion based on the total number of contenting nodes around the neighborhood of a node. An Adaptive NAV-Assisted Routing (ANAR) protocol is proposed to alleviate the network congestion where the existing NAV information of nodes along a path within the IEEE 802.11 protocol is utilized for determination of the feasible route [112]. The ANAR protocol adaptively switches between the selected paths while the level of network congestion changes.

The routing protocol ANAR injects route discovery packets into the network, while the protocols in [109–111] inject additionally control packets for gathering

neighborhood information, which increase the network congestion problem to some extend for the purpose of alleviating it.

A random route discovery packet drop (R2DPD) strategy to alleviate congestion under heavy traffic in IEEE 802.11 based multi-hop networks is proposed in [113], which drops routing packets in the MAC layer according to the on-line measuring of local contention state (i.e. load factor). Stations in heavy contention environment drop route discovery packets with high probability so that the congestion is relieved.

6.2 Load-Adaptive Contention-Aware Route Selection Algorithm

In this section, we present a Load-Adaptive Contention-Aware Route Selection (LACAR) algorithm that adapts the hop-count of routing algorithms according to the network traffic load considering the MAC contention in multi-hop wireless networks. The proposed route selection algorithm may be used by both proactive and reactive routing algorithms with no additional control packet overhead in order to increase goodput and energy performance in IEEE 802.11 DCF based multi-hop wireless networks.

The proposed scheme, LACAR is called as a route selection algorithm rather than a routing algorithm, because it does not include a definition for route discovery or route maintenance, rather it uses a path set composed of both long-hop and short-hop routes to all destinations, and selects either long-hop or short-hop routes network-wide depending on the network and traffic load.

The objective function of the adaptive route selection algorithm proposed is the maximization of average node goodput and minimization of the EPB performance, which are shown to exhibit similar behavior for changing traffic loads.

The results of the preceding two chapters show that, minimizing EPB, minimizes the inter-successful-receptions time and thus maximizes the average node goodput. Maximization of throughput is of secondary importance in multi-hop networks compared to maximization of goodput since throughput is the rate achieved at the link layer whereas goodput is the rate achieved at the application layer. Thus, throughput maximization is not considered as an objective of the adaptive route selection algorithm.

The optimum route selection algorithm for goodput and energy performance is illustrated to be network and traffic load dependent. Moreover, the physical layer and MAC layer parameters affect the optimum hop-count. The results of the preceding two chapters show that, goodput is maximized and EPB is minimized by short-hop routing for light-to-moderate traffic loads and by long-hop routing for heavy traffic loads. Recall that, these results are obtained under the assumption that all routes in the network are composed of equal number of hop-counts. In this chapter, we assume a quasi-stationary traffic in the network where the average traffic load changes for all nodes in the network at some discrete points in time. Thus, rather than small traffic load variations per node, we are concerned with sharp variations in traffic load, such as daily changes. Nodes are assumed to be stationary. In fact, the LACAR algorithm is appropriate to function with mobile nodes, but mobility necessitates updates of information on available short hop and long hop routes, which may degrade the performance and needs a future investigation.

Recall that LACAR is a route selection algorithm rather than a routing algorithm. Thus, LACAR functions on top of a base routing algorithm, i.e. route discovery, maintenance, etc. are done according to the rules of the routing algorithm. We have no assumption regarding the routing algorithm, it may be proactive, reactive or any other adaptive algorithm.

LACAR is a learning-based route selection algorithm that has two phases: the initialization phase and forwarding phase, which are explained next. Learning happens in all phases.

6.2.1 Initialization phase

Step 1:

Each node has a specific route to the destination, which is determined by the rules of the base routing algorithm. Node i routes packets according to the route selected by the base routing algorithm and measures the following quantities:

- $\Delta T(i)$, the time interval between two consecutive DATA receptions by the intended destinations,
- $\lambda_o(i)$, the average packet generation rate of node i,
- EPB(i), which is the energy per bit expenditure of node i measured over duration $\Delta T(i)$.

However, $\Delta T(i)$ is not known by node i immediately for multi-hop routes, since the source node i gets an acknowledgement at the network layer with a delay. In this case, two different calculation methods exist for obtaining $\Delta T(i)$:

1. If node i is destination of some path $\in \Gamma$, $\Delta T(i)$ is approximated by the average time between two successfully received packets, whereas an exact calculation requires the time between two successfully *transmitted* packets.
2. If node i is not the destination of any path $\in \Gamma$, node i waits for network layer acknowledgements over paths in set Γ_i to predict $\Delta T(i)$. This is an exact method for obtaining $\Delta T(i)$ for multi-hop routes but introduces a delay.

From the measured $\Delta T(i)$, node i calculates $G(i)$ by Equation (4.11), which is the rate at which source node i delivers DATA frames successfully to the destination nodes of the paths in the set Γ_i.

Node i records the measured $\lambda_o(i)$ and $EPB(i)$ values and the calculated $G(i)$ values, and obtains two graphs for the goodput and EPB versus $\lambda_o(i)$ for the route determined by the base routing algorithm.

Step 2:

The route discovery of the base algorithm is run again in this phase with a constraint of hop-count, which forces the routes to be switched between long hop routing and short hop routing. If the base routing algorithm uses long hop routing in Step 1, the base routing algorithm is forced to select a short hop route in Step2. And if the base routing algorithm uses short hop routing in Step 1, then the base routing algorithm is forced to select a long hop route in Step2. Step 1 is redone for this second route.

Through Step 1 and Step 2, goodput and EPB for different traffic loads for short hop and long hop routing are obtained by all source nodes in the wireless network. This way, each node obtains the necessary data that maps the traffic load to an optimum routing strategy. Note that, this mapping is special for that network topology, the network size, the physical layer and MAC layer parameters used in communications. And one advantage of LACAR is that, this mapping is obtained with no given information about these parameters. Moreover, no extra control packets are injected to the network for obtaining this mapping.

6.2.2 Adaptive phase

With the data obtained in the initialization phase, node i has the knowledge of the optimum hop-count for a given average generated traffic for maximizing goodput and minimizing energy expenditure. In the adaptive phase, node i measures the average generated traffic load and selects the route with the optimum number of hops. Learning of the LACAR algorithm keeps going in the adaptive phase, where the mappings are updated according to changing conditions, such as node removals, traffic pattern changes, or position changes.

6.2.3 An example

The LACAR algorithm may be implemented by both the proactive and reactive routing algorithms with modifications to the algorithm structure.

For example, let the base routing algorithm be AODV, which is a shortest path algorithm. The cost metric is energy if minimizing EPB is the optimization function or the cost metric is delay if maximizing goodput is the optimization function. Let's say that the shortest path selected by the base algorithm is a multi-hop route with cost $4 + 3 + 2$, but a longer hop route exists where the minimum cost of a direct transmission route is 11. LACAR uses the multi-hop route in Step 1 of initialization phase to obtain a mapping of goodput and EPB versus average generated traffic load. Route discovery of AODV is activated in Step 2 in order to find the minimum cost one-hop route in this step. Step 1 is redone for the minimum cost longer hop route, where another mapping of goodput and EPB versus average genrated traffic load is obtained for a longer hop route. During the adaptive phase, each node calculates goodput and EPB for the average generated traffic load and selects the optimum route based on the mappings obtained in the initialization phase.

Let us also consider a proactive routing algorithm with route tables. LACAR modifies the route tables so as to handle two kinds of routes: one for the shortest multi-hop route, and one for the shortest one-hop route. At the initialization phase, LACAR obtains mapping of goodput and EPB versus traffic load for these two routes. At the adaptive phase, either the multi-hop route or the one-hop route is selected depending on the load.

6.3 Numerical Results

In this section, computed simulation results for p, τ, average node goodput, average node throughput and EPB of the adaptive route selection algorithm LACAR are compared with the simulations for the non-adaptive cases with $h = 1$ and $h = 3$. The LACAR algorithm is implemented on top of the fixed routing protocol. The average offered traffic load per node is taken as 10 packets per second for the first half of the simulations and varied to 100 packets per second for the second half of the simulation duration. For the $h = 1$ and $h = 3$ cases, the hop counts of all paths are fixed throughout the simulation duration, whereas the network-wide hop-count is changed adaptively according to the traffic load for the adaptive case. Fig. 6.1 illustrates the parameters p, τ, average node goodput, average node throughput and EPB with the adaptive routing protocol compared with the non-adaptive cases for the 127-node hexagonal topology. The parameters used for the simulations are the same as listed in Table 3.2 and Table 5.1.

Recall that the average node goodput is maximized with $h = 3$ for the moderate traffic load of $\lambda_o = 10$ packets/sec, whereas it is maximized with $h = 1$ for the heavy traffic load of $\lambda_o = 100$ packets/sec as illustrated in Fig. 4.3(a). LACAR algorithm adapts the routing strategy according to the varying traffic load conditions, where nodes transmit by multi-hopping for the first half of the

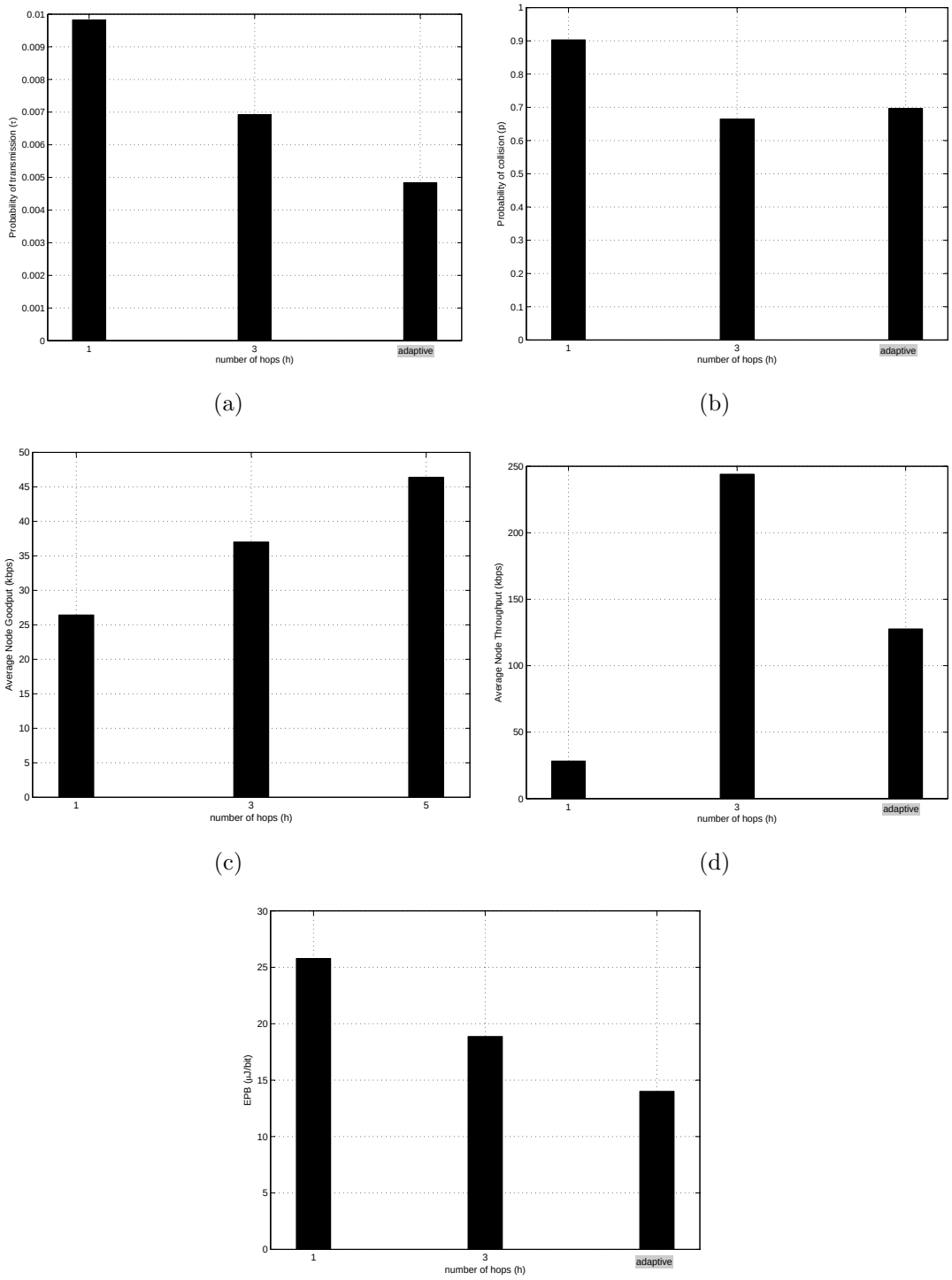

Figure 6.1: Comparison of performance of the adaptive route selection algorithm LACAR with non-adaptive cases with $h = 1$ and $h = 3$ for the 127-node hexagonal topology for a) probability of transmission, b) probability of collision, c) average node goodput, d) average node throughput and e) EPB with ideal sleeping regime

simulation duration when the average traffic load per node is 10 packets/sec and nodes transmit directly when the average traffic load per node becomes 100 packets/sec. LACAR algorithm performs the best resulting with the highest node goodput as shown in Fig. 6.1(c). A goodput gain of about 75% is achieved compared with direct transmissions, and a gain of about 25% is achieved compared with multi-hop transmissions for the 127-node hexagonal topology.

The average node throughput is shown in Fig. 4.5(a) to be maximized with $h = 3$ for all traffic loads. Thus, the $h = 3$ regime provides the maximum throughput as shown in Fig. 6.1(d) and LACAR algorithm performs worse than the $h = 3$ case since it adapts the routing strategy according to the varying traffic load conditions.

EPB with perfect sleeping regime is depicted in Fig. 6.1(e) for comparison of energy performance of LACAR with other regimes. Recall that EPB is minimized with $h = 3$ for the moderate traffic load of $\lambda_o = 10$ packets/sec, whereas it is minimized with $h = 1$ for the heavy traffic load of $\lambda_o = 100$ packets/sec as illustrated in Fig. 5.2(a). Thus, LACAR provides the minimum energy consumption compared to direct transmissions and multi-hopping as shown in Fig. 6.1(e). An energy gain of about 46% is achieved compared with direct transmissions, and a gain of about 26% is achieved compared with multi-hop transmissions for the 127-node hexagonal topology.

The average value of the MAC parameter τ is given in Fig. 6.1(a). It is observed that LACAR results with a minimum probability of transmission compared with other routing strategies. τ is decreased by 51% compared with direct transmissions and by 30% compared with multi-hop transmissions strategy. The reason behind the minimum τ obtained by the adaptive route selection algorithm becomes obvious with an inspection of Fig. 3.13(a). Note that, τ is the primary MAC parameter that affects the goodput and EPB performance metrics. The goodput is maximized and EPB is minimized as τ decreases.

The average value the MAC parameter p is plotted in Fig. 6.1(b). It is observed that adaptive route selection algorithm decreases p by 22% compared to direct transmissions and increases p by 5% compared with multi-hop transmissions strategy. The probability of collision parameter affects goodput and energy performance significantly, but the mechanism of this effect is not as clear as the effect of τ.

Similar simulation results are obtained for the 469-node hexagonal topology for which the results are given in Fig. 6.2. LACAR algorithm is compared with the direct transmissions regime and multi-hopping regime with $h = 6$ under varying traffic load. For the 469-node hexagonal topology, a goodput gain of about 222% is achieved compared with direct transmissions, and a gain of about 18% is achieved compared with six-hop transmissions, whereas an energy gain of about 68% is achieved compared with direct transmissions, and a gain of about 21% is achieved compared with six-hop transmissions. The goodput and energy gain increases significantly with increasing network size for direct transmissions with LACAR algorithm. The gain of adaptive routing is not that much compared to six-hop transmissions for the 469-node hexagonal topology. The reason for the high goodput gain is due to the higher absolute value of goodput gain obtained by six-hop transmissions for $\lambda_o = 10$ packets/sec, compared to the absolute value of the gain obtained by direct transmissions for $\lambda_o = 100$ packets/sec, as illustrated in Fig. 4.3. Likewise, the reason for the high energy gain is due to the relatively low EPB obtained by six-hop transmissions compared to direct transmissions for $\lambda_o = 10$ packets/sec as illustrated in Fig. 5.2.

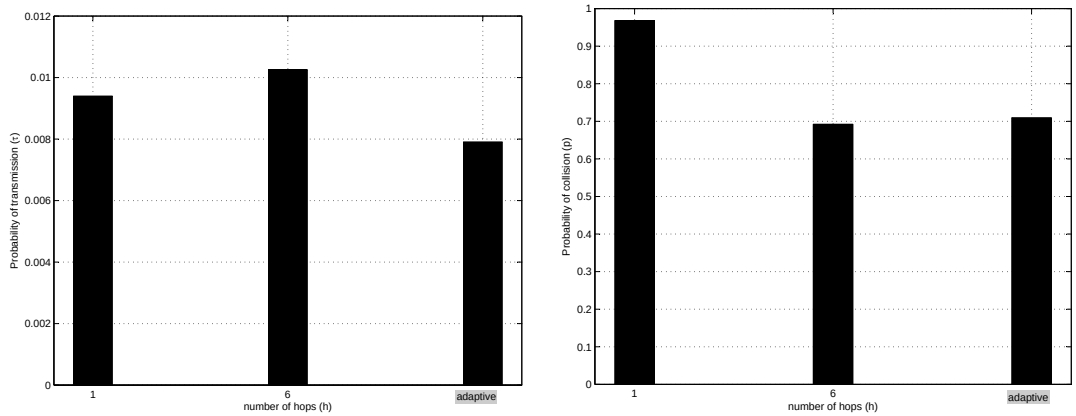

(a)

(b)

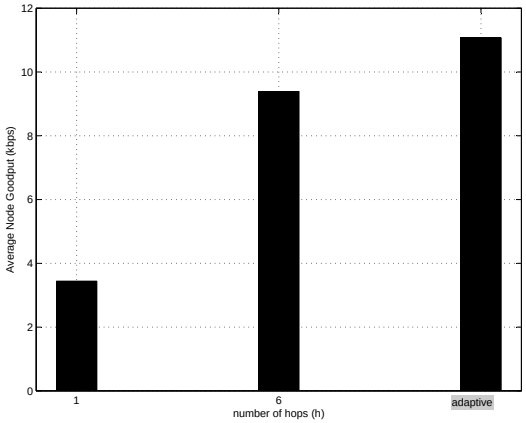

(c)

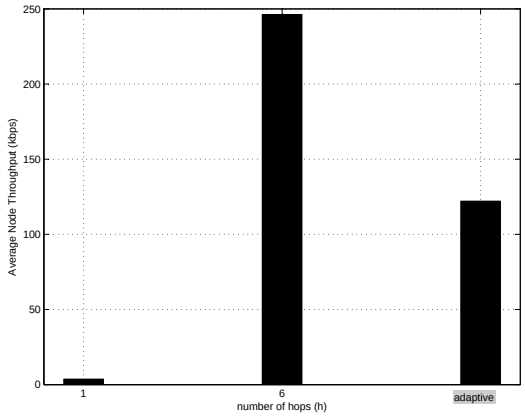

(d)

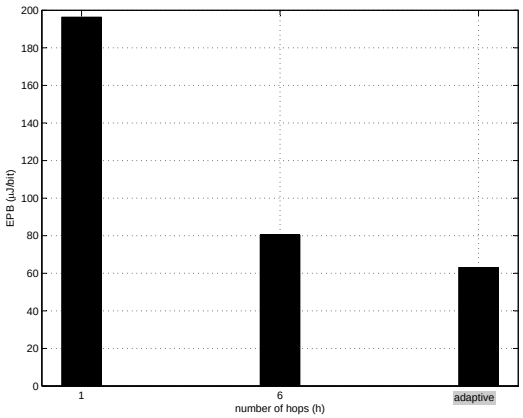

(e)

Figure 6.2: Comparison of performance of LACAR algorithm with non-adaptive cases with $h = 1$ and $h = 3$ for the 469-node hexagonal topology for a) probability of transmission, b) probability of collision, c) average node goodput, d) average node throughput and e) EPB with ideal sleeping regime

6.4 Conclusions

A load-adaptive contention-aware route selection algorithm, LACAR, which determines the optimum route adaptively according to the network and traffic conditions in multi-hop wireless networks is proposed in this chapter. The results show that a cross-layer traffic and network adaptive routing protocol provides a goodput gain of about $75-222\%$ compared with direct transmissions, and a gain of about $18-25\%$ compared with multi-hop transmissions; whereas an energy gain of about $46-68\%$ is achieved compared with direct transmissions, and a gain of about $21-26\%$ is achieved compared with multi-hop transmissions for the hexagonal topologies considered.

Chapter 7

Conclusions and Future Work

An analytical IEEE 802.11 DCF model, a goodput model, a throughput model and an energy model for the performance analysis of multi-hop wireless networks is developed in this dissertation. Extensive numerical studies and simulations are conducted and it is shown that these analytical models accurately compute MAC parameters as well as performance metrics such as energy, goodput and throughput over a wide range of scenarios.

Moreover, an adaptive routing approach where routes are selected adaptively according to the network and traffic conditions is proposed in Chapter 6 and the results show that a cross-layer traffic and network adaptive route selection algorithm significantly increases performance.

The answer of when a routing protocol should use a single long hop or multiple short hops in wireless networks for an increased energy and goodput performance under IEEE 802.11 DCF, is found out to be highly traffic and network dependent, whereas parameters such as contention window size, DATA packet size, maximum retry count have some impact. The answer for an increased throughput, on the other hand, is found out to be network dependent, mostly favoring multi-hop transmissions.

Viewed from energy aspect the results are as follows: Under light traffic, energy spent during idle mode dominates in the energy model, making any routing strategy nearly optimum. Under moderate traffic, energy spent during idle and receive modes dominates and multi-hop transmissions become more advantageous where the optimum hop number varies with processing power consumed at relay nodes. At the very heavy traffic conditions, where multi-hopping becomes unstable due to increased collisions, direct transmission becomes more energy-efficient and stable. The results show that the energy-efficient routing strategy depends not only on the processing power as shown before [37–40], but also depends on the traffic load. It is shown that the dependence on processing power is valid only for a specific range of traffic loads. Previous studies, e.g., [14, 15], that consider solely the energy consumption due to transmissions, state that multi-hop paths are more energy-efficient. Our results show that this is valid for low-to-moderate traffic loads with a perfect sleeping regime or for moderate traffic loads with no sleeping regime and dense topologies with more energy-efficient alternative multi-hop paths.

Viewed from goodput aspect similar results are obtained: Under light traffic, arrival rate of packets is dominant, making any routing strategy equivalently optimum. Under moderate traffic, parallel intra-path and inter-path transmissions dominate and multi-hop transmissions become more advantageous. At heavy traffic, multi-hopping becomes unstable due to increased packet collisions and excessive traffic congestion, and direct transmission increases goodput. And finally from a throughput aspect, it is shown that throughput is topology dependent rather than traffic load dependent, and multi-hopping is optimum for large networks whereas direct transmissions may increase the throughput for small networks.

We have also investigated the effect of the contention window size, the DATA packet size and maximum retry limit on goodput, throughput and energy performance. Goodput and throughput are shown to increase whereas the energy expenditure is shown to decrease significantly with increasing contention window size, DATA packet size and maximum retry limit.

The choice of routing strategy is observed to affect energy-efficiency and goodput more for large and homogeneous networks where it is beneficial to use multiple short hops each covering similar distances. The results indicate that a cross-layer routing approach, which takes energy expenditure due to MAC contentions into account and dynamically changes the routing strategy according to the network traffic load, can increase goodput by at least 18% and save energy by at least 21% in a realistic wireless network where the network traffic load changes in time. The goodput gain may increase up to 222% and energy saving may increase up to 68% for denser networks where multi-hopping with higher number of hop-count is possible.

The analytical IEEE 802.11 DCF model is based on a single average SMC that models the average behavior of nodes in a wireless network. Hence, as illustrated by the results, the accuracy of the model degrades as the network topology and traffic pattern becomes more irregular. The model introduced in this dissertation can be modified so as to model each link behavior separately by solving SMCs as many as the link number jointly. This method is not realized in this dissertation due to high computational complexity, but it can be studied as a future work in order to increase the accuracy of the model for irregular topologies and traffic patterns.

Two simplifying assumptions are used in the development of the analytical IEEE 802.11 DCF model: i) equal receiving and carrier sensing ranges and ii) no capture effect. It is shown in [114] that the relative values of the receiving

and carrier sensing ranges and the capture effect play a crucial role in the performance of the IEEE 802.11 protocol in multi-hop wireless networks, where the metrics spatial reuse and fairness are investigated. As a future work, the proposed DCF model can be extended by relaxing these two assumptions and the energy, goodput and throughput performance of the protocol can be investigated under varying ratios of receiving and carrier sensing ranges together with capture effect. Moreover, the proposed DCF model can be extended further by relaxing the assumptions of error free channel, unified disk graph model, etc.

The results obtained in this dissertation are specific to the IEEE 802.11 DCF. We want to investigate the validity of the results given in Chapter 4 and Chapter 5 for other MAC protocols. We wonder if the traffic dependency of the optimum routing strategy persists by other medium access control layers. The medium access control protocol MCF, which is based on DCF and is used as the medium access control protocol for the mesh networking standard IEEE 802.11s may be a candidate MAC for future analysis. Furthermore, the analysis conducted in this dissertation can be extended to the MAC protocol EDGA of IEEE 802.11e standard, which defines a set of Quality of Service enhancements for wireless LAN applications through modifications to the MAC layer.

The performance of the proposed adaptive route selection algorithm, LACAR, is investigated for a quasi-stationary traffic model where all nodes in the network change their traffic at the same time. The performance of LACAR under other dynamic traffic models will be examined and the route selection algorithm will be improved in order to increase energy and goodput performance under different traffic models.

The LACAR algorithm is based on the assumption of stationary nodes in this dissertation. However, LACAR is appropriate to function also with mobile nodes. Mobility necessitates updates of information on available short hop and long hop

routes, which may degrade the performance. As a future work, the performance of the LACAR algorithm in wireless mobile networks may be investigated.

Appendix A

Derivation of P_{ifq} and q

The steady state probability of dropping packets at the interface queue, P_{ifq}, and the probability that the node's buffer is empty after the node finishes processing a packet in backoff, q, is calculated in this section.

The MAC and energy model are developed assuming finite buffer space at interface queue at nodes, which is more realistic than the infinite buffer assumption. The interface queue model is characterized by the arrival process and the service time distribution with certain service discipline. The packet arrivals at each mobile station follow the Poisson process with average arrival rate λ_t computed in Equation (3.6). Packets are served by the first in first out discipline, by a single server. The MAC layer service time is a non-negative random variable denoted by random variable T_S, which has a discrete probability of $Pr(T_S = t_s(i))$ for T_S being $t_s(i)$. The service time distribution is as follows:

$$\begin{aligned} \Pr\{T_S = t_s(i)\} &= \begin{cases} (1-p)p^i & \text{if } 0 \le i < m \\ p^M & \text{if } i = M \end{cases} \\ t_s(i) &= \begin{cases} T_{ts} + iT_{tc} + \sum_j^{i+1} W_j \frac{\bar{\sigma}}{2} & \text{if } 0 \le i < m \\ MT_{tc} + \sum_j^{M} W_j \frac{\bar{\sigma}}{2} & \text{if } i = M \end{cases} \end{aligned} \tag{A.1}$$

Thus, the IFQ is an M/G/1/K queue and is solved by the techniques in [78], the details of which is given below.

Let p_n represent the steady-state probability of n packets in the queueing system, and let π_n represent the probability of n packets in the queueing system upon a departure at the steady state, and let $\mathbf{P} = p_{ij}$ represent the queue transition probability matrix:

$$\mathbf{P} = \begin{bmatrix} k_0 & k_1 & k_2 & \dots & k_{K-2} & 1 - \sum_{n=0}^{K-2} k_n \\ k_0 & k_1 & k_2 & \dots & k_{K-2} & 1 - \sum_{n=0}^{K-2} k_n \\ 0 & k_0 & k_1 & \dots & k_{K-3} & 1 - \sum_{n=0}^{K-3} k_n \\ \vdots & \vdots & \vdots & & \vdots & \vdots \\ 0 & 0 & 0 & \dots & k_0 & 1 - k_0 \end{bmatrix} \tag{A.2}$$

where k_n denotes the probability of finding n packets upon a departure and is calculated as

$$\begin{aligned} k_n &= \Pr\{n \text{ arrivals during service time } T_S\} \\ &= \sum_{i=0}^{\infty} \frac{e^{-\lambda_t t_s(i)} (\lambda_t t_s(i))^n}{n!} \Pr\{T_S = t_s(i)\}. \end{aligned} \tag{A.3}$$

π_n is obtained by the normalization equation and the balance equation $\pi\mathbf{P} = \pi$. The steady state probability of n packets in the queueing system, p_n, is obtained by the following equations [78]

$$\begin{aligned} p_n &= \frac{\pi_i}{\pi_0 + \lambda_t E[T_S]} (0 \le n \le K-1), \\ p_K &= 1 - \frac{1}{\pi_0 + \lambda_t E[T_S]}, \end{aligned} \tag{A.4}$$

where $E[T_S]$ is the expected value of service time. The steady state probability of dropping packets at the interface queue, P_{ifq}, is equal to p_K:

$$P_{ifq} = p_K. \tag{A.5}$$

Also, the probability that the node's buffer is empty after the node finishes processing a packet in backoff, q, becomes

$$q = \pi_0. \tag{A.6}$$

Appendix B

Derivation of $E[T_W]$

$E[T_W]$ of an M/G/1/K queue is calculated by summing up the waiting times for the packets in the queue and for the residual service time of the packet in service [78]:

$$E[T_W] = min(E[N_q] - 1, 0)E[T_S] + (1 - q_0)E[T_R], \tag{B.1}$$

where $E[N_q]$ is the expected number of packets in the system seen by an arrival that does join the IFQ, q_0 is the probability that an arrival that does join the system finds the queue empty and $E[T_R]$ is the residual service time upon an arrival that does join the IFQ. In [78], the probability of n packets in system upon arrival that does join the system is denoted by q_n and the probability of n in system upon departure is denoted by π_n and the following relation is given

$$\pi_n = q_n, (0 \leq n \leq K - 1). \tag{B.2}$$

Thus q_0 becomes

$$q_0 = \pi_0 = q,$$

which is also equal to q, i.e. the probability of empty queue upon departure calculated in A.

$E[N_q]$ is given by,

$$\begin{aligned} E[N_q] &= \sum_{i=0}^{K-1} iq_i \\ &= \sum_{i=0}^{K-1} i\pi_i \\ &= \sum_{i=0}^{K-1} ip_i(\pi_0 + \lambda_t E[T_S]) \\ &= (\sum_{i=0}^{K} ip_i - KP_{ifq})(\pi_0 + \lambda_t E[T_S]), \end{aligned} \tag{B.3}$$

where $\sum_{i=0}^{K} ip_i$ corresponds to average number of packets in the system denoted by $E[N_{sys}]$.

$E[T_R]$, the residual service time upon an arrival that does join the IFQ, is given by [78]

$$E[T_R] = \frac{E[T_S^2]}{2E[T_S]}. \tag{B.4}$$

Hence, Equation (B.1) is expressed by

$$\begin{aligned} E[T_W] = min((E[N_{sys}] - KP_{ifq})(q + \lambda_t E[T_S]) - 1, 0)E[T_S] \\ + (1-q)E[T_S^2]/(2E[T_S]). \end{aligned} \tag{B.5}$$

Bibliography

[1] S. Cherry, "Edholm's law of bandwidth," *IEEE Spectrum*, vol. 41, pp. 58–60, July 2004.

[2] "Wireless LAN medium access control (MAC) and physical layer (PHY) specifications," Tech. Rep. Std 802.11, R2003, ANSI/IEEE, 1999.

[3] N. Bambos, "Toward power-sensitive network architectures in wireless communications: concepts, issues and design aspects," *IEEE Personal Communications*, vol. 5, no. 3, pp. 50–59, 1998.

[4] S. Chakarabarty and A. Mishra, "QoS issues in adhoc wireless networks," *IEEE Communications Magazine*, 2001.

[5] A. Giovanidis, *Modeling and Analysis of Wireless Communication Systems using Automatic Retransmission Request Protocols*. PhD thesis, Technical University Berlin, 2010.

[6] S. Ci and H. Sharif, "Improving goodput in IEEE 802.11 wireless LANs by using variable size and variable rate (VSVR) schemes," *Wireless Communications and Mobile Computing*, vol. 5, pp. 329–342, May 2005.

[7] G. Bianchi, "Performance analysis of IEEE 802.11 distributed coordination function," *IEEE Journal on Selected Areas in Communications*, vol. 18, no. 3, pp. 535–547, Mar. 2000.

[8] F. Alizadeh-Shabdiz and S. Subramaniam, "Analytical models for single-hop and multi-hop ad hoc networks," *Mobile Networks and Applications*, vol. 11, no. 1, pp. 75–90, Feb. 2006.

[9] F. Ye, Q. Chen, and Z. Niu, "End-to-end throughput-aware channel assignment in multi-radio wireless mesh networks," in *IEEE Global Telecommunications Conference*, pp. 1375–1379, Nov. 2007.

[10] W. Yu, J. Cao, X. Zhou, X. Wang, K. C. C. Chan, A. T. S. Chan, and H. V. Leong, "A high-throughput MAC protocol for wireless ad hoc networks," *IEEE Transactions On Wireless Communications*, vol. 7, no. 1, pp. 135–145, 2008.

[11] H.-Y. Hsieh and R. Sivakumar, "Improving fairness and throughput in multi-hop wireless networks," in *in Proc. of IEEE ICN*, pp. 569–578, July 2001.

[12] A. J. Goldsmith and S. B. Wicker, "Design challenges for energy-constrained ad hoc wireless networks," *IEEE Wireless Communications Magazine*, vol. 9, no. 4, pp. 8–27, Aug. 2002.

[13] C. E. Jones, K. M. Sivalingam, P. Agrawal, and J. C. Chen, "A survey of energy efficient network protocols for wireless networks," *Wireless Networks*, vol. 7, no. 4, pp. 343–358, Jan. 2001.

[14] S. Singh, M. Woo, and C. S. Raghavendra, "Power-aware routing in mobile ad hoc networks," in *Proc. of the* 4^{th} *Annual ACM/IEEE International Conference on Mobile Computing and Networking*, pp. 181–190, Oct. 1998.

[15] K. Scott and N. Bambos, "Routing and channel assignment for low power transmission in PCS," in *Proc. of the* 5^{th} *IEEE International Conference on Universal Personal Communications (lCUPC)*, vol. 2, pp. 498–502, Oct. 1996.

[16] C. Toh, "Maximum battery life routing to support ubiquitous mobile computing in wireless ad hoc networks," *IEEE Communications Magazine*, vol. 39, no. 6, pp. 138–147, June 2001.

[17] M. A. Youssef, M. F. Younis, and K. A. Arisha, "A constrained shortest-path energy-aware routing algorithm for wireless sensor networks," in *Proc. of the IEEE Wireless Communications and Networking Conference 2002 (WCNC 2002)*, vol. 2, pp. 794–799, Mar. 2002.

[18] S. Shakkottai, T. S. Rappaport, and P. C. Karlsson, "Cross-layer design for wireless networks," *IEEE Communications Magazine*, vol. 41, no. 10, pp. 74–80, Oct. 2003.

[19] Q. Wang and M. A. Abu-Rgheff, "Cross-layer signalling for next-generation wireless systems," in *Proc. IEEE Wireless Communications and Networking Conference (IEEE WCNC'03)*, (New Orleans, USA), pp. 1084–1089, Mar. 2003.

[20] T. ElBatt and A. Ephremides, "Joint scheduling and power control for wireless ad hoc networks," *IEEE Transactions on Wireless Communications*, vol. 2, no. 1, pp. 74–85, Jan. 2004.

[21] U. C. Kozat, I. Koutsopoulos, and L. Tassiulas, "A framework for cross layer design of energy-efficient communication with QoS provisioning in multi-hop wireless networks," in *Proc. of the* 23^{rd} *Annual Joint Conference of the IEEE Computer and Communications Societies*, vol. 2, pp. 1446–56, Mar. 2004.

[22] R. Bhatia and M. Kodialam, "On power efficient communication over multi-hop wireless networks: joint routing, scheduling and power control," in *Proc. of the* 23^{th} *Annual Joint Conference of the IEEE Computer and Communications Societies (INFOCOM)*, Mar. 2004.

[23] W. Yuen, H. Lee, and T. Anderson, "A simple and effective cross-layer networking system for mobile ad hoc networks," in *Proc. of IEEE PIMRC*, (Lisbon , Portugal), pp. 1952–6, Sept. 2002.

[24] Z. Yao, P. Fan, Z. Cao, and V. O. K. Li, "Cross-layer design for service differentiation in mobile ad-hoc networks," in *Proc. of IEEE PIMRC*, (China), Sept. 2003.

[25] K. B. Johnsson and D. C. Cox, "An adaptive cross-layer scheduler for improved QoS support of multiclass data services on wireless systems," *IEEE Journal on Selected Areas in Communications*, vol. 23, no. 2, pp. 334–343, Feb. 2005.

[26] L. Alonso and R. Agusti, "Automatic rate adaptation and energy-saving mechanisms based on cross-layer information for packet-switched data networks," *IEEE Communications Magazine*, vol. 42, no. 3, pp. 15–20, Mar. 2004.

[27] S. Toumpis and A. Goldsmith, "Performance optimization and cross-layer design of media access protocols for wireless ad hoc networks," in *ICC 2003*, pp. 2234–2240, May 2003.

[28] G. Carneiro, J. Ruela, and M. Ricardo, "Cross-layer design in 4G wireless terminals," *IEEE Wireless Communications*, vol. 11, no. 2, pp. 7–13, Apr. 2004.

[29] M. Conti, G. Maselli, G. Turi, and S. Giordano, "Cross-layering in mobile ad hoc network design," *IEEE Computer*, vol. 37, no. 2, Feb. 2004.

[30] S. Singh, M. Woo, and C. S. Raghavendra, "Power-aware routing in mobile ad hoc networks," in *Proc. of the* 4^{th} *Annual ACM/IEEE International Conference on Mobile Computing and Networking (Mobicom)*, pp. 181–190, Oct. 1998.

[31] X. Li and Z. Bao-yu, "Study on cross-layer design and power conservation in ad hoc network," in *Proc. of the* 4^{th} *International Conference on Parallel and Distributed Computing, Applications and Technologies*, pp. 324–328, Aug. 2003.

[32] A. Safwat, H. Hassanein, and H. Mouftah, "Optimal cross-layer designs for energy-efficient wireless ad hoc and sensor networks," in *Proc. of the* 22^{nd} *IEEE International Performance Computing and Communications Conference*, Apr. 2003.

[33] M. Park, J. G. Andrews, and S. M. Nettles, "Wireless channel-aware ad hoc cross-layer protocol with multi-route path selection diversity," in *Proc. of the* 58^{th} *IEEE Vehicular Technology Conference (VTC)*, vol. 4, (Orlando, FL, USA), pp. 2197–2201, Oct. 2003.

[34] P. Agrawal, "Energy efficient protocols for wireless systems," in *Proc. of the* 9^{th} *IEEE Personal, Indoor and Mobile Radio Communications (PIMRC)*, vol. 2, pp. 564–569, Sept. 1998.

[35] J. M. Kahn, R. H. Katz, and K. S. Pister, "Emerging challenges: Mobile networking for smart dust," *Journal of Communications and Networks*, vol. 2, no. 3, pp. 188–196, Sept. 2000.

[36] J. Rabaey, J. Ammer, J. L. D. S. Jr., and D. Patel, "Picoradio: Ad-hoc wireless networking of ubiquitous low-energy sensor/monitor nodes," in *Proc. of IEEE Computer Society Workshop on VLSI*, pp. 9–12, Apr. 2000.

[37] P. Chen, B. O'Dea, and E. Callaway, "Energy efficient system design with optimum transmission range for wireless ad hoc networks," in *Proc. of IEEE International Conference on Communications (ICC)*, vol. 2, pp. 945–952, May 2002.

[38] Z. Shelby, C. Pomalaza-Raez, and J. Haapola, "Energy optimization in multihop wireless embedded and sensor networks," in *Proc. of* 15^{th} *IEEE*

International Symposium on Personal, Indoor, and Mobile Radio Communications, Sept. 2004.

[39] E. I. Oyman and C. Ersoy, "Overhead energy considerations for efficient routing in wireless sensor networks," *Computer Networks*, vol. 46, no. 4, pp. 465–478, Nov. 2004.

[40] W. R. Heinzelman, A. Chandrakasan, and H. Balakrishnan, "Energy-efficient communication protocol for wireless microsensor networks," in *Proc. of the* 33^{rd} *International Conference on System Sciences*, pp. 1–10, Jan. 2000.

[41] S. Banerjee and A. Misra, "Energy-efficient reliable communication for multi-hop wireless networks," *Journal of Wireless Networks (WINET)*, 2004.

[42] M. Haenggi, "Twelve reasons not to route over many short hops," in *IEEE Vehicular Technology Conference (VTC'04 Fall)*, (Los Angeles, CA), Sept. 2004.

[43] V. Srivastava and M. Motani, "Cross-layer design: A survey and the road ahead," *IEEE Communications Magazine*, vol. 43, pp. 112–119, Dec. 2005.

[44] Z. Ning, L. G. ;and Xingwei Wang, Y. Peng, and W. Hou, "Key technology and solution to improve throughput in wireless mesh networks," in *International Conference on Information Networking and Automation (ICINA)*, vol. 1, pp. 549–553, Oct. 2010.

[45] M. Walia and R. Challa, "Performance analysis of cross-layer MAC and routing protocols in MANET," in *Second International Conference on Computer and Network Technology (ICCNT)*, pp. 53–59, Apr. 2010.

[46] C. Ibars, A. del Coso, Y. Grunenberger, F. Theoleyre, and F. Rousseau, "Increasing the throughput of wireless mesh networks with cooperative

techniques," in *Mobile and Wireless Communications Summit*, pp. 1–5, 2007.

[47] S. J. Lee and J. Shin, "Cross-layered MAC and routing algorithm for enhanced packet-delivery-ratio over wireless multi-hop networks," in *ICUIMC 2007*, Feb. 2007.

[48] J. Premalatha, P. Balasubramanie, and C. Venkatesh, "Cross layer design to improve QoS in ad hoc networks," *Journal of Mobile Communication*, vol. 2, no. 2, pp. 52–58, 2008.

[49] D. Clark, C. Partridge, R. Braden, B. Davie, S. Floyd, V. Jacobson, D. Katabi, G. Minshall, K. Ramakrishnan, T. Roscoe, I. Stoica, J.Wroclawski, and L. Zhang, "Making the world (of communications) a different place," July 2005.

[50] J. Chang and L. Tassiulas, "Energy conserving routing in wireless ad-hoc networks," in *Proc. of the* 19^{th} *Annual Joint Conference of the IEEE Computer and Communications Societies (INFOCOM)*, March 2000.

[51] I. Kang and R. Poovendran, "Maximizing static network lifetime of wireless broadcast adhoc networks," in *Proc. of ICC*, (May 11-15, 2003), Anchorage, Alaska.

[52] R.Wattenhofer, L. Li, P. Bahl, and Y.Wang, "Distributed topology control for power efficient operation in multihop wireless ad hoc networks," in *Proc. of the* 20^{th} *Annual Joint Conference of the IEEE Computer and Communications Societies (INFOCOM)*, 2001.

[53] Y. Xu, J. Heidemann, and D. Estrin, "Geography-informed energy conservation for ad hoc routing," in *ACM SIGMOBILE*, (Rome, Italy), July 2001.

[54] C. K. Toh, "Maximum battery life routing to support ubiquitous mobile computing in wireless ad hoc networks," *IEEE Communications Magazine*, pp. 138–147, June 2001.

[55] W. Liang, "Minimizing energy and maximizing network lifetime multicasting in wireless ad hoc networks," in *Proc. of IEEE ICC*, vol. 5, (Seoul), pp. 3375–3379, May 2005.

[56] M. Stemm and R. Katz, "Measuring and reducing energy consumption of network interfaces in hand-held devices," *IEICE Transactions on Fundamentals of Electronics, Communications, and Computer Science*, 1997.

[57] S. Udani and J. Smith, "Power management in mobile computing," a survey, University of Pennsylvania, 1996.

[58] A. Chandrakasan and R. Brodersen, *Low Power Digital CMOS Design*. Kluwer Academic, Norwell, MA, 1995.

[59] G. Welch, "A survey of power management techniques in mobile computing operating systems," vol. 29, pp. 47–56, 1995.

[60] G. Hiertz, D. Denteneer, S. Max, R. Taori, J. Cardona, L. Berlemann, and B. Walke, "IEEE 802.11s: The WLAN mesh standard," *IEEE Wireless Communications*, vol. 17, pp. 104–111, Feb. 2010.

[61] J. Camp and E. Knightly, "The IEEE 802.11s extended service set mesh networking standard," *IEEE Communications Magazine*, vol. 46, pp. 120–126, Aug. 2008.

[62] X. Wang and A. O. Lim, "IEEE 802.11s wireless mesh networks: Framework and challenges," *Ad Hoc Networks*, vol. 6, pp. 970–984, August 2008.

[63] H. Y. Hsieh and R. Sivakumar, "IEEE 802.11 over multi-hop wireless networks: problems and new perspectives," in *Proc. of IEEE* 56^{th} *Vehicular Technology Conference*, vol. 2, pp. 748–752, 2002.

[64] S. Xu and T. Saadawi, "Does the IEEE 802.11 MAC protocol work well in multihop wireless adhoc networks?," *IEEE Communications Magazine*, vol. 39, pp. 130–137, June 2001.

[65] I. S. Hwang and C. A. Chen, "Saturation throughput analysis in IEEE 802.11 DCF using semi-markov model," *International Mathematical Journal*, vol. 1, no. 5-8, pp. 289–296, 2006.

[66] K. Duffy, D. Malone, and D. J. Leith, "Modeling the 802.11 distributed coordination function in non-saturated conditions," *IEEE Communications Letters*, vol. 9, no. 8, pp. 715–717, Aug. 2005.

[67] Y. Barowski, S. Biaz, and P. Agrawal, "Towards the performance analysis of IEEE 802.11 in multi-hop ad-hoc networks," in *IEEE Wireless Communications and Networking Conference*, vol. 1, pp. 100–106, Mar. 2005.

[68] M. M. Carvalho, C. B. Margi, K. Obraczka, and J. J. Garcia-Luna-Aceves, "Modeling energy consumption in single-hop IEEE 802.11 ad hoc networks," in *Proc. of the* 13^{th} *International Conference on Computer Communications and Networks*, pp. 367–372, 2004.

[69] M. Carvalho and J. Garcia-Luna-Aceves, "Modeling single-hop wireless networks under rician fading channels," in *IEEE Wireless Communications and Networking Conference (WCNC)*, vol. 1, pp. 219–224, Mar. 2004.

[70] T.-H. Lee, A. Marshall, and B. Zhou, *Autonomic Management of Mobile Multimedia Systems*, vol. 4267/2006 of *Lecture Notes in Computer Science*, ch. Modelling Energy Consumption in Error-Prone IEEE 802.11-Based Wireless Ad-Hoc Networks, pp. 61–73. Springer Berlin/ Heidelberg, 2006.

[71] M. M. de Carvalho, *Analytical Modeling of Medium Access Control Protocols in Wireless Networks*. Ph. D. thesis, University of California, Santa Cruz, Mar. 2006.

[72] K. Duffy, D. J. Leith, T. Li, and D. Malone, "Modeling 802.11 mesh networks," *IEEE Communications Letters*, vol. 10, no. 8, pp. 635–637, Aug. 2006.

[73] A. Tsertou and D. I. Laurenson, "Revisiting the hidden terminal problem in a CSMA/CA wireless network," *IEEE Transactions on Mobile Computing*, vol. 7, no. 7, pp. 817–831, July 2008.

[74] P. C. Ng and S. C. Liew, "Throughput analysis of IEEE802.11 multi-hop ad hoc networks," *IEEE/ACM Transactions on Networking*, vol. 15, pp. 309–322, Apr. 2007.

[75] B. R. Haverkort, *Performance of Computer Communication Systems: A Model-Based Approach.* Chichester, UK: John Wiley & Sons Ltd., 1998.

[76] K. Duffy, D. Malone, and D. J. Leith, "Modeling the 802.11 distributed coordination function in non-saturated heterogeneous conditions," *IEEE/ACM Transactions on Networking*, vol. 15, no. 1, pp. 159–172, 2007.

[77] S. Ray and D. Starobinski, "On false blocking in RTS/CTS-based multihop wireless networks," *IEEE Transactions on Vehicular Technology*, vol. 56, pp. 849–862, Mar. 2007.

[78] D. Gross and C. M. Harris, *Fundamentals of Queueing Theory.* Wiley Series in Probability and Mathematical Statistics, New York: John Wiley & Sons Ltd., 2^{nd} ed., 1985.

[79] "The network simulator ns-2." [Online]. Available: http://www.isi.edu/nsnam/ns.

[80] P. Gupta and P. R. Kumar, "The capacity of wireless networks," *IEEE Transactions on Information Theory*, pp. 388–404, Mar. 2000.

[81] B. Xu, S. Hischke, and B. Walke, "The role of ad hoc networking in future wireless communications," in *International Conference on Communication Technology Proceedings (ICCT 2003)*, vol. 2, pp. 1353–1358, 2003.

[82] J. Li, C. Blake, D. S. J. D. Couto, H. I. Lee, and R. Morris, "Capacity of ad hoc wireless networks," in *Proc. of ACM Mobicom*, July 2001.

[83] M. Grossglauser and D. Tse, "Mobility increases the capacity of ad-hoc wireless networks," in *Proc. of IEEE INFOCOM 2001*, vol. 3, (Anchorage, AL), pp. 1360–69, Apr. 2001.

[84] R. Negi and A. Rajeswaran, "Capacity of power constrained ad-hoc networks," in *Proc. of IEEE INFOCOM 2004*, (Hong Kong, China), Mar. 2004.

[85] S. Toumpis and A. Goldsmith, "Capacity regions for ad hoc networks," *IEEE Transactions on Wireless Communications*, vol. 2, no. 4, pp. 736–48, Jul. 2003.

[86] S. Toumpis and A. J. Goldsmith, "Large wireless networks under fading, mobility, and delay constraints," in *Proc. of IEEE INFOCOM 2004*, (Hong Kong, China), Mar. 2004.

[87] A. Behzad and I. Rubin, "High transmission power increases the capacity of ad hoc wireless networks," *IEEE Transactions on Wireless Communication*, vol. 5, no. 1, pp. 156–165, 2006.

[88] K. Jain, J. Padhye, V. Padmanabhan, and L. Qiu, "Impact of interference on multi-hop wireless network performance," in *ACM MobiCom*, (San Diego, CA), Sept. 2003.

[89] D. S. J. D. Couto, D. Aguayo, B. A. Chambers, and R. Morris, "Performance of multihop wireless networks: Shortest path is not enough," in *Proc. of* 1^{st} *Workshop on Hot Topics in Networks*, Oct. 2003.

[90] S.-J. Park and R. Sivakumar, "Quantitative analysis of transmission power control in wireless ad-hoc networks," in *Proc. of International Conference on Parallel Processing Workshops*, pp. 56–63, 2002.

[91] Y. Wang, J. C. S. Lui, and D.-M. Chiu, "Understanding the paradoxical effects of power control on the capacity of wireless networks," *IEEE Transactions on Wireless Communications*, vol. 8, pp. 406–413, Jan. 2009.

[92] M. M. Hira, F. A. Tobagi, and K. Medepalli, "Throughput analysis of a path in an IEEE 802.11 multihop wireless network," in *IEEE Wireless Communications and Networking Conference (WCNC 2007)*, pp. 441 – 446, Mar. 2007.

[93] K. Wang, F. Yan, Q. Zhang, and Y. Xu, "Modeling path capacity in multihop IEEE 802.11 networks for QoS services," *IEEE Transactions on Wireless Communications*, vol. 6, pp. 738 – 749, Feb. 2007.

[94] Y. Yang, J. Hou, and L.-C. Kung, "Modeling the effect of transmit power and physical carrier sense in multi-hop wireless networks," in *Proc. of* 26^{th} *IEEE International Conference on Computer Communications (INFOCOM 2007)*, pp. 2331 – 2335, May 2007.

[95] J. W. Yang, J. K. Kwon, H. Y. Hwang, and D. K. Sung, "Goodput analysis of a WLAN with hidden nodes under a non-saturated condition," *IEEE Transactions on Wireless Communications*, vol. 8, pp. 2259–2264, May 2009.

[96] M. Haenggi and D. Puccinelli, "Routing in ad hoc networks: A case for long hops," *IEEE Communications Magazine*, vol. 43, pp. 93–101, Oct 2005.

[97] M. Haenggi, "On routing in random rayleigh fading networks," *IEEE Transactions on Wireless Communications*, vol. 4, pp. 1553–1562, July 2005.

[98] M. Stemm and R. Katz, "Measuring and reducing energy consumption of network interfaces in hand-held devices," *IEICE Transactions on Communications*, vol. 80, no. 8, pp. 1125–1131, Aug. 1997.

[99] L. Feeney and M. Nilsson, "Investigating the energy consumption of a wireless network interface in an ad hoc networking environment," in *Proc. of the* 20^{th} *Annual Joint Conference of the IEEE Computer and Communications Societies (INFOCOM)*, vol. 3, pp. 1548–1557, 2001.

[100] J. Ebert, S. Aier, G. Kofahl, A. Becker, B. Burns, and A. Wolisz, "Measurement and simulation of the energy consumption of an WLAN interface," Tech. Rep. TKN-02-010, Technical University Berlin, Telecommunication Networks Group, Germany, June 2002.

[101] J. Ebert, B. Burns, and A. Wolisz, "A trace-based approach for determining the energy consumption of a WLAN network interface," in *European Wireless Conference*, pp. 230–236, Feb. 2002.

[102] J. Chen, K. Sivalingam, and P. Agrawal, "Performance comparison of battery power consumption in wireless multiple access protocols," *Wireless Networks*, vol. 5, no. 6, pp. 445–460, Nov. 1999.

[103] R. Bruno, M. Conti, and E. Gregori, "Optimization of efficiency and energy consumption in p-persistent CSMA-based wireless LANs," *IEEE Transactions on Mobile Computing*, vol. 1, no. 1, pp. 10–31, Jan. 2002.

[104] W. K. Kuo, "Energy efficiency modeling for IEEE 802.11 DCF system without retry limits," *Computer Communications*, vol. 30, no. 4, pp. 856–862, Feb. 2007.

[105] AT&T, *WaveMODEM 2.4GHz Data Manual, Release 2*, 1995.

[106] C. E. Perkins and P. Bhagwat, "Highly dynamic destination-sequenced distance-vector routing (DSDV) for mobile computers," in *Proc. of ACM SIGCOMM*, vol. 24, pp. 234–244, 1994.

[107] C. E. Perkins and E. M. Royer, "Ad hoc on-demand distance vector routing," in *Proc. of 2nd IEEE Workshop on Mobile Computing Systems and Applications WMCSA*, pp. 90–100, 1999.

[108] D. B. Johnson and D. A. Malt, "Dynamic source routing in ad hoc wireless networks," *IEEE Transactions in Mobile Computing*, vol. 353, pp. 153–181, 1996.

[109] S. J. Lee and M. Gerla, "Dynamic load-aware routing in ad hoc networks," in *Proc. of IEEE International Conference on Communications (ICC)*, vol. 10, pp. 3206–3210, 2001.

[110] H. Hassanein and A. Zhou, "Routing with load balancing in wireless ad hoc networks," in *Proc. of 4th ACM International Workshop on Modeling, Analysis and Simulation of Wireless and Mobile Systems (MSWiM)*, pp. 89–96, 2001.

[111] B. C. Kim, J. Y. Lee, H. S. Lee, and J. S. Ma, "An ad-hoc routing protocol with minimum contention time and load balancing," in *Proc. of IEEE GLOBECOM*, vol. 1, pp. 81–85, 2003.

[112] Y.-P. Hsu and K.-T. Feng, "Cross-layer routing for congestion control in wireless sensor networks," in *IEEE Radio and Wireless Symposium*, pp. 783 – 786, 2008.

[113] Y. Peng and S. Cheng, "Random route discovery packet drop using load factor of MAC layer in IEEE 802.11 ad hoc networks," in *International Conference on Communication Technology Proceedings ICCT*, vol. 2, pp. 1215–1219, 2003.

[114] M. Durvy, *Modelling the IEEE 802.11 Protocol in Wireless Multi-Hop Networks*. PhD thesis, EPFL, 2007.